Performance and Emissions of ASTM-Approved Alternative Jet Fuels in Compression Ignition Engines

By

Darren Julian Pinto

Submitted to the graduate degree program in The Department of Mechanical Engineering and the Graduate Faculty of the University of Kansas in partial fulfillment of the requirements for the degree of Master of Science

Chair: Dr Christopher Depcik

Dr. Susan Williams

Dr. Xianglin Li

Date Defended: 26th August 2019

The thesis committee for Darren Julian Pinto certifies that this is the approved version of the following thesis:

Performance and Emissions of ASTM-Approved Alternative Jet Fuels in Compression Ignition Engines

Chair: Dr. Christopher Depcik

Date Approved: 26th August 2019

Abstract

The use of aviation fuels in compression ignition engines rose from the single forward fuel policy (SFFP) that mandated all vehicles at military bases be operated on JP-8. Since CI engines are designed to operate on diesel fuels, the switch to aviation fuels would affect both performance and emissions due to the difference in physical properties and chemical composition between aviation and diesel fuels. Hence, the first section of the study is a comprehensive review of all research pertinent to CI engines fuelled with aviation fuels for the SFFP. The tests indicate that CI engine combustion was affected by the change in viscosity, density, and cetane number (CN) of the fuel. The lower CN resulted in delayed ignition and a high premixed burn rate while the lower viscosity led to improved atomization. However, the lower viscosity also reduced fuel penetration in the cylinder while increasing spray angles and leakages past the fuel pump clearance volumes that reduced engine performance. Conversely, fuels with a greater lower heating value (LHV) and CN resulted in improved combustion as compared to diesel fuels. Finally, the CI engine test with blends of Jet-A and a coal-to-liquid (CTL) jet fuel from Sasol Ltd. at the University of Kansas pointed at a possible combination of lower CN and a low viscosity that impeded combustion and limited the synthetic blend to 20 percent by volume.

Acknowledgements

This thesis was made possible under the able guidance and motivation by Dr. Christopher Depcik at the Mechanical Engineering department at the University of Kansas. Additionally, timely assistance by Dr. Susan Williams, Dr. Ray Carter Jr., and Dr. Karen Peltier proved important in directing my research efforts on the right path. The constant advice from Jonathan Mattson, Saud Shah Alam, Charu Srivatsa, and Bailey Spickler were invaluable in achieving the goals set for this research topic. Finally, this thesis would have been impossible without the help, love, and support of close family and friends.

Table of Contents

List of Figures

List of Tables

Nomenclature

2-EHN	2-Ethylhexyl Nitrate
AFSO21	Airforce Smart Operations for the 21st Century
AMP	Aggregation Mode Particles
ASTM	American Society of Testing and Materials
ATDC	After Top Dead Center
BMEP	Brake Mean Effective Pressure
BSFC	Brake Specific Fuel Consumption
BTDC	Before Top Dead Center
BTE	Brake Thermal Efficiency
CAAFI	Commercial Aviation Alternative Fuels Initiative
CCD	Condensate Collection Device
CH_3CHO	Acetaldehyde
CH_4	Methane
CCI	Calculated Cetane Index
CI	Compression Ignition
CO	Carbon Monoxide
CO_2	Carbon Dioxide
CRC	Coordinating Research Council
CTL	Coal to Liquid
DCN	Derived Cetane Number
DI	Direct Injected
DF2	Diesel Fuel #2
DLA	Defense Logistics Agency
DoD	Department of Defense
DSB	Defense Scientific Board
ECU	Electronic Control Unit
EGR	Exhaust Gas Recirculation

EPA	Environmental Protection Agency
FAA	Federal Aviation Administration
FAME	Fatty Methyl Ester
FFA	Free Fatty Acids
FID	Flame Ionization Detector
FPGA	Field Programmable Gate Array
FSJF	Fully Synthetic Jet Fuel
FT	Fischer Tropsch
FTIR	Fourier Transform Infrared
GEP	General Electric Products
GHG	Greenhouse Gas
GM	General Motors
GSE	Ground Support Equipment
GTL	Gas to Liquid
H_2O	Water
HCHO	Formaldehyde
HCN	Hydrogen Cyanide
HMMWV	High Mobility Multipurpose Wheeled Vehicle
HNCO	Isocyanic Acid
ICAO	International Civil Aviation Organization
IMEP	Indicated Mean Effective Pressure
IDI	Indirect Injected
IPK	Isoparaffinic Kerosene
IVC	Intake Valve Close
JP	Jet Propellant
KU	University of Kansas
LHV	Lower Heating Value
LT	Low Temperature
N_2O	Nitrous Oxide

NASA	National Aeronautics and Space Administration
NATO	North Atlantic Treaty Organization
NH_3	Ammonia
NMP	Nucleation Mode Particles
NO_2	Nitrogen Dioxide
NO_x	Nitrogen Oxides
NTC	Negative Temperature Coefficient
OE	Operational Energy
PM	Particulate Matter
pph	parts per hour
SFFP	Single Forward Fuel Policy
SPK	Synthetic Paraffinic Kerosene
TARDEC	Tank Automotive Research, Development and Engineering Center
TDC	Top Dead Center
TEL	Tetraethyl Lead
THC	Total Hydrocarbons
U.S.	United States
UCO	Used Cooking Oil
ULSD	Ultra-Low Sulfur Diesel
USAF	U.S. Air Force
VNT	Variable Nozzle Turbocharger

Chapter I: Research Overview

Introduction

Crude oil is the primary energy source in the world with a total annual consumption expected to exceed 99 million barrels by 2018 [1]. However, it will not be long before this current period of oil dependence ends as the remaining crude reserves become more difficult to access. Furthermore, with crude oil consumption growing at an exponential rate, atmospheric carbon dioxide (CO_2) emissions have crossed 400 ppm in Figure 1 [2], and its effects are evident through a rise in global average temperatures, sea levels, intense rainfall, floods, droughts, wildfires, and other natural calamities. A major source of these CO_2 emissions come from the combustion of liquid fuels by the transportation sector, both civilian and military, and account for about 32% of all CO_2 emissions [3]. In addition, other by-products of combustion like Particulate Matter (PM), nitrogen oxides (NO_x), carbon monoxide (CO), and total hydrocarbons (THC) all have detrimental health effects on living organisms. As a result, world governments continue to introduce tougher environmental legislation to battle global warming and pollution.

One possible solution to reduce global greenhouse gas emissions and our dependence on fossil fuels is through the utilization of biofuels and alternative fuels in compression ignition (CI) engines. CI engines are advantageous for their higher thermal and fuel conversion efficiencies while maintaining low pumping work because of the absence of a throttling device [4]. Although CI engines are designed to ideally operate on petroleum diesel fuel, their higher compression ratios (in comparison to spark ignition engines) and subsequent fuel auto-ignition process allows for the utilization of other heavy liquid fuel distillates; e.g., relatively cheaper bunker fuel oil used to propel large freight ships. In spite of the relatively low number of CI passenger vehicles sold in the United States (U.S.), petroleum diesel fuel

accounts for approximately 21% of fuel used solely for transportation and presents a viable opportunity to reduce the net carbon footprint [5]. Moreover, the use of CI engines with alternative fuels becomes all the more important when analyzing the energy requirements of the United States (U.S.) military.

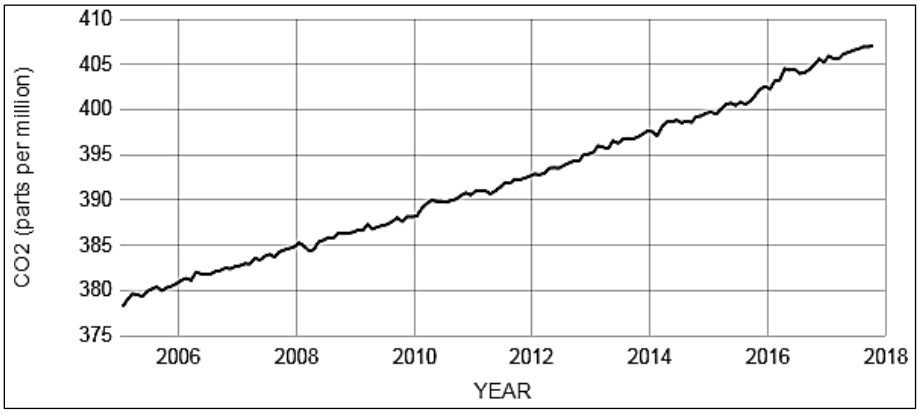

Figure 1: Atmospheric CO_2 levels demonstrating a significant rise over the last decade [2]

The U.S. Department of Defense (DOD) is the largest federal executive department and accounts for the greatest energy consumption of any national agency in the world. Specifically, 57% of the total energy required by the different arms of the DoD come in the form of liquid fuel consumption at nearly 86 million barrels in 2015 for a cost of almost $14 billion [6]. A break-up of this expenditure for different services of the U.S. military is listed in Table 1. Of this expenditure, close to 70% went towards Operational Energy (OE) requirements in order to train and mobilize troops along with deploying advanced weapons platforms for various military operations, as displayed in Figure 2. Investigating OE requirements further finds that the United States Air Force (USAF) uses 52% of this fuel [7]. Furthermore, this dependency on petroleum feedstock can be problematic for the U.S. military because of fluctuating oil prices associated with the unstable and unpredictable geopolitics of the Middle East, Nigeria, and Venezuela that account for 60% of the total fuel imports. Although the recent crude oil price slump has helped abate the DoD's expenditure on fuel, the U.S. Air Force, U.S. Army, and U.S. Navy have enforced stringent policies to decrease energy consumption, reduce gross carbon emissions, and

increase the utilization of green technologies to combat climate change [8]. Ironically, civilian airline companies have been pursuing a switch to alternative fuels more aggressively than the military, considering the huge spurt in domestic and international air travel. These initiatives have impelled new research, particularly in the field of fuels and combustion, which is the purpose of this study conducted at University of Kansas (KU).

Table 1: DoD fuel assessment of recent and estimated annual expenditure on procurement of fuel for the United States military [6]

		2011	2012	2013	2014	2015	2016	2017e	2018e
Energy Demand, (Million Barrels)	Army	20.2	16.1	12.7	10.1	7.3	7.1	8.4	8.4
	Navy	31.1	31.5	28.4	28.2	28.5	28.5	26.4	26.6
	Air Force	*61.3*	*55.7*	*47.8*	*48.6*	*52.0*	*49.6*	*51.5*	*51.3*
	Marine Corps	0.3	0.2	0.2	0.2	0.2	0.2	0.5	0.5
	Other DoD	0.3	0.4	0.7	0.3	0.5	0.4	0.9	0.9
	Demand	113.5	103.9	89.8	87.4	88.6	85.7	87.7	87.7
	Expenditure (Billion $)	$16.6	$16.3	$14.8	$14.0	$14.1	$8.7	$9.2	$9.2

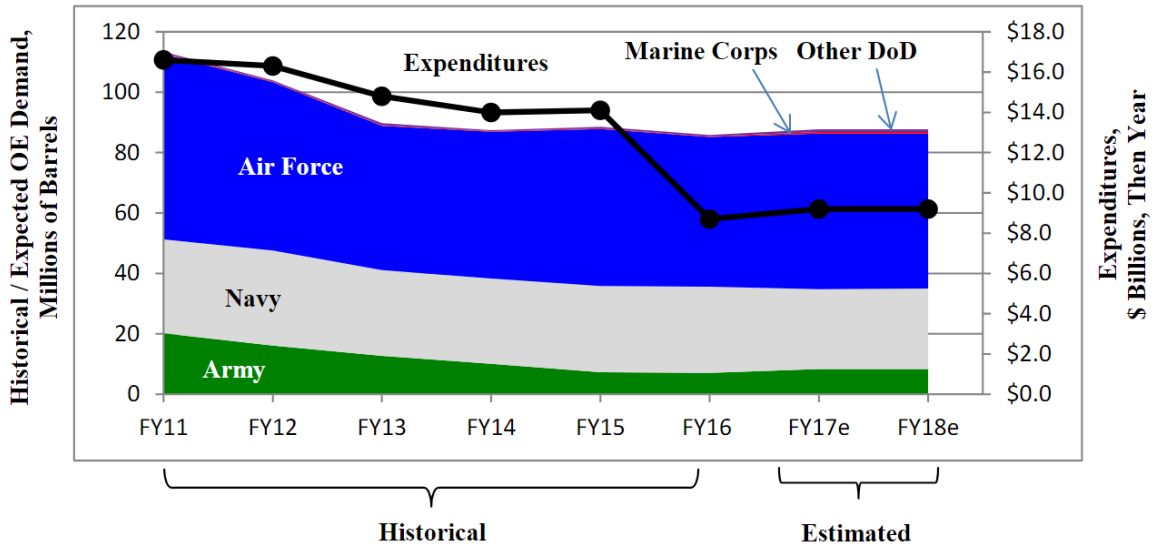

Figure 2: OE demand of the U.S. DoD highlighting the large proportion of fuel costs for the USAF [6]

The Single Fuel Concept and its Implementation

In 1951, the U.S. government introduced the 'wide-cut' Jet Propellant # 4 (JP-4) fuel as the main jet propellant [9] (MIL-DTL-5624A). However, this fuel has a high volatility and an infamous reputation for building up static charge in fuel lines, subsequently increasing the risk of fires [10]. In particular, Bachman et al. [11] reported fifteen fire incidents attributed to static electricity generated by fuel in fuel pipes during the period between 1959 and 1969. As a result, Beery et al. [12] published a detailed analysis in 1975 suggesting the use of Jet Propellant # 8 (JP-8) fuel as a replacement for JP-4 (a comparative table of fuel properties is in the Appendix) in an effort to address fire safety during combat and noncombat conditions. This study also recommended a systematic conversion from JP-4 to JP-8 for all North Atlantic Treaty Organization (NATO) and U.S. forces around the world.

Meanwhile, hostile relations between the U.S. and Russia during the Soviet invasion of Afghanistan in 1979 resulted in large deployments of troops and military equipment to Europe to form a coalition with NATO forces. During winter months, ground support vehicles, generators, and armed infantry vehicles were deemed inoperable as paraffins in the traditional ground transportation fuels (F-54 and DF-2) congealed in fuel lines and tanks, subsequently affecting fuel pumps and filters [13]. Hence, the DOD recommended blends of JP-5 or JP-8 with these fuels as a stopgap measure to prevent wax formation; however, this presented a huge logistical obstacle in transporting different fuels to multiple military bases.

This issue resulted in the NATO Standardization Agreement (NATO STANAG 4362) in 1987 to use JP-8 as a single fuel on the battlefield. In the following year, the DOD directive 4140.43 specified JP-8 as the primary fuel for land and air forces overseas. This directive, backed by several research reports, highlighted the positives of using JP-8 on the battlefield. Specifically, Bowden et al. [14] conducted an

exhaustive fuel properties study of JP-8, Jet-A1, and JP-5 fuels from different parts of the world at the Belvoir Fuels and Lubricants Research Facility at the Southwest Research Institute. It was determined that JP-8 properties were similar to that of DF-1, DF-2, and NATO F-54. Furthermore, Montemayor et al. [15] listed all the benefits in using JP-8 for both U.S. and NATO forces during both conflict and peacetime operations, such as simplified logistics, reduced lubricant degradation, reduced exhaust emissions, and increased readiness. Other efforts by Likos et al. [16] involved the evaluation of four U.S. Army engines with JP-8 fuel. They found that JP-8 increased engine efficiency at maximum power conditions, lowered the rate of cylinder combustion chamber deposit formation, lessened contamination of the engine lubricant, reduced the wear of the upper piston ring area, and reduced the rate of depletion of the lubricant additives. Along similar lines, Butler et al. [17] presented their comprehensive engine tests where DF-2 fuel was substituted with JP-8 in over 2800 different combat vehicles at Fort Bliss, Texas. The entire study took place for over two years and demonstrated that JP-8 is a suitable substitute for DF-2 without requiring any engine modifications. In addition, this study illustrated that the higher heating value of JP-8 offset a slight loss in power output because of its lower viscosity. Additionally, the report highlighted tactical and economic advantages like simplified logistics, improved war preparedness, and reduced costs.

Shortcomings of JP-8 as a Single Battlefield Fuel

An engine and its auxiliary components are designed optimally around a single fuel; hence, using a different fuel with dissimilar physical and chemical properties can have drastic effects on the functionality of the engine. For instance, the switch from diesel fluid #2 (DF-2) or F-54 to JP-8 on the battle frontlines of the Euro-Russian border during the height of the cold war affected engines that employed fuel-lubricated rotary pumps. Along similar lines, Pera [13] highlighted problems using JP-8

like hot starts, poor operation, fuel pump failures, improper replacement parts, corrosion, use of fuel without additives, etc., as reported by maintenance crews during Operation Desert Shield and Operation Desert Storm. Interestingly, these problems did not arise during the tests at Fort Bliss with a possibility being that JP-8 fuel properties, such as viscosity and Cetane Number (CN), were different from the fuel obtained in the Middle East. Moreover, the tests at Fort Bliss took place in a monitored, idealized, and controlled environment, far from an actual battlefield scenario. Likewise, the arid and sandy regions of Kuwait, Iraq, and Saudi Arabia can influence the long-term performance of engines. An important point to note is the MIL-DTIC standards for JP-8 prescribe a range for the CN number. This can often lead to change in fuel injection events as a difference in 10 units of CN results in approximately a 30% difference in ignition delay [18, 19]. However, these issues were partially solved in the Middle East by adjusting the fuel injection process and improving the quality control on fuel pump accessories.

In addition to shortcomings in engine performance, several studies have reported the toxic effects of JP-8 fuel on U.S. military personnel. The performance additives and organic solvents that are components of JP-8 can lead to neurobehavioral deficits, including degraded motor learning, memory, attention, and visual-spatial performance along with reductions in processing speed. In this area, Mattie and Sterner [20] compiled a review on toxicology studies for jet fuel. They reported instances of short-term dermal toxicity, hearing loss, sub chronic dosing, immunological defects, neuro-behavioral, developmental, reproductive, and mutative effects of JP-8 on different species of laboratory rats. Ironically, in spite of JP-8 being in use for over three decades, there is a lack of research on how this fuel affects military service personnel under prolonged exposure.

USAF Transition to Synthetic and Renewable Fuels

In 1998, the Defense Scientific Board (DSB) performed a study on how the DoD could reduce energy consumption for its weapons systems [21]. Their study focused on streamlining procurement and improving fuel efficiency of weapon systems. The period from the year 2000 to 2005 saw several governmental committees and private enterprises make efforts to push alternative fuels into the mainstream. The most important legislation to initiate the commercial development of strategic non-conventional fuels was the Energy Policy Act of 2005 [8]. The act paved a way for research of alternative fuels for the transportation sector. In 2006, the JASON report [22] presented to the DoD, listed possible reduction in fossil fuel utilization using various advanced technologies and alternative energy sources. The USAF first purchased a batch of synthetic Fischer-Tropsch fuel (S-8) from Syntroleum Inc. for a series of tests on military transport, surveillance, and combat aircraft. Following these successful demonstrations, the USAF presented the Air Force Energy Plan in 2009 to reduce fuel demand, increase alternate fuel supply and change the working culture for the USAF on a whole, to promote sustainability. The USAF aimed at setting 50% of their domestic fuel requirement via cost effective alternative fuel blends procured from continental U.S. manufacturers. In addition to the USAF, the DOD listed its goals for alternative fuels to include the use of up to 50% 'drop-in' fuels without modifying engines along with deriving fuels from non-food crops and having life cycle greenhouse gas emissions lower than petroleum-derived fuels. By this time, the civilian aviation industry made several advancements in the alternative fuel sector with several airlines investing in the research of drop-in fuels. By 2010, synthetic paraffinic kerosene fuel derived from the Fischer-Tropsch process (FT-SPK) and biomass derived hydroprocessed esters and fatty acids (HEFA) were already approved by the Federal Aviation Administration (FAA) for 50% blends with conventional Jet-A. The Commercial Aviation Alternative Fuels Initiative (CAAFI) supervised the testing of these fuels for the FAA and the USAF being member of the

CAAFI soon began certifying these alternative fuels for their own domestic operations. NASA published a series of test reports with data from their Alternative Fuel Effects on Contrails and Cruise Emissions Study (ACCESS I and II) programs that demonstrated the reduction in aerosol emissions at high altitude cruise conditions after using a 50-50 blend of Jet-A and camelina bio jet fuel [23]. FT-SPK fuels in particular have been observed to decrease soot by almost 50 to 90% and reduce CO_2 by 2.4% with a total absence of sulfurous byproducts of combustion [7]. In particular, the lower aromatic content of FT-SPK has been found to lower CO emissions by almost 20% [24]. Furthermore, the excellent low temperature properties of the FT-SPK at higher altitudes meant good fuel thermal stability, essential for military use in colder climates. Moreover, the availability of coal and natural gas reserves in the continental U.S. present FT-SPK aviation fuel as an economically viable alternative to Jet-A [7]. According to some sources, life-cycle greenhouse gas (GHG) emissions from alternative fuels can be up to 80% lower than traditional fossil jet fuel emissions [25].

In 2009, the International Civil Aviation Organization (ICAO) of the United Nations (who establishes standards and recommended practices) set a goal for international aviation to achieve carbon-neutral growth starting in 2020 [26]. This use of alternative fuels, especially in the aviation sector, has gained momentum in the last decade because of the potential development of the airplane industry: e.g., the North American region will grow by 2.3% annually and carry 1.2 billion passengers in 2036, an additional 452 million passengers per year [27]. As a result, several airlines have committed to going carbon neutral while reducing emissions within the next decade, with alternative fuels at the core of their long-term environmental policies. To date, the American Society of Testing and Materials (ASTM) has approved five alternative fuel pathways (see Appendix Tables 5 to 11 for detailed fuel properties) based on extensive tests conducted with the help of industrial fuel manufacturing partners, fuel testing and certification laboratories, and the U.S. military with the entire process overseen by the FAA. An overview

of the fuel pathways prescribed by the ASTM 7566 16b standard has been listed in Table 2. Various research groups have explored several other bio jet fuel pathways; however, the ASTM process to certify aviation fuel is rigorous due to the high safety standards associated with aircraft.

Table 2: Alternative jet fuel pathways approved for manufacturing by the ASTM D7566 16b standard

Fuel	*Acronyms*	*Pathways*	*Feedstock*	*Maximum blend %*	*Year Approved*
Fischer Tropsch synthetic paraffinic kerosene	FT-SPK	Coal/natural gas to jet (Fischer Tropsch Synthesis, gas fermentation)	Coal, natural gas, Biomass	50	2009
Hydroprocessed esters and fatty acids	HEFA	Hydroprocessed renewable jet, catalytic hydrothermolysis, hydrotreated depolymerized cellulosic jet	Vegetable oil, animal fat, recycled oils	50	2011
Synthetic iso-paraffins	SIP	Catalytic conversion of sugars to fuel, direct biological sugar to hydrocarbons	Sugar	10	2014
Fischer Tropsch synthetic kerosene with aromatics	FT-SKA	Same as FT-SPK	Coal, natural gas, Biomass	50	2015
Alcohol to jet	ATJ	Ethanol to jet, butanol to jet	Starch, sugar, cellulosic biomass	50	2016

USAF Transition to Commercial Jet-A Fuel

In an effort parallel to the utilization of alternative fuels, the USAF worked to reduce fuel expenditures by converting all national air bases to operate on commercially available Jet-A. This process began in 2009 as a part of the Airforce Smart Operations for the 21st Century (AFSO21) cost savings initiative [28]. In partnership with the Defense Logistics Agency, 130 air bases were converted to operate with standard Jet-A under this program leading to annual savings of almost $25 million, along with the benefits of enhanced energy security and operational flexibility. Fuel additives for enhanced cold weather performance, corrosion inhabitance, and static dissipation could be added on site, as needed. This fuel standardization allowed additional local and regional fuel suppliers to supply fuel to the military, which further reduced the price of fuel. With the inclusion of alternative fuels and standardization to Jet-A, the

single fuel concept becomes expensive and complicated, invariably prompting a steady decline in the utilization of JP-8 by the USAF. As a result, refineries have reduced or terminated the production of JP-8 citing an increase in procurement, storage, and handling costs to support a supply chain specific to this fuel [29]. This incentivizes the possibility of exploring the use of new approved alternative fuels in CI engines of ground support equipment in an effort to reduce operational and logistical costs.

The Single Fuel Concept and Alternative Fuels at Airports

Of importance, the single fuel concept for the U.S. military could potentially be applicable to commercial airports. Airports rely on a large fleet of ground support equipment (GSE) to ensure timely transit of aircraft and passengers including terminal buses, catering trucks, passenger stands, cargo loaders, baggage tractors, security vehicles, garbage trucks, hydrant trucks, deicers, fuel trucks, engine starters, generators, and auxiliary power units [30]. Most of these prime movers operate on ultra-low sulfur diesel (ULSD#2) fuel that could be swapped for aviation jet fuel to simplify airport logistics or in times of emergency. Additionally, the use of alternative fuels like FT-SPK can result in lower particulate emissions from these vehicles, subsequently improving airport air quality. For example, Donohoo-Vallett [31] modeled the improvement in air quality at Atlanta Hartsfield Jackson International Airport when moving from using low sulphur jet fuel to FT-SPK. She found that utilization of synthetic paraffinic kerosene in jet engines could potentially reduce PM in the airport vicinity by 64%. Her models further indicated that the use of alternative fuels lower or maintain pollutant emission levels for both aircraft and ground support vehicles. In this area, Miller et al. [32] listed the necessary guidelines to integrate alternative jet fuels in to airports. They listed a complete framework consisting of a complete investor analysis, screening of technological and logistical options followed by an evaluation of each option to optimize finances. However, for optimum efficacy when shifting to an alternative fuel, fuel injection events

should be modified to ensure the greatest power delivery and reduced emissions. Hence, relating fuel properties to CI engine performance and emissions is a critical need in the area of alternative jet fuels. This is where the single-cylinder engine test cell in the Department of Mechanical Engineering at University of Kansas (KUME) can be employed.

Engine Test Cell

The power plant of the KUME single-cylinder engine test cell is a Yanmar L100V naturally aspirated, CI engine with engine construction and instrumentation documented by Langness et al. [33]. It is paired to a Dyne Systems, Inc. Dymond Series air-cooled regenerative dynamometer. An Inter-Loc C OCS controller allows the dynamometer to run in speed mode or torque mode. A FUTEK (model #TRS-605) torque transducer installed between the shaft of the dynamometer and engine measures up to 200 N-m with an error of ±0.2% at full load. A Bosch MS15.1 Diesel Electronic Control Unit (ECU) controls fuel injection events. A Bosch CP3.2 pump, driven by a Leeson (model #C42D17FK1C) 0.5 hp electric motor, pressurizes the Bosch fuel rail (model # 261-B1-135-201) and prevents drawing power away from the engine while testing. An Emerson Elite Coriolis mass flow meter (model #CMF-010M) measures the fuel flow rate from the fuel tank to the fuel pump. An Omega pressure sensor (model #EWS-BP-A) measures the ambient pressure while another sensor (model #EWS-RH) measures the atmospheric temperature and humidity. Engine intake air is determined using a Meriam volumetric laminar flow element (model #50MW20-2) and an Omega differential pressure transducer (model #PX277-30D5V). A 30-gallon resonator barrel acts as a plenum to reduce unsteady flow. The temperature of air entering the engine is measured by an Omega (model #TC-K-NPT) K-type thermocouple and pressure is measured by an Omega (model #TC-K-NPT) K-type thermocouple.

The high-frequency data collection system for this engine consists of a Kistler encoder (model #2614B1) and a Kistler piezoelectric pressure transducer (model #6052C) that records in-cylinder pressure. The analog signal from the encoder is converted to a digital signal with a Kistler signal converter (model #2614B2). A Kistler pulse multiplier (model #2614B4) then converts the digital signal to an appropriate crank angle. An NI CRIO (model# cRIO-9014) data acquisition system fitted with real time controllers along with analog and digital modules allows for real time data acquisition from the sensors on the engine. A high-speed computer with a field programmable gate array (FGFA) chip samples and stores data up to 200 Hz through a LabVIEW program. This program also generates artificial signals for the camshaft speed required by the ECU as the cam speed sensor cannot be appropriately installed.

An AVL SESAM Fourier Transform Infrared Spectroscopy (FTIR) emissions analyzer connected to a second LabVIEW program measures the carbon dioxide (CO_2), carbon monoxide (CO), nitric oxide (NO), nitrogen dioxide (NO_2), water (H_2O), nitrous oxide (N_2O), methane (CH_4), ammonia (NH_3), isocyanic acid (HNCO), hydrogen cyanide (HCN), formaldehyde (HCHO), acetaldehyde (CH_3CHO), aromatic hydrocarbons, and other hydrocarbons. A Flame Ionization Detector (FID) quantifies total hydrocarbons with a Magnos oxygen sensor used to determine oxygen content. An AVL Smoke Meter (model #415SE) collects PM and outputs its concentration to the LabVIEW program. A MATLAB code developed by a previous graduate student is used for post processing data to remove noise, average data over used defined intervals, and determine standard deviations in measurements. Finally, a data diagnostic tool developed by Mattson [34, 35] is used to investigate the performance of engine and calculate the heat release of the fuel via both the first and second laws of thermodynamics.

Thesis Focus

Overall, the KUME experimental setup along with the heat release model allows for quantification and qualification of the influence of fuel properties on engine performance along with regulated and unregulated emissions. This is used here to investigate alternative drop-in fuels approved by the FAA for civilian use. Moreover, the findings are additionally applicable for the Single Fuel Concept of the U.S. military. Unique to the KUME engine testing methodology is the combustion normalization employed when studying different alternative fuels and their blends with Jet-A. This is critically important when testing fuels without the predilection of combustion phasing as different properties of fuel have a noteworthy effect on the ignition delay. Specifically, the influence of CN, viscosity, and density will affect both the physical and chemical ignition delay leading to dissimilar engine behavior while subsequently changing emissions like NO_x, PM, CO, and HC. In addition, chemistry factors in these alternative fuels, like the absence of aromatic compounds (leading to gasket leaks) or the removal of sulphur (reducing lubrication from the fuel), will be considered as part of this investigation.

To provide the appropriate background, Chapter 2 highlights a thorough investigation into jet fuels and alternative jet fuels that were used in CI engines. This chapter covers detailed performance analysis and emission profiles of fuels tested mainly for the U.S. military. It includes trends for in-cylinder pressure and temperature, heat release profiles, BMEP and IMEP curves, and tailpipe emission data. Since this topic has largely been experimental in nature, few authors have qualitatively analyzed their test results illustrating a significant issue in the literature. Furthermore, a large section of the summary focusses on JP-8, as it has been the main fuel for the USAF for nearly 30 years since it was first introduced on the battlefield.

The following Chapter 3 summarizes experiments conducted using the engine test cell at the University of Kansas to map the performance and emissions of a coal to liquid (CTL) fuel from Sasol. The fuel is tested in its neat form and with blends of Jet-A acquired from Lawrence Municipal Airport. A LabVIEW interface acquire data, like fuel and airflow rates, temperatures, in-cylinder pressure traces, and torque, which are then sampled and filtered through a MATLAB routine developed by Langness [36]. The first-law heat release model developed by Mattson [37] is used to obtain the rate of heat release of different blends, which is then validated with engine test data. The RHR model uses the in-cylinder pressure trace from test data and is calibrated against known combustion efficiency of the thermodynamic cycle as measured by the brake specific production of partially oxidized combustion species [38]. Results from this test will be used to validate the use of CTL fuel for the single forward fuel policy.

Chapter 2: Literature Review of FAA Approved Alternative Jet Fuels Testing in Compression Ignition Engines

Abstract

The use of alternative jet fuels in compression ignition engines has gained importance with the implementation of the Single Fuel Forward Policy (SFFP) of the U.S. Department of Defense (DOD). Through the SFFP, the U.S. DoD aimed at reducing the operational and logistical costs associated with multiple supply chains of liquid fuels. With the selection of JP-8 as the main battlefield fuel, CI engines originally designed to operate on ULSD#2 could show a decrease in performance and compromise soldiers' safety. Through preliminary studies, the drop-in engine performance was indicative of the differences in physical and chemical properties of JP-8 and ULSD#2. With focused research, issues with autoignition, ignition delay, fuel injection, lubricity, and most importantly emissions were highlighted. In addition, advances in bioengineering have led to the formulation of alternative fuels that are sustainable and promise substantial reductions in greenhouse gas emissions. Consequently, the ASTM has approved five production pathways for alternative jet fuel for use in civil and military aviation, which has widened the scope of the SFFP to synthetic fuels. Hence, this work presents a comprehensive review of jet fuels used in CI engines to give readers an overview of engine parameters that are affected by the difference in properties of aviation fuels and ULSD#2. Furthermore, the factors influencing emissions are discussed as synthetic fuels show promise in reducing both NO_x and soot emissions. Finally, suggestions are provided that highlight the methodologies to effectively use aviation fuels to enhance combustion.

Introduction

Before the invention of the gas turbine, a high-octane gasoline called AvGas fueled piston engine operated aircraft. However, the higher operating temperatures of supercharged piston engines and

issues with fuel injection at higher altitudes led to pre-ignition and unstable engine operation. Additionally, the included antiknock additive tetraethyl lead (TEL) was highly toxic, leading to severe lead poisoning. With the invention of the gas turbine in the 1940s, fuel combustion temperatures in the turbine section necessitated the use of a fuel with a higher flash point and thermal stability. Furthermore, to increase payload, the fuel was required to be a stable heat transfer medium to cool or lubricate engine components like pumps. Based on several decades of research highlighting the advantages of kerosene-based propellants, this formulation of jet fuel is extensively used in aircraft, ships, helicopters, and other vehicles that use gas turbines.

Conventional kerosene-based aviation fuel is mainly produced from crude oil by fractional distillation. Typically, these fuels are mixtures of approximately 60% of iso and n-paraffins, about 20% mono-, di-, and tri-cycloparaffins, and aromatics [39]. These fuels have the advantages of lower viscosity for enhanced atomization that improves performance and lowers emissions [40]. Furthermore, a higher heating value for a jet fuel significantly improves aircraft range, subsequently minimizing operational costs [41]. In addition, the lower flash point of jet fuel makes the fuel safe to handle and reduces the risk of fire. In addition to being stable at elevated temperatures, jet fuels have low freezing points that allow optimal fuel injection at higher altitudes where other viscous fuels would form waxes and clog fuel filters. Moreover, jet fuel's higher yield from crude oil can lower its cost below that of ULSD#2. For example, the current price of jet fuel by bulk supply is around $1.60/gal; whereas, the price for ULSD#2 is around $2.10/gal [42].

As a result, NATO forces during the height of the cold war in the 1980s identified the benefit of reduced operational costs with the use of aviation fuel in CI engines. Later in 1988, the U.S. DoD passed the SFFP where it was decided that all military equipment was to be fueled with JP-8 to eliminate the supply chain logistics of ULSD#2. As a result, aviation fuel found use in CI engines as well as gas turbines. In

addition, the use of JP-8 put an end to the waxing of diesel fuels in harsh winter climates of northern Europe. The other incentive behind utilizing a single battlefield fuel was the enhancement of operational readiness. Furthermore, preliminary analysis of using JP-8 and blends of ULSD#2/JP-8 in CI engines was found to increase engine performance and reduce emissions. Additionally, the U.S. DoD emphasized reducing dependence on foreign oil by exploring alternative aviation fuels for the military. Recently, the USAF has converted all its bases to operate on commercially available Jet-A fuel to minimize the use of JP-8 that would decrease operational costs for the U.S. DoD [29]. Since most crude oil refineries produce Jet-A, it was tangible that switching to a more widely used product would lower costs.

With the formulation of alternative jet fuels, the SFFP was extended to include newer synthetic fuels that were produced from non-petroleum sources like coal and organic waste. Specifically, aviation fuels derived from coal and natural gas used mature technologies, like the Fischer Tropsch synthesis and steam reforming, to produce coal-to-jet or gas-to-jet fuels. As an example, Sasol Ltd. highlighted a benefit of alternative jet fuel, where coal to jet fuel was produced to take advantage of abundant coal reserves in South Africa to reduce dependence on foreign crude oil imports. However, the U.S. DoD emphasized the importance of renewable fuels to reduce overall carbon emissions. As a result, biojet fuels are being derived from alcohols, plant waste, animal fats, sugars, and vegetable oils through several novel bioengineering processes. Hence, the ASTM developed the ASTM 7566 certification to specify the physical and chemical properties of new turbine fuels.

Originally designed to operate on diesel fuels, CI engines have been the backbone of the U.S. military since they have a higher thermal efficiency and torque than SI engines; hence, necessary for heavily armored military vehicles with a large range. However, using fuels other than ULSD#2 might negatively affect power output, emissions, and reliability due to differences in fuel properties. As a result, this study aims to consolidate research performed on CI engines operated on ASTM approved fuels for the

SFFP. Relevant research is chronologically discussed to highlight the formulation of different fuels and the effects of fuel properties and engine operating conditions on the overall performance and emissions. Predominantly, the effects of low density, viscosity, and variable CN are elaborated in detail. With the inclusion of high-pressure fuel injection systems, exhaust gas recirculation (EGR), forced-induction, multiple injection, and sophisticated computers in engines, modern CI engines operating on alternative fuels are more complicated to analyze than older mechanically injected engines. Thus, the combined result of implementation of SFPP, conversion of USAF bases to operate on Jet-A, and the emphasis on zero emissions has led to the need for continued research on CI engines operating using different aviation fuels.

Conventional Jet Fuel (Jet-A/Jet-A1/JP-8/JP-5)

The invention of the gas turbine in the 1940s created the need for a new fuel with properties suiting high altitude flight. As a result, traditional AvGas was replaced with a mixture of kerosene and gasoline (wide-cut JP-1) with good low temperature stability. However, in subsequent years, the USAF required fuels that burned with less smoke and had higher flash points for fire safety. As a result, the composition of jet fuel evolved in stages from JP-1 to JP-8, with improved stability and handling characteristics. For example, Jet-A was developed as a commercial, high quality jet fuel for civilian applications. Next, JP-5 with a high flash point was developed specifically for the naval aircraft and helicopters deployed on aircraft carriers. Furthermore, JP-8 (MIL-DTL-83133), a kerosene fraction developed from Jet-A that had a higher flash point than JP-4, was formulated by including additives like a static dissipater, corrosion inhibitor, lubricity improver, fuel system icing inhibitor, antioxidants, and metal deactivators for additional stability in extreme climates [43]. However, the production pathways and chemical composition of JP-8 fuel is highly classified information that is not available in public domain.

Jet-A or JP-8, derived from either crude oil or shale oil, is a complex mixture of hydrocarbons and additives engineered for aviation turbines. These hydrocarbons include aromatics, n-paraffins, iso paraffins, and cycloparaffins in varying proportions. Mostly, fractional distillation is used to separate the different hydrocarbons from impurities in crude oil before selectively blending products for specific properties. The typical boiling range is 150 to 270^{o}C, which falls between gasoline and diesel fuel. Moreover, these fuels have stringent limitations regarding the freeze point, end point and viscosity limit; hence, jet fuels have carbon numbers ranging from C_8 to C_{17} [44]. In general, typical jet fuels are found to contain 20% n-paraffins, 40% isoparaffins, 20% cycloparaffins, and 20% aromatics [45].

The need to test these aviation fuels in CI engines stemmed from a 1988 directive [46] where the U.S. military was instructed to follow the SFFP to minimize logistical costs by operating all CI engine powered vehicles and generators on JP-8. However, with the recent conversion of all military installations from JP-8 to Jet-A [28], the SFFP has assumed importance with both JP-8 and Jet-A. Numerous researchers have investigated the performance of jet fuels in CI engines along with their effects on fuel injection systems. However, since the specification of jet fuel varies with batches, production pathways, and feedstocks, this has led to a wide variation in properties. Subsequently, this makes it difficult to establish a trend or predict performance of CI engines operating on these aviation grade fuels. For example, the ASTM D1655 specification for JP-8/Jet-A does not specify the CN, which is an important fuel property to optimize CI engine performance and reduce emissions. Therefore, to provide an overview of previous research efforts of aviation fuels for the SFFP, the following section summarizes research on JP-5, JP-8, and Jet-A in CI engines.

Literature Review of JP-8 Fuel

As early as 1965, Wise et al. [47] presented a report highlighting the logistical problems faced by the U.S. Navy outside the continental U.S.. As a result, the Navy Civil Engineering laboratory was directed to

conduct several tests using JP-5 as a fuel in construction equipment and other auxiliary power units as a replacement for ULSD#2. For this test, the power plants included two Continental Motors 5D402 engines with Roosa Master injection pumps and CAV injectors, two Detroit Diesel 3-71 engines with GMC unit injectors, two International UD-ISA engines with IHC injection equipment, and two Cummins Model 3T-6 engines with a Cummins PT injection system. Overall, a 500-hour engine endurance test revealed no damage to engine components with the use of JP-5. It was in this publication that the authors highlighted the absence of a CN rating that could increase the chance of obtaining low CN fuel and cause engine starting and operation difficulties in combat. In addition, the reduced viscosity of jet fuels could affect the injection system and shorten the length between overhauls and service intervals.

In the same year, Wise et al. [48] conducted a series of tests in heavy equipment fueled with JP-5. A few engines reported a slight power loss due to internal leakages in the injection systems associated with the low viscosity of JP-5. However, the performance of the engine was not impacted sufficiently to modify the fuel injection settings to compensate for this loss in power.

In November 1965, Watson [49] undertook an engine test conducted at the Navy Civil Engineering laboratory to determine the possible shortcomings of using jet fuels in a large bore low speed CI engine. These tests aimed to address factors like fuel water content, injection nozzle parameters, injection timing, wear, and lubricity. Again, no performance degradation was observed over the entire 500-hour duration of the test. However, it was recommended that changes be made to the injection nozzles, injection pressures, and injection timing to maintain optimal fuel spray penetration for low viscosity jet fuels.

A few years later, Lestz [50] conducted a performance evaluation of JP-5 in a GMC DD Engine and reported a 2.5 to 6.3% loss in power after switching from DF2 to JP-5. This reduction in power was a

consequence of the decreased heating value of JP-5. In addition, the higher volatility of this fuel improved atomization that reduced fuel consumption slightly, resulting in a lower BSFC at an operating speed near peak torque.

In 1974, Marvin [51] performed tests on seven Detroit Diesel Allison Division engines fueled with JP-4, JP-5, and DF2. They reported a reduced power output with the use of JP-5 fuel that correlates with the lower volumetric heat content of JP-5.

Moon [52] in 1979 carried out a performance and endurance test on a single-cylinder Cooperative Universal Engine at the Air Force Research Lab. The engine indicated a 3% increase in fuel consumption with JP-5 without any wear in the fuel injection system. Additionally, there was no significant loss in power output.

Towards the end of 1979, Lee [53] performed a 400-hour evaluation of an AVDS-1970-2C CI engine at Teledyne Continental Motors. The author inferred that the engine power reduced from 2.6 to 3.5% of values comparable to the tests with DF2. However, the study mentioned the issues with the variability or quality control of the CN of each batch of fuel. The author recommended additional research since CN standards were not mandatory for jet fuels; hence, a deviation in fuel properties could affect engine performance, particularly in critical combat environments.

Bowden et al. [54] studied the effects of shale derived JP-5 and JP-8 for stability, corrosion, and compatibility with diesel fuels in 1980. The shale JP-5 fuel indicated a 6% decrease in power of a Detroit Diesel compared to JP-5 derived from conventional petroleum. In contrast, the JP-8 based fuels from both petroleum and shale sources did not show any significant loss in performance.

In December 1981, Montemayor et al. [55] tested four engines using JP-5 to determine its overall performance in a comprehensive report. The engines selected were the Detroit Diesel (DD) 4-53T,

Continental Motors LDT-465-1C, Cummins NTC-350, and Caterpillar 3208T with the fuels consisting of JP-4, Jet-A, kerosene, heavy aromatic naphtha, and heavy oil and blends of the fuels. Their results indicated that only the low viscosity fuels resulted in internal injection pump leakages and a loss of power. Meanwhile, the low CN associated with the presence of a larger proportion of aromatic compounds in some of the fuels slightly impacted engine performance via a longer ignition delay. Elsewise, the other fuels did not affect engine performance when analyzing energy input, CN, viscosity, 10% boiling point, and aromatic content. Overall, the other minor variations in performance were attributed to the differences in injection systems of the engines.

In 1986, Montemayor et al. [56] at the Belvoir Fuels and Lubricants Research Facility at SwRI compared the Arctic 6.2L and Stanadyne fuel pumps for compatibility with a low viscosity JP-8 fuel. In all, six fuel pumps were analysed for wear: three Arctic 6.2L and three from a commercial utility cargo vehicle. The tests were performed on a GM 6.2L DI engine at 700 rpm/no-load, 1500 rpm/100 lb-ft load, and 1600 rpm/full-load for 200 hours. The Arctic pump was found to be superior to the standard fuel pump. However, the lower viscosity, reduced LHV, and decreased density of JP-8 caused a slight reduction in power. The authors suggested that pump component wear could lead to a reduction of fuel supply that might result in a loss of power caused by excessive wear.

A couple years later in 1988, Likos et al. [16] presented a laboratory evaluation of MIL-T-83133 JP-8 fuel in army CI engines that led to the directive issuing the SFFP. The engines selected for the tests were the two-stroke General Motors (GM) Detroit Diesel (DD) 6V-53T, the naturally aspirated DD 6V-53N, the Teledyne Continental Motors LDT-465-IC, a GM 6.2L HMMWV engine, and the Cummins NHC-250. The engines were tested over the Army/Coordinating Research Council (CRC) 240-hour cycle for tracked-vehicles, or the Army/CRC 210-hour cycle for wheeled-vehicles. The tests with JP-8 fuel indicated a decrease in power with engines that did not feature fuel density compensating devices. This drop in

efficiency was the result of lower fuel injection rates based on the reduced density and viscosity of JP-8. However, the LDT-465-IC engine was designed for multi-fuels and, as a result, showed an increase in power output at part load operation with this fuel. Next, all engines except the GM 6.5L showed an increase in thermal efficiencies due to the higher volatility of JP-8 and subsequent better atomization. Of note, inefficiencies in the GM 6.5L engine were repercussions from the poorly built Arctic fuel injection pump. Furthermore, JP-8 had a lower CN than ULSD#2 that increased the premix combustion phase additionally fostering a greater thermal efficiency due to a greater level of constant volume combustion. However, at higher loads and speeds, the timing effects of optimal combustion phasing reduced and thermal efficiency declined. Overall, the engines that were fuel-compensated saw the net effect of a thermal efficiency gain that offset the decreased volumetric heating value of JP-8; hence, resulting in an improved vehicle range over ULSD#2. In addition, an engine oil analysis and engine teardown indicated insignificant wear, sludge, and deposit formations.

The next year in 1989, Owens et al. [57] conducted vehicle acceleration and fuel consumption tests when converting from DF2 to JP-8 fuel. The vehicles included multiple infantry vehicles featuring eight different CI engines (GM 6.2 L, Cummins NHC-250, DD 6V-53N, Teledyne Continental AVDS-1790-2DR, Avco- Lycoming AGT-1500, Cummins VTA-903T, AVDS-1790-2C). Overall, JP-8 was found to decrease the acceleration and response of the vehicles. This was a result of the lower viscosity of JP-8 causing leakages past the clearances in the fuel pump and injector, subsequently reducing fuel delivery rates. Secondly, the lower volumetric energy density of JP-8 compared to ULSD#2 caused an additional power loss; hence, for the same operating conditions, JP-8 fueled vehicles had a higher BSFC.

In 1991, Lacey and Lestz [58] from the Belvoir Fuels and Lubricants Research Facility at SwRI performed a tear down on five Stanadyne mechanical fuel pumps from CI generators to estimate wear and lubricity issues with the use of Jet-A. The results did not indicate that Jet-A caused lubricity issues and

subsequent wear on the internal components of the pumps. On the contrary, the authors found that dirty fuel, excessive hydraulic loading, misalignment between components, plugging of discharge lines, and corrosion were the main causes of pump failures.

In the same year, Lacey [59] studied Stanadyne rotary fuel injection pumps obtained from combat vehicles in Operation Desert Shield in addition to three commercially sourced fuel pumps. The wear-prone components from each pump were dismantled and analysed. It was found that the increase in wear of certain components contributed to the premature failure of fuel pumps; however, it was impossible to ascertain that JP-8 was the main cause of failure.

The following year in 1992, Lacey and Lestz [60] presented a study on low-lubricity fuels in CI injection pumps after several reports of fuel-lubricated Stanadyne rotary pump failures during Operation Desert Shield. In all, the authors performed teardowns of 12 pumps sourced from combat vehicles and three pumps from civilian vehicles. The analysis indicated that low lubricity fuels increased the wear on certain components of pumps but were not the major cause for failure. In specific, wear increased as the low-viscosity fuel had a weaker hydrodynamic lubricating film on certain moving components. However, most failures occurred due to corrosion, particulate contamination, poorly seated valves and pistons, and failure of seals, springs, and elastomeric parts. Nevertheless, it was suggested that improvements in design and metallurgy and addition of lubricity additives would significantly improve the life of the pump.

In a continuation of their previous work in 1992, Lacey and Lestz [61] described the durability of Stanadyne rotary fuel injection pumps running low-lubricity aviation fuels. They tested five Arctic pumps and four standard Stanadyne pumps with commercially available Jet-A1. The test rig consisted of a mounting arrangement like a GM 6.2L engine and the pumps were run at full capacity for a period of

200 hours. One of the standard Stanadyne pumps indicated a 38.5% reduction in engine power delivery; whereas, the other pumps showed a 1% to 13% reduction in engine power. This was the result of the low viscosity fuel causing leakages in the pumping mechanism. Furthermore, it was established that a wear scar diameter of less than 0.6 mm on the standard Ball on Cylinder Lubricity Evaluator (BOCLE) wear test would produce mild wear while a wear scar of 0.7 mm would lead to pump failure. In addition, it was found that the Arctic version of the Stanadyne pumps showed lesser wear than the standard pumps. This was result of the improved surface hardening metallurgy of components used in the Arctic pumps. In conclusion, the authors suggest that improvements in fuel formulation and additives and metallurgy would make fuel pumps compatible with most aviation fuels.

In the same year, Butler Jr. et al. [17] compiled a report highlighting field demonstrations of JP-8 fuel in military CI engines. In all, 2807 vehicles and other ground support systems were surveyed for the demonstration program. Summarizing data for fuel consumption, no vehicle showed a decrease in mileage after switching from ULSD#2 to JP-8. Meanwhile, minor power losses were reported in some vehicles that were proportionate to the differences in the heating values of JP-8 and ULSD#2. Further, fuel injection systems, fuel check valves, and fuel filters functioned as intended, without any catastrophic failures. However, a few vehicles with rotary fuel pumps experienced lubricity induced wear after prolonged use of JP-8. Nonetheless, the clean burning nature of JP-8 fuel prevented the formation of a smoke screen, an essential tactic required to hide the movement or location of military vehicles. Overall, the tests covered 1,689,071 miles for combat vehicles and 811,818 miles for transportation vehicles.

In 1996, Yost et al. [62] from the SwRI conducted a U.S. Army investigation of exhaust emissions using JP-8 fuels with varying sulfur content of 0.06, 0.11, and 0.26% by weight respectively. The test cells included a DD Series 60 (DI) engine and an Army GM 6.2L (IDI) engine utilizing the transient hot-start

section of the heavy-duty CI engine Federal Test Procedure (FTP). In addition, the fuel injection settings were compensated for the lower viscosity and reduced volumetric energy content of JP-8 to enable peak power output. For the DD engine, HC emissions were higher than the reference EPA fuel. Next, the CO emissions for the same engine on JP-8 were lower than the EPA standard for diesel, as leaner combustion was thought to occur with this low viscosity fuel. Furthermore, an increase in sulfur content grew PM emissions while a higher CN lowered PM emissions. Hence, the lower sulphur fuels (0.06% and 0.11%) had reduced PM emissions than the EPA standard; whereas, the 0.26% sulfur JP-8 sample had higher PM. Meanwhile, the GM 6.2L engine did not show significant variation in emissions with all three samples of fuel. Overall, the emissions data indicated that the DD engine had an equivalent sulfur level of 0.21% while the GM 6.2L engine had an equivalent sulfur level of 0.3% as compared to the 0.035% EPA certification for diesel fuel.

In 1997, Kouremenos et al. [63] investigated the performance and emissions on an experimental Ricardo R6 IDI engine fueled by JP-8 and DF2. The combustion chamber was designed for swirl formation via a turbulence-augmenting combustion piston head. In addition, the compression ratio was fixed at 20 and injection was achieved with a mechanical plunger type injector. Next, the experiments were conducted at 50%, 66%, 83%, and 100% of full load at 1000, 1500, and 2000 rpm for a total of 12 runs for each fuel. The static injection timing was 38^{o} CA BTDC for both fuel tests and an extra test was specifically conducted with static injection at 33^{o} CA BTDC to check the effects of unstable combustion with JP-8 fuel. From the analysis, in-cylinder pressure was higher for JP-8 at all test conditions as the ignition delay increased the premix burn. Additionally, JP-8 caused large cycle-to-cycle pressure oscillations accompanied by noisier operation in all test conditions as the change in viscosity and density affected the fuel injection process. Furthermore, the dynamic fuel injection system timing was faster for JP-8 as the aviation fuel had lower viscosity and density than DF2. Further for tests at 38^{o} BTDC, JP-8 showed a

lower exhaust gas temperature as the intense rate of burning resulted in a faster expansion of gases and subsequent heat transfer to the cylinder walls. When the injection was retarded to 33^{o} BTDC, the exhaust gas temperatures were similar for both DF2 and JP-8. For fuel consumption of JP-8, BSFC values were higher at lower loads as the greater level of premix burn during the compression stroke reduced available work. Also, the BSFC of JP-8 was lower at higher loads as the increased ignition delay pushed combustion into the expansion stroke, increasing fuel consumption. This increase in BSFC for JP-8 could be eliminated by advancing the injection timing. For emissions, NO_x levels were identical for both JP-8 and DF2 at all tests with the 38^{o} BTDC injection. When injection was delayed to 33^{o} BTDC, the lower in-cylinder temperatures significantly reduced the formation of NO_x for JP-8. Next, HC and CO emissions were negligible for both fuels at both 38^{o} and 33^{o} injection timing as IDI engines create more homogenous mixtures before the start of ignition. Meanwhile, the higher ignition delay of JP-8 caused an increase in PM emissions for the 38^{o} case compared to DF2. When the injection timing was retarded to 33^{o} BTDC, there was no change in PM emissions. Based on the observations, the authors conclude that delaying static injection to its optimal value could improve the overall combustion characteristics of JP-8.

In the year 2000, Stoecklein et al. [64] evaluated CI military vehicles with a JP-8 fuel containing a thermal stability additive called +100. The additive was a dispersant with detergent that prevented hot surface fuel deposition problems in gas turbines. However, in ground vehicles, the additive permanently disabled water separators in fueling systems allowing water to enter the fuel tanks. Furthermore, the additive removed scale and dirt from fuel lines that could plug filters. To identify its effect in a CI engine, a test was performed using a CS200 HMMWV engine. The results from this analysis indicated that JP-8 and JP-8+100 act like solvents and cause a temporary rise in fuel particles when the fuel system previously utilized diesel fuel. This condition is a function of the fuel quality and the original fuel system

before switching to JP-8+100. Moreover, a particle test indicated a large increase in contaminants with sizes ranging from 2 µm to 15 µm. As a result, the authors recommended further investigation regarding particle concentration levels that might affect the durability of the engine and fuel injection system.

In 2001, Kotsiopoulos et al. [65] evaluated the use of JP-8 in a Petter AV1 laboratory IDI CI engine fitted with a mechanical fuel injection system while operating with a compression ratio of 19. Tests were conducted at 25%, 50%, 75%, and full load conditions. From the results, it was observed that JP-8 had a higher in-cylinder pressure than diesel due to a delayed combustion caused by low-viscosity induced irregular fuel delivery. When changing loads, the pre-chamber pressure was found to be unstable as the low viscosity of JP-8 causes poor injection performance. Next, its reduced LHV caused a higher BSFC. Additionally, the differences in CN, density, and viscosity of diesel and JP-8 were the main causes of irregular combustion. Discussing emissions, NO_x levels were only slightly higher in the case of JP-8 as its lower viscosity enabled better atomization. Next, THC emissions were low in all cases, a common observation for IDI engines as the fuel has more time to burn in the main chamber. In addition, CO emissions were similar for both engines, following THC emission trends. Furthermore, PM was reduced across all loads for JP-8 as its lower viscosity allowed better premixing and enhanced homogenization of air and fuel. The authors conclude that shortcomings of using JP-8 can be overcome by optimizing the injection timing.

In 2003, Arkoudeas et al. [66] studied the emissions of a stationary Petter AV1 CI engine fueled with JP-8 and two types of biodiesel with blends at 10%, 20%, and 50% by volume with JP-8. The biodiesels were derived from methyl esters produced from sunflower oil and olive oil. For the sunflower oil derived biodiesel, with test blends lower than 10% of biodiesel, NO_x emissions were reduced. For blends between 10% and 20% biodiesel, the NO_x emissions increased except at low loads. At 50% blends of biodiesel, NO_x emissions increased. For the olive oil derived fuel at blend percentages less than 20%

biodiesel, there was a decrease in NO_x emissions for lower loads; whereas, at higher loads NO_x emissions increased. This growth in NO_x emissions at higher loads was attributed to the increased oxidation rate of nitrogen due to the additional oxygen content in biodiesel. Meanwhile, PM emissions were reduced at all engine loads because of this extra oxygen while additionally factoring in the absence of aromatics and sulfurous compounds in this fuel. However, fuel consumption increased for the same power produced as blend percentage grew since the LHV of biodiesel was lesser than JP-8.

In 2004, Rakopoulos et al. [67] provided a comparison of the emissions of JP-8 with those of DF2, based on experiments with DI and IDI single-cylinder CI engines. The DI engine was a naturally aspirated, four-stroke, air-cooled, Lister LV1 engine with a Bryce high-pressure fuel pump. The IDI engine was a naturally aspirated, water-cooled Ricardo R6 engine fitted with a CAV fuel injection pump. The engines were tested at loads of 20%, 40%, 60%, and 80% of full load, and three speeds (1500, 2000, and 2500 rpm). For the DI engine, since JP-8 has a lower CN, ignition delay grew while its lower viscosity and density caused a reduced pressure in the fuel system. As a result, JP-8 lowered NO_x and CO emissions but increased HC emissions. Furthermore, PM emissions rose with load, as local and global equivalence ratios increased. Meanwhile for the IDI engine, no significant changes in engine performance were observed with JP-8. However, NO_x emissions were reduced as NO formation was limited to the pre-combustion chamber and the injection of fuel at higher loads resulted in a rich mixture; hence, reducing NO_x. Beyond the stated outcomes, the overall performance of the engines running on JP-8 indicated no significant changes in comparison to ULSD#2.

In the same year, Korres et al. [68] tested emissions of JP-8 along with DF2 and biodiesel in a single cylinder Petter AV1 laboratory CI engine. Across all loads, DF2 blends with the low CN JP-8 decreased NO_x emissions due to a reduced in-cylinder temperature. Meanwhile, the use of biodiesel increased NO_x emissions because of its higher oxygen content. For the same reasons, PM emissions were reduced with

the addition of biodiesel; whereas, the slightly higher content of aromatics and sulphur increased PM when JP-8 was tested with blends of ULSD#2. Finally, addition of JP-8 and biodiesel to ULSD#2 increased fuel consumption due to a reduced density and LHV, respectively.

At the end of 2004, Frame and Blanks [69] investigated the exhaust emissions of a 6.5 L HMMWV engine operating on JP-8 fuel. The engine was operated on SDF2 for 100 hours followed by an 11-mode steady state testing event and a San Antonio Transient (SAT) cycle. The engine tests indicated a 7.3% drop in power with the JP-8 fuel, caused by a reduction in fuel volumetric energy density. With respect to emissions, JP-8 produced 11% less NO_x and 28% less PM than ULSD#2 as cylinder temperatures were lower and combustion duration was shortened.

In 2005, Fernandes et al. [70] conducted a thorough investigation regarding the use of JP-8 in a military engine. The engine was a 12.7 L, six cylinder, variable vane turbocharged, and electronically injected CI engine. They operated the engine at 1200 rpm with 20% load, 1200 rpm with 50% load, and 1500 rpm with 75% load. For the initial baseline tests at low load, a lower density and amplified leakages associated with the reduced viscosity of JP-8 decreased the fueling rate that led to a loss in torque. However, when the injection duration was increased to match the mass flow rate of diesel, JP-8 performance bettered that of diesel by increasing torque along with lowering BSFC. Here, the IMEP for JP-8 was higher than diesel in the case of fueling adjustment as the JP-8 tested had a higher LHV. However, an increase in injector and mechanical losses amplified the fueling rate and lowered BSFC at higher loads. For this experiment, similar trends were observed for the medium and high load cases as in the low load scenario. Moreover, a change in injection pressure occurred due to the low viscosity and higher compressibility of JP-8. Furthermore, a heat release analysis indicated a larger premix burn for JP-8 due to the growth in ignition delay caused by a lower CN. Based on this study, the injection timing could be optimized by considering ignition advance, premix burn, diffusion burn, and combustion

duration. Meanwhile, BSFC and torque remained unaffected by injection timing advance. However, this advance in injection had a negative effect on the optimized combustion phasing because of a high premix burn phase for JP-8. After adjusting the injection duration of JP-8 to that of diesel in comparison to the baseline diesel tests, NO_x emissions dropped. In addition, the higher volatility and lower sulphur content of JP-8 reduced PM emissions as compared to the baseline diesel. In combination, the absence of aromatic hydrocarbons in JP-8 resulted in lower NO_x emissions than diesel as flame temperatures were considerably lower. For unknown reasons, the effects of cooled EGR did not have drastic effects on emissions across all loads. As a result, JP-8 was deemed as a viable substitute for DF2 for the SFFP.

A year later, Papagianniakis et al. [71] analyzed the use of DF2 and JP-8 in DI and IDI engines for performance and emissions. The DI engine was a single-cylinder air cooled, direct injection, high speed Lister LV-1 series, experimental engine while the IDI CI engine was a single cylinder, water-cooled, Ricardo E-6 experimental engine. The tests with the DI engine were conducted at loads of 20%, 40%, 60%, and 80% of full load and speeds of 1500, 2000, and 2500 rpm while the tests with the IDI engine were taken at 50%, 66%, 83%, and 100% of full load at 1000, 1500, and 2000 rpm. Upon examination of the test results for the DI engine, the lower CN of JP-8 resulted in a greater pressure rise with a lower ignition delay at low load and high-speed conditions. However, the effects of lower CN were diminished at higher load as ignition delay reduced with a higher cylinder temperature. In addition, the BSFC for JP-8 grew at high loads since it has a lower volumetric energy density. Moreover, NO levels were reduced considerably while HC and CO emissions were less during the tests under high load and high speed. Furthermore, PM emissions increased at part load for all engine speeds. In comparison, the pre-chamber for the IDI engine allowed for a more homogenized air fuel mixture and, hence, there was a slight increase in-cylinder pressure. As with an IDI engine, ignition delay periods were longer as combustion is first initiated in the pre-chamber. Next, NO levels were comparable to the DI engine while CO and HC

emissions grew at greater engine speeds as less time is available for the species to oxidize completely. Furthermore, soot formation was comparable with the DI engine. Based on the tests, the authors recommended adjustments in fuel injection for both engines to optimize performance and emissions for JP-8.

Also in 2006, Schihl et al. [72] studied the evaporation of JP-8 in DI engines to predict heat release to understand better how CN variations affected engine performance. A poorly performing engine was selected based on a set of tests performed by Miklos. Here, JP-8 was studied in detail to obtain multi-component surrogates of the fuels. After analyzing various fuel properties using the evaporation coefficient method (MEC), the final JP-8 surrogate composition was selected to be 18% tetradecane and 82% dodecane. Moreover, a 12-cylinder CI engine was selected for the study. The engine had a combustion chamber with an offset bowl and pent head that could burn both diesel and JP-8. In addition, an engine cycle simulation was used to provide thermodynamic data that were missing from tests conducted with the 12-cylinder engine. The model predicted a lower evaporation rate for JP-8 as compared to ULSD#2. Next, the vapor fraction of JP-8 was 15-30% higher than ULSD#2 that resulted in a higher heat release rate and pressure rise. Furthermore, a first law analysis investigating the spray tip penetration of the jet indicated an increase in evaporation rate with respect to a decreasing CN. As a result, this longer spray penetration led to a larger premix fuel vapor fraction with better air-fuel mixing. This method helped to correlate pressure rise with injection, fuel evaporation, and ignition for low viscosity fuels like JP-8.

In 2007, Kalligeros et al. [73] performed a fuel consumption and emission analysis on a stationary single cylinder CI engine with a mechanical fuel injection system. The test fuels were JP-8 and mixtures of JP-8 and FAME biodiesels derived from sunflower seeds and olive oil. For blends with olive and sunflower FAME, the 10 and 20% blends reduced NO and NO_x emissions for all load cases as compared to

emissions from JP-8. For 50% blends of FAME biodiesels and JP-8, the higher oxygen content in the fuel grew the level of NO_x emissions. Meanwhile, PM emissions were reduced in all cases as combustion efficiency increased with the additional oxygen content in the biodiesel and its respectively lower sulphur content. Finally, blends of FAME biodiesels and JP-8 had higher fuel consumption due to a reduced heating value for biodiesel.

Again in 2007, Kotsiopoulos et al. [74] compared the performance and emissions of JP-8, biodiesel, and diesel in a DI engine with a fuel injector that was mechanically actuated. The tests were conducted for 16 cases with loads ranging from 12%, 37%, 60%, and 80% of full load at 1200, 1600, 1800, and 2000 rpm. When comparing baseline diesel fuel with JP-8, it was found that maximum combustion pressure occurred in the case of diesel as the lower CN number of JP-8 increased the ignition delay; hence, combustion occurred later as the piston expanded. For low loads, the BSFC of JP-8 was higher than diesel due to JP-8's reduced heating value in addition to its longer ignition delay. With respect to emissions, this augmented ignition delay reduced the temperature within the combustion chamber subsequently decreasing NO_x formation. Next, at low engine speeds and low loads, a greater level of PM emissions were seen for JP-8 as ignition delay decreased as load increased. At higher loads, NO_x and PM emissions of both fuels were nearly the same. However, at higher engine speeds, JP-8 had greater PM emissions due to a later combustion phase caused by its lower viscosity. Based on the results, the authors suggested delaying the static injection timing of JP-8 to reduce the problems arising from its substitution in CI engines.

In 2008, Mosberger et al. [75] analyzed the effects of high sulfur military JP-8 fuel on heavy duty CI engine EGR cooler condensate. The engine was a DD 60 containing a variable geometry turbocharger and an EGR cooler. The exhaust gas from the EGR cooler could pass through a controlled condensation apparatus to measure SO_3, SO_2, and H_2SO_4 concentrations. Next, the engine was tested at 1200 and

1800 rpm, at 20% and 50% loads with 10% and 30% EGR concentrations. For simulating a high sulfur level, the fuel was doped with an additive called di-tert-butyldisulfide ($(CH_3)_3CSSC(CH_3)_3$). Firstly, the operating test at normal coolant temperatures did not indicate a presence of H_2SO_4. Here, this was explained due to the limited time available for the oxidation of SO_2 and SO_3 to H_2SO_4. Furthermore, an SO_2 concentration increase showed a strong correlation with the growth in fuel sulfur content. Hence, sulfur emissions increased mainly with engine load, as fuel flow rate grew. Lastly, the PM in the exhaust rose with the presence of sulfates in the soot particles that additionally lowers the growth of SO_2 emissions. Consequently, the presence of sulfates were the main cause of EGR condenser corrosion and fouling in combination with the formation and absorption of H_2SO_4 during cold start events and during engine shut down occurrences.

In the same year, Korres et al. [76] studied the use of naval aviation turbine fuel JP-5 as a suitable replacement for JP-8. The fuels for this analysis were JP-5, diesel, and biodiesel derived from animal fat. The fuels were tested in their neat form, as well as in different blends in a single cylinder, mechanically injected CI engine. Subsequently, fuel consumption and emissions were analyzed under various loads with ordinary diesel as the reference fuel. Their findings indicated that NO_x emissions rose in the case of biodiesel blends as the additional oxygen molecule in biodiesel enhanced the oxidation of nitrogen in the intake air. However, blends of JP-5 up to 40% showed a reduction in NO_x levels in comparison to the reference ULSD#2 due to lower in-cylinder temperatures. In contrast, NO_x emissions increased when JP-5 was added in ratios exceeding 60% by volume. Furthermore, PM emissions were reduced using blends of JP-5 and biodiesel because its lower density and viscosity enabled better atomization. At higher loads, a marginal reduction in fuel consumption was observed for blends exceeding 60% of JP-5 due to an increase in ignition delay with a decrease in CN. Overall, the superior CN of biodiesel and the extra oxygen content improved the combustion process of both ULSD#2 and JP-5 for the SFFP.

In 2010, Pandey et al. [77] conducted performance, emissions, and pump wear analyses of JP-8 fuel for military use. They employed a CI engine that was a supercharged, 12-cylinder, DI unit rated at 585 kW. Engine tests started at 1000 rpm and then increased in increments of 100 rpm to 2000 rpm at full load. Results from this test indicated the effects of a lower CN on the RHR with JP-8 having a greater ignition delay than ULSD#2. Furthermore, the lower density and volumetric energy of JP-8 led to a subsequent loss in power. For the same reason, BSFC increased with the use of JP-8, in spite of its slightly greater heating value. Concerning emissions, the higher volatility and lower viscosity of JP-8 led to better atomization and improved combustion that reduced both CO and HC emissions. Now, while NO_x emissions usually increase for fuels with a low CN, the absence of aromatic fractions of hydrocarbons can exert a more pronounced effect on NO_x. As a result, NO_x emissions decreased by more than 40% for JP-8. For the same reason of a lower level of aromatic hydrocarbons, PM emissions decreased by 26% as compared to ULSD#2. Finally, a 100-hour test on the pump components indicated a greater rate of wear with JP-8 since its reduced viscosity generates less lubrication than ULSD#2.

In the same year, Nargunde et al. [78] investigated the effects of using JP-8 and ULSD#2 in a CI engine. The engine was a single-cylinder, high speed engine, equipped with a solenoid operated Bosch high pressure fuel pump and a swirl control mechanism. The engine was tested at 1500 rpm with injection pressures of 600, 1000, and 1200 bar that normalized combustion to achieve 5 bar IMEP. From the data presented, the delay between injection timing and start of injection was different for both fuels as the density, viscosity, and bulk modulus of the fuel affected the opening of the injector. Here, a larger duration of injection occurred for JP-8 with its properties affecting both fuel and energy flow rates. Next, the enhanced evaporation of JP-8 resulted in a 3.72% greater apparent rate of heat release (AHRR) than ULSD#2. For the same reason of a better evaporation process, JP-8 had a lower ignition delay than ULSD#2 as there was a negligible difference in CN of both fuels. Since the ignition delay for ULSD#2 was

higher than JP-8, the maximum cylinder pressure was greater for ULSD#2. Consequently, cylinder temperatures are larger for ULSD#2 as this longer ignition delay allowed more fuel to be injected before ignition began. Moreover, the enhanced evaporation of JP-8 resulted in lower exhaust temperatures that pointed to greater combustion efficiency and a lower ISFC. From the emissions analysis, a lower peak pressure and reduced aromatic content of JP-8 resulted in decreased NO_x levels. Furthermore, the higher volatility of JP-8 increased homogeneity that resulted in more complete combustion and less CO and HC emissions. Finally, the lower aromatic content of JP-8 resulted in fewer PM emissions than ULSD#2 given the same injection pressure. However, the formation of nucleation mode particles (NMP) for JP-8 was higher than ULSD#2, as the amount of aggregation mode particles (AMP) were lowered, resulting in a lesser amount of NMPs being absorbed on AMPs.

Also in 2010, Smith et al. [79] investigated the effects of high sulfur JP-8 on engine emissions and EGR cooler condensate to improve on an earlier research effort in 2008. The engine setup and condensate collection device (CCD) were the same as described in the authors' previous research work [75] explained earlier. However, the problem of erroneous H_2SO_4 measurements in the CCD was eliminated by decoupling condensers and adding a collector after each condenser to capture condensate. In addition, a second impinge was added to increase the collection efficiency of condensate. Furthermore, the tests were performed at 1200 rpm and 3 BMEP with 10 and 50% EGR. For the analysis, an MKS Fourier Transform Infrared (FTIR) was used to measure levels of H_2SO_4 and SO_2 in case the CCD method was not accurate. Additionally, JP-8 was doped with tert-butyl disulfide ($(CH_3)_3CSSC(CH_3)_3$) to 2870 ppm and 3512 ppm of sulfur. Meanwhile, an analytical chemical equilibrium method was derived to predict the gaseous sulfur emissions. Results from the tests indicated a constant level of H_2SO_4 in the exhaust stream across the different tests and an increase in SO_2 emissions with the growth in fuel sulfur content. Interestingly, the low sulfur fuel indicated a higher experimental level of SO_2 than the predicted

concentration, while it was exactly opposite in the case of the high sulfur fuel. In an extension to the analysis, the test matrix for the FTIR was kept at 1200 rpm with a load of 3 to 7 BMEP at 0 and 15% EGR. The FTIR method indicated higher levels of SO_2 and experimental values were only marginally higher than predicted values. However, experimental SO_2 levels were greater than predicted values at low sulfur levels but lower than the predicted values at tests with the high sulfur fuel. The differences in values for the CCD and FTIR were mainly caused by sulfur content in lubricating oil and the presence of sulfates. A particulate size distribution analysis was used to test whether sulfates contribute to particle mass. The analysis revealed the formation of larger particles due to accumulation when using high sulfur fuel that leads to the increase in mass of PM. To conclude, the authors' indicated that the CCD and FTIR results are agreeable; hence, SO_2 levels grow with an increase in sulfur content with and without EGR. Furthermore, the authors conclude that the emission levels of H_2SO_4 from 2-5 ppm do not change significantly when varying sulfur content in JP-8, EGR levels of the engine, and condenser temperatures in the CCD.

In 2010, Wadumesthrige et al. [80] studied the performance of a generator unit powered by a turbocharged, five-cylinder, four-stroke, DI CI engine fitted with a mechanical fuel injection system. The fuels tested were ULSD#2, S-8, JP-8, and B20 with an emphasis on properties like CN, lubricity, flash points, heat releases, and cold flow characteristics. The tests were performed for 240 hours under a stationary load at 60% of full load with no changes to engine calibration while testing. From the results, S-8 was found to have the lowest fuel consumption and highest thermal efficiency. This was attributed to S-8 having respectively excellent atomization and a higher CN. The BSFC was found to increase in the following order: B20, ULSD, JP-8, and S-8, respectively, based on the lower heating value. However, with their lowered viscosity, JP-8 and S-8 had higher fuel leakages past the injector and fuel pump. Furthermore, ULSD and B20 had a greater bulk modulus that could result in a sharper pressure spike,

subsequently requiring an advance in fuel injection timing. The BTE of S-8 was the highest due to its high CN, LHV, low viscosity, and increased level of atomization. Here, a decreasing trend of BTE over time was witnessed for S-8 that was caused by leaking of fuel due to the improper sealing of fuel lines. Additionally, S-8 and JP-8 showed higher EGTs due to their lower viscosities resulting in a delay in the start of injection; hence, more combustion took place closer to the exhaust valve opening. For generator operation, S-8 showed low smoke opacity measurements because of its absence of aromatics and sulphur. In addition, the lower boiling point of S-8, as compared to the base fuel ULSD, facilitated an enhanced level of evaporation at lower temperatures. Despite the perceived combustion advantages of S-8 as a generator fuel, the tests revealed that JP-8 and S-8 resulted in unstable performance in terms of power and frequency as engine calibration was optimized for ULSD.

The following year, Lee and Bae [81] used an optical engine to study the application of JP-8 in a CI engine. A four-stroke, single-cylinder, naturally-aspirated, direct injection CI engine with a high-pressure electronic fuel injection system was used to perform experiments at 30 and 140 MPa, for low and high load conditions, respectively. Furthermore, the injection quantity was 60 mg/stroke for diesel fuel, and 58.8 mg/stroke for JP-8. On analysis of the macroscopic spray, an asymmetric spray pattern was observed for the JP-8 fuel as the internal flow structure in the nozzle cavities were affected by changes in fuel properties. In addition, the strong turbulence intensity of JP-8 caused an asymmetry of the boundary layer in the internal nozzle where some holes had separated boundary layer flows while the others showed a reattachment of the separated boundary layer along their walls. As a result, the fuel indicated a cone-type spray and a partially hydraulic flip spray. Next, the lower viscosity and higher volatility of JP-8 resulted in a shorter fuel jet penetration and wider spray angle than ULSD#2. Additionally, the surface tension between the spray boundary and air was reduced due to JP-8's decrease in density and viscosity. This led to an instable shear layer between the gas and liquid phases.

Furthermore, the presence of lower proportion of aromatics decreased the overall latent heat of evaporation to enhance evaporation and mixing. Moving on to the HRR analysis, the lower CN of JP-8 resulted in a longer ignition delay, cancelling out the advantages of enhanced evaporation and atomization. For the same reason, the peak RHR was higher than ULSD#2 for both injection pressures, resulting in a greater level of premix burn and augmented heat transfer to the cylinder wall. As a result, NO_x emissions were higher than ULSD#2. Furthermore, since JP-8 had shorter burn duration with a higher level of premixed combustion, the combustion efficiency of JP-8 was lower than ULSD#2 resulting in more HC emissions. Besides, the rapid heat transfer to the cylinder walls led to heightened quenching that additionally increased HC emissions. Finally, the lower aromatic content of JP-8 along with its enhanced air-fuel mixing resulted in reduction of PM formation as compared to ULSD#2.

In 2011, Brandt et al. [82] conducted tests to determine the use of JP-8 in commercial engines fitted with high pressure common rail fuel injections systems for the U.S. military. The engine selected for the study was a Ford 6.7L V8 turbocharged CI engine subjected to a 210-hour TWVC cycle. After the tests, examination of the fuel injection pumps and injectors did not indicate wear with JP-8. Here, the power output dropped by a maximum of 5% below baseline ULSD#2 performance due to a decrease in viscosity and heating value for JP-8. For the same reason of a lower viscosity, the volumetric fuel flow for JP-8 increased by about 4.5%. In addition, pre- and post-engine tests indicated 2.8% and 3% power loss at ambient and high temperature operating conditions, respectively. With respect to emissions, the enhanced mixing of JP-8 resulted in lower HC and CO levels as compared to ULSD#2. Moreover, the researchers anticipated high NO_x levels due to a longer ignition delay; hence, a pilot injection was used to lower in-cylinder temperatures. Overall, all tests were operated without any fuel related failures.

Again in 2011, Henein et al. [83] performed experiments to determine the autoignition characteristics of low CN JP-8 fuels (CN = 44.1 and 31) and SPK (CN > 74) in a military CI engine. In addition, the authors

discuss the impact of CN on LT and NTC combustion regimes with the help of a simulation tool. The engine was a 4.5L, Partnership for New Generation of Vehicles (PNGV), direct injection, four-valve, water-cooled, high speed CI engine equipped with a common rail injection system. Turbocharging was simulated by externally supplying hot compressed air. Initially, the engine was tested under the standard OEM strategy, followed by a CFD simulation of charge temperatures during ignition delay. Then, the JP-8 fuel with CN = 31 was tested in the CI engine and data for the lowest and highest load were discussed. At light loads of 5 bar IMEP, two injections were used while only one injection was used for the 10, 15, and 18 bar IMEP tests. They found that traces of cylinder gas pressure and ion current indicated that the engine misfired under low load conditions during the first injection event due to the prolonged ignition delay. Furthermore, the total ignition delay for both injection events was larger than the single combustion event of ULSD#2. Subsequently, a PV trace indicated an improvement in combustion and charge temperature with increasing loads, which was investigated through CFD and experimental data. Simulations using STAR-CD CFD software indicated combustion failure at intake air temperatures lower than 80^{o}C. Moreover, simulation of autoignition above intake air temperatures of 80^{o}C depicted the relationship between the formations of different radicals and the role of HCHO on the reactions defining the LT and NTC regimes. Furthermore, simulations with air intake temperatures greater than 190^{o}C led to a higher rate of evaporation during physical delay, an enhanced rate of endothermic reactions, lowered HCHO formation, and high rates of oxidation reactions. Next, the standardized experimental results indicated a large ignition delay and significant premix burn with the low CN JP-8 as compared to the other three fuels. Although the injection was advanced to compensate for the low CN JP-8, its RHR was the lowest among all fuels. Moving on, the authors conducted engine tests based on the approach required to improve combustion while using a low CN fuel. The first suggestion was to increase the charge temperature, followed by an increase in engine load. Both these

methods improved the RHR from the fuel and reduced the NTC regime of combustion. In addition, the authors stated that the fuel economy for the regular JP-8 and low CN JP-8 could be the same if injection timing was advanced. Finally, the authors suggest multiple injections to overcome noise, vibration, and harshness, as combustion phasing of JP-8 becomes similar to ULSD#2.

In the same year, Lutz and Modiyani [84] demonstrated the modifications required to remove EGR and operate a CI engine on JP-8 and reach 48% brake thermal efficiency since the EGR system was prone to fouling due to the high sulfur content of JP-8 fuel. In addition, another goal was to maintain emissions within the levels specified by the EPA. The engine used was a Cummins 8.9L ISL commercial over tie shelf unit rated at 425 HP. Here, the authors first evaluated engine modifications, then tested the recommended hardware changes, and finally conducted a durability test. The modifications included increasing peak cylinder pressure to 3200 psi, boosting the compression ratio, creating wider and shallower piston bowl geometry, reducing swirl ratios, enhancing injector cup flow, creating a low-pressure drop port and manifold flow, and improving the turbocharging matching. Next, the standard, non-modified test results with JP-8 indicated an insignificant effect on engine performance and formation of NO_x as compared to ULSD#2; however, there was a 1 to 2% of drop in power. Meanwhile, smoke levels were considerably lower for JP-8 with the absence of aromatic hydrocarbons. After the EGR system was removed, a new set of experiments were performed. The general trends from the subsequent tests with injector cup flow indicated a BTE growth with injector flow increase. From the three injectors tested, the 165 pph injector cup was recommended for increasing the BTE with JP-8 fuel. Secondly, the modification of increasing the compression ratio increased BTE by 2%, with a slight increase in NO_x. Thirdly, the effect of backpressure due to a diesel particulate filter was studied by adjusting a valve in the exhaust stack. Interestingly, this process increased BTE by 1.60 to 1.63%. Next, a modified cylinder head with a wide and shallow bowl was used to study changes in the BTE. The results

from this test along with a reduction in backpressure increased BTE by 3.2% at part load and 3.8% at full load. Moving on, the next modification was a change in bowl profile and an increased injector cup flow. The recommendation was to use a 180 pph injector and 19:1 CR piston with a scaled production bowl. However, a resulting increase in peak pressures required structural changes to the engine, which was not recommended. Finally, four types of turbochargers were analyzed for an improvement in BTE. The turbocharger demonstrated limited success in increasing BTE as most turbochargers on commercial engines are tailored to operate with EGR. Overall, the authors were able to demonstrate a BTE increase of 43.8% instead of 48% as control of emissions presented constraints on performance.

In the same year, Murphy and Rothamer [85] carried out a performance and emissions evaluation of low CN fuels under high operating loads. The engine used was a 2.44 L Caterpillar 3401 single-cylinder oil-test engine with a Bosch common rail and 2-injector body. They employed ULSD#2 as the baseline fuel against Jet-A, SPK, a 50-50 blend of Jet-A and SPK (JB1), and a 25-75 blend of Jet-A and SPK (JB2). Furthermore, performance parameters were measured using two different intake camshafts for dissimilar intake valve timings at -143º intake valve close (IVC) and -85º IVC. Experimental results illustrated that CN was the main parameter that affected pressure rise rate, ignition delay, and fraction of energy release, particularly during the premixed burn phase. In addition, the pressure rise was inversely related to CN (i.e., pressure rise increased with decreasing CN) with the JB1 blend illustrating the highest premix pressure rise among all fuels tested. Along similar lines, the results from the apparent heat release rates indicated the influence of CN on the magnitude of heat release. Consequently, the JB1 blend had the highest heat release rate during the premix phase since it had the longest ignition delay and lowest viscosity that allowed more time for mixing smaller droplets of fuel; hence, resulting in a higher entrainment of air into the fuel that promoted rapid autoignition reactions. Furthermore, the effects of late combustion were accentuated in the case of the camshaft with -85º IVC.

In addition, the net ISFC indicated a drop in fuel consumption with increasing CN, because of the large premix burn that enables more constant volume-like combustion as a larger fraction of energy is converted into work during the premix phase. Meanwhile, the low aromatic content and higher volatility of the JB1 blend led to lower PM formation as compared to both Jet-A and ULSD#2. For exactly the opposite reasons, NO_x emissions were lower in the case for JB1 fuel, particularly for the -143º IVC camshaft, where in-cylinder temperatures were lower. Both the emissions and combustion parameters suggested the dominating influence of CN on overall engine performance.

In the same year, Lee et al. [86] used two-color thermometry to visualize combustion in a CI engine fueled with JP-8 to correlate engine performance and emission results. The engine was a four-stroke, water-cooled, single-cylinder, naturally-aspirated, direct injection CI version equipped with a high pressure, electronic fuel injection system. Further, the engine was operated at 1200 rpm with injection pressures of 30 MPa and 140 MPa while using a regulated quantity of each fuel to maintain mid-load performance. Even though both fuels had the same injection timing, combustion began earlier for ULSD#2 due to its higher CN. For JP-8, the effects of its enhanced atomization did not overcome the effect of CN. However, this greater level of atomization facilitated a higher peak RHR and premix burn event. In terms of emissions, this larger premix burn resulted in greater HC and NO_x levels as the augmented evaporation and greater ignition delay resulted in a mixture that was more homogenous and closer to stoichiometric conditions. Additionally, local overleaning due to the high vaporization rate resulted in incomplete combustion and low combustion efficiency. However, smoke levels were reduced considerably as the enhanced mixing resulted in the elimination of fuel rich zones. Next, the two-color image thermometry indicated that the flame luminosity of JP-8 diminished rapidly with enhanced vaporization. In addition, this implied that JP-8 had a larger premix burn than ULSD#2. Furthermore, luminosity intensity analysis and spatial distribution analysis indicated a shorter fuel jet penetration into

the combustion chamber that resulted in more homogenized combustion. Finally, the flame temperature field indicated locally high temperature regions within the combustion chamber for JP-8 that acted like hotspots for the formation of thermal NO_x.

In 2012, Soloiu et al. [87] investigated the performance of neat ULSD#2 and its blends with JP-8. The engine was an IDI, single-cylinder, four-stroke engine with a three-vortex swirl chamber having a compression ratio of 23.5. The tests were conducted at full load and 2400 rpm with ULSD#2, 20% JP-8 (J20), 35% JP-8 (J35), and 50% JP-8 (J50). Based on the in-cylinder pressure data, instantaneous volume averaged maximum gas temperature, heat flux through the cylinder walls, and heat release, there was negligible difference between the different fuels tested. Moreover, the test results indicated less than a 0.3% difference in engine mechanical efficiency for all the blends. However, the ignition delay was found to increase with JP-8 blend, contrary to the fuel with a higher CN having shorter delay. This was attributed to the fact that military documentation does not contain the specification for CN and it could differ vastly by source. In addition, BSFC decreased while overall efficiency increased with a greater proportion of JP-8. In terms of emissions, NO_x decreased with JP-8 content until the J35 blend. Beyond that, there was a slight increase in NO_x emissions until J50. Hence, it was suggested that a 20% blend by weight resulted in a substantial reduction of NO_x. Moreover, soot emissions increased with JP-8 content; thus, displaying the typical NO_x-soot formation trade-off. Based on the findings, it was suggested that JP-8 was a suitable fuel for power generation.

In 2012, Yost and Brandt [88] at the SwRI evaluated a commercial off-the-shelf engine with JP-8 at high temperatures. The Ford 6.7L engine selected for this study was a V8, DI, turbocharged, and intercooled engine that was fitted with a fuel lubricated, high pressure common rail fuel injection pump with piezoelectric fuel injectors. For the purpose of their tests, an external coolant fuel loop was maintained at elevated temperatures to keep the fuel at 70^{o}C. Moreover, the test cycle for their analysis was a

modified 210-hour tactical wheeled vehicle cycle for compatibility tests, performed with JP-8 at ambient conditions and JP-8 at 70^{o}C. In addition, a pre- and post-test was conducted to determine the durability of the engine over the entire test. After the 210-hour long testing event, engine power dropped by 3% at ambient fuel temperatures and 1.9% at 70^{o}C. However, the engines indicated no significant power loss or wayward tailpipe emissions at elevated fuel temperatures. Finally, a hardware check on the components of the high-pressure injection system indicated no wear. As a conclusion, JP-8 was recommended for use in CI engines.

In 2012, Yu et al. [89] studied the in-cylinder soot formation of ULSD and JP-8 in an optically accessible engine, single-cylinder, naturally-aspirated CI engine with a mechanical common rail injector. The authors used three methods to study the soot formation: tailpipe emission analysis with a micro soot meter, optical laser based in-cylinder measurements using a two colored high-speed camera, and in-cylinder numerical analysis of line of sight calculations applied to a chemical-kinetic CFD simulation. Based on the results, the properties of JP-8 and ULSD influenced the needle lift for the fuel injection. The lower viscosity of JP-8 allowed for a longer travel of the needle, consequently increasing volumetric flow rate of JP-8. Moreover, JP-8 had a lower soot formation than ULSD due to better atomization aided by its lower viscosity and aromatic content. On analyzing the results from the two-color high-speed camera measurements, fewer high soot temperature zones were observed in the case of JP-8. In addition, JP-8 had a smaller soot optical thickness than ULSD across all load conditions. When comparing the CFD results and the in-cylinder optical measurements using the two color line of sight integration model, there was a close agreement with the optical measurements and experimental data. However, a few data sets showed erroneous results due to a limitation in the direct range of camera. Through the experimental and optical results, it was concluded that the volatility of fuel was the key parameter in defining soot emissions.

In 2012, Mangus and Depcik [90] investigated the use of ULSD, UCO biodiesel, and JP-8 fuel in a single cylinder direct injection CI engine operating with a mechanical fuel pump. The combustion phasing, emissions, and fuel consumption were studied as a function of fuel density, viscosity, CN, and calorific value. Here, JP-8 was found to have a delayed combustion because of lower bulk modulus, density, and viscosity. These characteristics also explained its lower combustion temperature, combustion efficiency, and NO_x emissions than that of ULSD and UCO biodiesel as JP-8 had a reduced residence time in the combustion chamber. However, JP-8 showed higher CO and HC emissions as compared to ULSD and UCO because of lower cylinder pressures and flame temperatures and a shorter in-cylinder residence time. Next, NO_x emissions were reduced in the case of JP-8 as aromatic contents were absent. All three fuels were found to have the same fuel consumption as the higher volatility of JP-8 increased its vaporization that offset the lower combustion efficiency as compared to ULSD and UCO biodiesel. Moreover, the thermal efficiency, fuel conversion, and thermal efficiency of JP-8 were lower than the other fuels tested because of reduced in-cylinder temperatures and a lessened residence time of the reacting air-fuel mixture. Furthermore, JP-8's later injection was attributed to the slow buildup of fuel pressure in the fuel injector and slow pressure waves in the pump line nozzle system.

In 2012, Jayakumar et al. [91] studied the performance of a single cylinder, high speed, high compression CI engine with electronic fuel injection. The tests with JP-8, biodiesel and ULSD#2 were normalized by adjusting the injection timing of the premixed combustion fuel fraction and conducted at 1500 rpm and 5 bar IMEP by adjusting the location of peak pressure. The intake was connected to a plenum maintained at 1.1 bar to simulate turbocharging. Based on the results, the authors determined that B100 has the shortest ignition delay because of its higher CN that is aided by the additional oxygen atom in the fuel molecule. Next, JP-8 had a shorter ignition delay than ULSD because of its higher volatility. Furthermore, the highest LHV of JP-8 amongst all the three test fuels described the lower BSFC

of JP-8. For emissions, NO_x levels were lowest for B100 because of the shorter ignition delay followed by JP-8 and ULSD. Along similar lines, the additional oxygen atom in B100 reduced PM and CO emissions by enhancing combustion efficiency. Meanwhile, the intermediate properties of JP-8 meant that PM and CO emissions of JP-8 were between levels shown from tests with B100 and ULSD. Furthermore, JP-8 was found to have lower NMPs than B100 but higher NMPs than ULSD, mainly due to a similar trend in fuel volatility, AMP concentration, and aromatic content. In addition, an augmented diffusion burn caused higher AMPs that resulted in lower NMPs. Finally, JP-8 produced lower exhaust temperatures than B100 and ULSD due to a slightly later burn.

In the same month, Jayakumar et al. [92] proceeded to study the effects of swirl and injection pressure on the emissions of JP-8 in a single-cylinder, high-speed, DI CI engine with a common rail fuel injection system and swirl control mechanism. For their experiments, injection pressures were set to 400 bar, 600 bar, 800 bar, 1000 bar, and 1200 bar with the engine running at 1500 rpm and 5 bar IMEP. In addition, a low swirl ratio of 1.44 and high swirl ratio of 7.12 were selected to estimate the effects of variation in turbulence on atomization and combustion. From the initial test results, it was observed that the higher swirl ratios needed slightly advanced injection timing due to lower charge temperatures caused by higher heat losses. In addition, higher injection pressures needed a delay in injection timing to maintain normalized combustion as the spray speeds an enhanced fuel breakup and atomization process. Nevertheless, swirl increased turbulence and enhanced fuel evaporation but did not affect injection duration. Next, higher injection pressures and swirl ratios significantly increased the premix burn phase; however, the combination of a higher injection pressure and swirl ratio caused wall quenching. Due to JP-8 propensity to enhance atomization and mixing, its combustion efficiency increased with a growth in swirl ratios, subsequently, reducing the formation of HC, CO, and PM emissions. Meanwhile, this resulted in higher in-cylinder temperatures leading to the formation of NO_x. For the soot emissions that

occurred, AMPs was lessened while the NMPs increased with the intensification in swirl ratios. Overall, the results indicated that a higher swirl ratio improved combustion, but an optimized swirl ratio could achieve lower NO_x and NMP emissions.

In 2013, Labeckas et al. [93] conducted tests to determine the combustion, performance, and emission characteristics of a CI engine operating on Jet-A1 fuel with a cetane improver. The CN improver selected was 2-ethylhexyl nitrate that was mixed with Jet-A1 in ratios of 0.04%, 0.08%, 0.12%, 0.16%, and 0.24% by mass. The engine was a single cylinder, four-stroke, DI MTZ D-243 engine with a mechanical injection system. Furthermore, engine load measurements were taken at 1400, 1800, and 2200 rpm. The low CN of Jet-A1 resulted in a 15.5%, 9.5%, and 17.0% longer ignition delay than ULSD#2 under full operating load at speeds of 1400, 1800, and 2200 rpm, respectively. Meanwhile, the addition of a CN improver in ratios greater than 0.12% by mass educes the ignition delay to levels acceptable for safe engine operation. Furthermore, the cylinder pressure reduced by 6.5% at low speed and 4.4% at high speed with neat Jet-A1. Moreover, the addition of 0.04 and 0.08% CN improver did not change the cylinder pressure at low speeds; however, at concentrations of 0.12% and above, adding the improver resulted in 16.1% and 24.7% lower pressures as compared to ULSD#2. Next, the engine BSFC with Jet-A1 decreased by 1.8% but increased by 2.4 and 2.5%, at 1800 and 2200 rpm respectively, compared to normal diesel. With the 0.12% CN improver, the BSFC increased by 2.3 and 1.2% at 1800 and 2200 rpm, respectively. Moving on, NO emissions for Jet-A were lower than ULSD#2 by 11.5%, 11.8%, and 17.1% at each test speed. Furthermore, the CN improver at 0.12% concentration reduced NO by 7.0%, 12.8%, and 17.7% over the test conditions since the premix burn phase was reduced with the increase in CN. In addition, HC and CO emissions decreased by 2.8 and 6.1 times as compared to ULSD#2, and smoke opacity decreased by 31.0%, 9.8%, and 1.4% for each of the three engine speeds. However, the addition of CN

improver resulted in combustion being closer to ULSD#2, resulting in an increase in emissions as compared to results with neat Jet-A1.

In the same year, Soloiu et al. [94] studied the combustion and emission characteristics of JP-8 blends with ULSD#2 in a single cylinder, direct injection CI engine. For their work, the JP-8 blends were 20% and 50% by weight with ULSD#2 with both fuels having a similar CN. Meanwhile, performance measurements were taken at engine loads of 3, 5, and 8 bar IMEP. Results for all three load conditions showed that JP-8 blends did not affect the peak in-cylinder pressure when compared to ULSD#2. Since the CN of JP-8 was one unit more than ULSD#2, JP-8 blends showed a slightly lower heat release rate as compared to ULSD#2. Next, thermal efficiency increased with an growth in the percentage of JP-8 as a function of its marginally higher CN and LHV. When emissions were concerned, NO_x emissions decreased with the percentage of JP-8 due to a higher CN. However, at low load conditions, NO_x levels for increasing JP-8 blends grew beyond ULSD#2 as low in-cylinder temperatures suppressed thermal NO. Moving on, at higher loads soot levels grew with the higher percentage of JP-8 blends as the increase in mass of fuel injected led to engine operation reaching the smoke level. Next, CO emissions decreased while CO_2 emissions rose across all loads for all the test fuels suggesting improvement in combustion efficiency with an increase in JP-8 blend ratio. In addition, THC emissions for each fuel blend decreased as combustion efficiency grew with greater loads. Overall, the marginal difference in CN was found to be the most important characteristic that determined the performance and emissions of ULSD#2 and JP-8.

In 2013, Rothamer and Murphy [95] studied the ignition delay of aviation fuels and ULSD#2 in a single cylinder, 2.44L heavy duty Caterpillar 3401 CI engine. For this study, five fuels were analyzed: DF2, jet-A (jet-A2), a blend of 50% jet-A and 50% Sasol iso-paraffinic kerosene (IPK) (JB1), a blend of 75% jet-A and 25% IPK (JB2), and a blend of 70% jet-A and 30% IPK (JB3). Ignition delay measurements were performed at different fuel densities from 15 to 40 kg/m^3 using 5 kg/m^3 increments and temperature was varied

from 875 to 1100 K. Here, the temperature and density of the ignition delay was determined by a two-zone equation of state. The ignition delay as a function of density for different fuel samples showed a linear trend on a log scale plotted for 1/T values. These ignition delays were found to be in strong agreement with the respective fuel CNs. Moreover, diesel fuel with its greater viscosity was found to have the longest ignition delay of all fuels. The blends of jet fuel and Sasol IPK and Jet-A have identical ignition delays. However, the CN of JB1 and JB3 fuels were close but indicated a difference in ignition delays. A possible explanation involved the varying sensitivity of ignition delay as a function of CN. Subsequently, these data were used to model the ignition delay using an Arrhenius equation with the results compared to those from shock tubes, constant volume combustion machines, and rapid compression machines. Overall, chemical delay was found to dominate in a temperature range of 800 to 1000 K while physical ignition delay became limiting after 1000 K.

In 2014, Ahmet et al. [96] studied the performance and emissions of JP-8 and methyl ester blends in a single-cylinder, naturally-aspirated DI CI engine. The tests were performed using six different fuels blends; i.e., 25% biodiesel (B25), 50% biodiesel (B50), and 75% biodiesel (B75) with JP-8, 100% biodiesel (B100), 100% JP-8 (J100), and ULSD#2. The tests were conducted at 2200 rpm and at loads of 7.5, 11.25, 15, and 18.75 N.m. At lower loads, combustion was delayed when using J100 and B100 fuels; whereas, it was advanced as biodiesel blend level increased. Here, the additional oxygen content and higher CN of biodiesel influenced the performance and emissions largely. This resulted in greater in-cylinder temperatures as the oxidation reactions proceeded at a higher rate resulting in increased conversion of nitrogen to NO. Instead, with a lower CN and reduced heat release rate, J100 fuel burns with decreased NO_x emissions. For the same reason of higher oxygen content, CO and soot emissions are lower for B100 while the lesser CN of J100 results in a reduced duration of combustion, consequently increasing the amount of partially combusted products. Overall, the authors suggested that the higher LHV of J100 and

oxygen content of B100 could be tailored to formulate fuel blends for optimal engine performance and reduced emissions.

In 2014, Labeckas et al. [97] studied the performance and emissions of an engine operating on JP-8 and ULSD#2. They used a four-stroke, four-cylinder, naturally aspirated, DI CI engine with a mechanical injection pump set at 19.0 MPa. The fuels were blended by volume including 100% JP-8 fuel (J), 90% JP-8 / 10% DF (J+D10), 70% JP-8 / 30% DF (J+D30), 50% JP-8 / 50% DF (J+D50), 30% JP-8 / 70% DF (J+D70), and 100% diesel fuel (DF). Furthermore, the engine was tested at full load at speeds of 1400 rpm and 2200 rpm. For their experiments, the higher density and CN of ULSD#2 led to a decrease in ignition delay at both engine speeds. Hence, with the growth in ignition delay for greater blends of JP-8, combustion became more constant-volume like, displaying an increase in the level of premix burn and subsequent rise in rate of heat release. Next, both BSFC and brake thermal efficiency remained fairly constant at lower loads across all the fuel blends. However, at 2200 rpm, the shortened ignition delay with ULSD#2 led to lower heat losses to the engine block and cooling fluid. With respect to emissions, formation of thermal NO increased with addition of ULSD#2. This was the outcome of reduced fuel atomization and the presence of a small fraction of rapeseed methyl ester in the fuel. Moving on, CO and HC emissions showed ambiguous variations across all loads; however, at low speed with low ULSD#2 blends, an increase in HC could be attributed to the largely heterogeneous combustion process. Finally, the smoke opacity of the exhaust was found to be analogous to the levels of CO and HC. Overall, the blends of 70% JP-8 / 30% DF (J+D30), 50% JP-8 / 50% DF (J+D50), and 30% JP-8 / 70% DF (J+D70) showed slight gains in performance and emissions across the entire experiment.

In the same year, Labeckas et al. [98] evaluated the impact of CN on the performance and exhaust emissions of a CI engine fueled with JP-8. They used a CN improver called 2-ethylhexyl nitrate in JP-8 in blends of 0.04%, 0.08%, 0.12%, 0.16%, and 0.24% by volume. The engine tests were performed at full

load at 1400 rpm and 2200 rpm. The engine was a four-stroke, four-cylinder, 60 kW, DI D-243 CI engine with a mechanical fuel injection system. Test results showed that the CN improver had the most profound effect during high load and high-speed engine operation. However, a highly advanced flame could reduce the time available for combustion to complete and reduce combustion efficiency. Further, the advanced ignition with an increase in CN improver percentage led to a lower premix burn as mixing time is reduced. On the contrary, the higher premix, RHR, and in-cylinder pressure happened later in the expansion stoke and hence engine operation was without excessive vibrations with JP-8 fuel. Next, the tests with JP-8 and the CN improver indicated a lower BSFC than ULSD#2 as atomization, evaporation, and mixing were superior to ULSD#2 at all operating conditions. Nevertheless, BSFC grew with greater CN improver percentages as it promoted a shorter ignition delay and lower maximum heat release rate further away from TDC. Furthermore, the addition of CN improver reduced the BTE at 1400 rpm but grew BTE with greater CN improver percentages at 2200 rpm. As far as emissions were concerned, NO_x levels decreased as the premix burn event associated with higher CN decreased. Because of the ensuing longer diffusion burn phase, soot emissions increased, displaying the classical NO_x-soot trade-off. Next, an increase in CN improver percentage resulted in an initial growth in CO and HC emissions while it began decreasing at high percentages of CN improver. This was explained by the lower time for combustion to complete as ignition delay was reduced with the rise in CN. Overall, the tests indicated that the addition of 0.12% 2-methylhexyl nitrate has an overall effect of increasing thermal efficiency and reducing BSFC and total emissions as compared to neat JP-8 or ULSD#2.

In the same year, Solmaz et al. [99] investigated the use of civilian Jet-A1 blends with ULSD#2 in CI engines. They used a single-cylinder, four-stroke, DI engine running on blends of 0%, 5%, 10%, 25%, and 50% Jet-A1 volumetrically blended with ULSD#2 abbreviated as J0, J5, J10, J25, and J50, respectively. The tests were conducted at full load with speeds ranging from 1750 to 3000 rpm. Their results indicated a

drop in torque with increasing Jet-A1 in the blend due to a drop in the heating value and delayed combustion as CN decreased. In addition, the lower density of Jet-A1 resulted in a reduced volumetric energy density of fuel within the combustion chamber. For the same reasons, BSFC increased with increasing blends of Jet-A1. When it came to emissions, NO_x levels decreased with growing percentages of Jet-A1 as the combined effect of lower heating value and high latent heat of evaporation led to reduced in-cylinder temperatures. Next, smoke levels increased with Jet-A1 blend percentages, typical of the NO_x-soot trade off. Finally, CO emissions grew with addition of Jet-A1 to ULSD#2 as fuels with a lower H to C ratio could lead to less efficient combustion. As a result, it was determined that Jet-A1 was not a suitable fuel for use in CI engines without increasing its CN.

Again in 2014, Yamik at al. [100] tested an engine with blends of a sunflower oil methyl ester and JP-8. They used a four-stroke, four-cylinder test engine running at full load between speeds of 1750 and 3000 rpm. Here, ULSD#2 served as the baseline fuel while biodiesel was blended with 5%, 10%, and 25% JP-8. Meanwhile, engine tests indicated an increase in power with growing biodiesel percentage in JP-8 blends as compared to ULSD#2. This was said to be caused by the higher viscosity of biodiesel that resulted in less fuel injection, penetration, and atomization into the combustion chamber. However, the addition of JP-8 in the biodiesel blend helped in evaporation and subsequent atomization that grew overall combustion efficiency as the percentage of JP-8 rose. Next, the BSFC showed exactly opposite trends to power output, suggesting that the blends of biodiesel and JP-8 resulted in delayed combustion that was inefficient. Moreover, their explanation for the increase in BSFC was a drop in volumetric energy density as more mass of fuel had to be injected into the cylinder to maintain power output. In addition, the heating value of biodiesel and JP-8 was lower than ULSD#2. In terms of emissions, NO_x decreased with blends of JP-8 as less oxygen was available for the conversion of nitrogen to NO. For the same reason, soot emissions diminished with an increase in biodiesel content as more oxygen is

available for combustion. In addition, the biodiesel tested had less aromatic compounds that led to lower amounts of soot precursors. Overall, the addition of JP-8 slightly compensated for the lower performance of biodiesel and reduced NO_x formation.

In 2015, Lee et al. [101] analyzed JP-8 combustion in an effort to minimize the formation of NO_x and PM emissions. They performed an engine test utilizing a four-cylinder CI engine with EGR and an electronic injection system to support multiple injection events. For their analysis, an initial pilot combustion event was set to offset the effects of a low CN fuel while a 30% EGR rate was used to optimize emissions. Initial single injection tests indicated delayed combustion in the low temperature heat release region and an increase in high temperature heat release region. This ignition delay resulted in cooler engine temperatures that led to a reduction in PM and NO_x and an increase in HC and CO as compared to ULSD#2. Meanwhile, during the multiple injection mode, the low temperature heat release region experienced a higher reactivity followed by a larger premix burn event as compared to ULSD#2. Subsequently, NO_x emissions increased while CO and HC emissions reduced considerably as the combustion temperature was higher and lasted longer. In addition, PM emissions rose, but were less than ULSD#2 as JP-8's higher level of atomization prevented formation of fuel rich zones. Furthermore, the multiple injection mode resulted in slightly lower temperatures where the accumulation mode of PM formation was predominant as compared to the nucleation mode for a single injection event. Moving on, tests with 30% EGR under the single injection mode indicated no difference between ULSD#2 and JP-8. During multiple injections and 35% EGR, ignition delay remained the same and the RHR grew for JP-8. This indicated that EGR could not cancel out the effects of the high reactivity JP-8 fuel and there was a loss of combustion efficiency. To determine the NO_x and PM reduction potential, the EGR rate was varied and JP-8 was shown to have lower emissions irrespective of engine operating

conditions. Hence, it was possible to control emissions (i.e., lower NO_x and PM) by adjusting a single injection event and dynamically changing EGR all while improving efficiency.

In 2015, Chu et al. [102] determined an injection strategy for dual fuel PCCI combustion with JP-8 and propane in an effort to reduce both NO_x and PM. The test was conducted using a high speed DI CI engine fitted with an electronic fuel injector, external pressure booster, and EGR system. In all, seven tests cases featuring single and multiple fuel injections were formulated for the analysis. The first test consisted of 32% EGR and propane injection. The second test was performed with 70% propane and no EGR. The third, fourth, and fifth tests consisted of no EGR and 70% propane with increasing start of ignition timings. The sixth and seventh tests featured a post injection event with 70% propane and 22% EGR. Comparing the first and second tests, EGR resulted in a later but higher RHR; whereas, the introduction of propane grew the diffusion burn phase. For the same reasons, NO_x emissions decreased with EGR while PM emissions rose for the first test. In addition, results for the first test indicated lower THC emissions. In the second test, the presence of propane resulted in enhanced late oxidation reactions that decreased PM. Next, a comparison of the RHR for the second, third, fourth, and fifth tests indicated the effect of advancing the injection strategy. In specific, the addition of low reactivity propane in the second test resulted in a delayed combustion while the earlier injection for the third, fourth, and fifth tests provided ignition delays that correlated with injection before TDC. Here, the excessively early combustion in case 5 reduced the in-cylinder temperature, subsequent decreasing NO_x emissions. Comparing the sixth and seventh test results, the combined effect of post injection strategy, propane injection, and EGR reduced NO_x and PM simultaneously as compared to the previous tests. As a conclusion, the authors suggest that the NO_x-PM trade-off with JP-8 could possibly be reduced by incorporating EGR, propane injection, and post injection strategies.

Again in 2015, Labeckas and Slavinskas [103] presented a detailed study of a D-243 engine tested with blends of JP-8 and RME. The tests were performed on a naturally aspirated, four-cylinder, four-stroke engine fitted with a mechanical fuel injection system and a compression ratio of 16. The base fuels for the tests included ULSD#2 (B5, with 5% biodiesel) and JP-8 (J100) while rapeseed methyl ether (RME) blends were prepared by mixing 5% (J5), 10% (J10), 20% (J20), and 30% (J30) RME by volume with JP-8. With respect to the injection process, it was found to be earlier than normal for RME blends at lower loads and speeds as the higher density of RME caused a faster propagation of pressure waves in the fuel lines. Additionally, the presence of the oxygen component of biodiesel improved the CN and subsequently reduced ignition delay as the biodiesel component in the blend increased. Moreover, the presence of heavy hydrocarbons in the blends affected fuel evaporation. In specific, the combustion of blends was later than that of jet fuel at low speeds; whereas, at high speeds combustion initiated earlier for the J30 blend with greatest CN and enhanced oxygen content. In conjunction with the ignition delay, the peak of heat release were larger for the fuel blends with a longer ignition delay since the fuel has more time to homogenize and mix. In addition, the position of peak heat release was advanced for fuels with a larger proportion of biodiesel. Next, BSFC slightly increased with the addition of biodiesel in jet fuel due to its lower LHV. Therefore, more fuel was injected into the cylinder to match the power requirement resulting in a reduced thermal efficiency. For emissions, NO_x emissions grew for J10 at low speeds and for J20 and J30 blends at higher speeds as the presence of additional oxygen enhances the formation of NO and NO_2. Next, CO emissions rose for J20 at lower speeds and intensified at higher rates for J10 at greater speeds due to a decreased time of combustion. Furthermore, J10 resulted in respectively large HC emissions at all loads, but decreased as the organic component blend percentages rose. Lastly, PM emissions increased drastically for J10 at higher speeds while decreasing with higher fuel blends.

In 2016, Soloiu et al [104] performed an analysis on the combustion and emission characteristics of Jet-A in an IDI and a DI CI engine. Both engines were tested at 4.5 bar IMEP at 2000 rpm. The test blend included a 75% Jet-A and 25% ULSD#2 blend (75JU) by mass with ULSD#2 as the baseline fuel. For the DI engine, there was a pronounced premix burn phase for both fuels while the pre-chamber equipped IDI engine showed a short ignition delay. In addition, the RHR indicated that the DI engine encountered a similar combustion event for Jet-A and diesel fuel. Analyzing the mass fraction burnt, DI engine exhibits sudden combustion for both fuels while the IDI engine indicated gradual burning across the entire combustion phase. Next, a higher in-cylinder temperature was obtained for the blend in the IDI engine. In terms of emissions, soot emissions for the DI engine were reduced using 75JU as compared to ULSD due to a better atomization process. In the IDI engine, soot emissions decreased for both fuels as its longer burn duration enabled more post-combustion oxidation reactions. Next, NO_x emissions were greater in the DI engine as the premix burn was elevated in lean conditions; whereas, the IDI engine had a pre-chamber that underwent rich combustion. Meanwhile, the use of 75JU slightly reduced NO_x emissions in the DI engine due to lower in-cylinder temperatures and a lessened heat release peak. In contrast, the IDI engine showed comparable NO_x levels for both fuels. Overall, the authors stated that these tests confirmed Jet-A could be a viable fuel for the SFFP.

In the same year, Szedlmayer et al. [105] studied the impact of variations in fuel CN on the performance of CI engines for unmanned aerial vehicles (UAV). They performed tests on a multi-cylinder, turbocharged, direct-injection, CI engine using six fuel samples having a CN from 30 to 55 in increments of 5 units. The test was conducted at four loads; i.e., ground idle, full power ascent, cruise, and descent idle. The ground idle, cruise, and descent idle modes used a pre-injection event along with a single main fuel injection while the full power ascent mode used a single main injection pulse. Based on the tests, the CN affected autoignition as the delay in combustion grew with a decreasing value of CN. In addition,

the pre-injection event could not improve the combustion quality when the CN was less than 35. In the case of full ascent mode, the high load reduced ignition delay that resulted in similar peak pressures for each of the fuel samples. Meanwhile, the cruise condition mode resulted in an increase in premix burn for fuels with a lower CN. However, in descent mode where the engine throttle is significantly reduced, the CN = 30 fuel showed highly unstable engine operation in spite of pre-injection. These tests indicated that pre-injection was too early in the cycle, leading to unstable combustion. For the heat release analysis, the same trends were observed for each of the operating modes with respect to the pressure traces. Furthermore, the net mean operating pressure and net specific fuel consumption showed no significant variation with CN, except during the descent loading cycle when engine performance greatly diminished. As a result, only low load conditions exhibited a strong dependence on CN and ignition quality.

Again in 2016, Solmaz et al. [106] performed experiments with blends of Jet-A1 and ULSD#2 in a single cylinder DI engine. The fuels tested were ULSD#2, Jet-A1 (A100), 25% Jet-A1 with 75% diesel (A25), 50% Jet-A1 with 50% diesel (A50), and 75% Jet-A1 with 25% (A75) diesel by volume with the engine set at 2200 rpm at 7.5, 11.25, 15, and 18.75 N.m. loads. Firstly, the in-cylinder pressure and crank angle data indicated an ignition delay with an increase in Jet-A1 fuel blend. This was the result of diesel having nearly twice the CN as Jet-A1. As a result, a later combustion of Jet-A1 blends allowed more time for the fuel-air mixing process and, hence, the premix burn level increased with blend level. Likewise, the lower density and viscosity of Jet-A1 means that less fuel was delivered into the cylinder, resulting in a reduced power output and greater fuel consumption for the same load conditions as ULSD#2. In addition, the improved atomization of Jet-A1 reduced the equivalence ratio, subsequently enabling leaner combustion. Furthermore, since Jet-A1 combustion happened later towards TDC, less time was available for combustion to complete, resulting in an increase in CO and HC emissions with a growth in blends of

Jet-A1. Additionally, a longer ignition delay led to less diffusion burn, reducing the formation of PM. Finally, the substantially reduced heating value of Jet-A1 resulted in a lower temperature of combustion that reduced the formation of NO_x. As a result, the authors suggested that Jet-A1 could be used to reduce NO_x emissions.

In the same year, Szedlmayer and Kweon [107] presented a study on the effects of altitude on the performance of a CI engine for a UAV. The engine was General Motors (GM) 6.6-liter Duramax turbocharged DI CI engine, which is equipped with a Bosch CRIN 3 common-rail fuel injection system and a Garrett single-stage variable nozzle turbocharger (VNT). For the tests, the engine was set to run at 1400 rpm at loads of 100, 400, and 800 BMEP, along with varying inlet pressure from 30 to 101 kPa. From the heat release data, the tests revealed a drop in pressure with a drop in intake pressure when simulating high altitudes. In addition, the ignition delay grew as the higher altitude resulted in a lower in-cylinder temperature and pressure at the time of fuel injection. This increase in ignition delay amplified with altitude and resulted in a larger premixed burn event as a greater amount of air and fuel mixture was combusted. With respect to in-cylinder temperatures, there was a shift in energy losses between coolant and exhaust gases. This shift was the result of lower mean in-cylinder temperatures early in the expansion stroke that decreased the cooling heat loss. In addition, at higher altitudes, an advance in injection timing did not have a significant impact on the premix burn event and combustion phasing. Moving on, the combustion noise level grew with the ignition delay and subsequent higher premix heat release rate. Next, the brake thermal efficiency rose at lower loads as the air is sufficient to sustain autoignition reactions. Meanwhile, the brake thermal efficiency decreased with rising altitudes because of heat loss during the combustion stroke. Additionally, the ISFC decreased at low load conditions with rising altitudes except at high load and high altitudes due to the larger ignition delay.

Based on these tests, the authors suggested multiple fuel injection strategies to attain maximum engine performance at greater altitudes.

In 2017, Sane et al. [108] investigated the autoignition and combustion of ULSD#2 and JP-8 during cold starts of a Volkswagen 2.0L TDI engine. The engine was fitted with a high-pressure common rail fuel injection system that can produce up to 1800 bar injection pressure. For the purposes of testing, 200 cycles of engine operation were documented to analyze the effects of cold starts. On initial firing, the engine reached 1042 rpm on ULSD#2 fuel but showed unstable operation for the first 35 to 40 cycles while stabilizing at a speed of around 850 rpm. With JP-8, the engine reached a speed of 1100 rpm and smoothened out at the 23rd cycle at around 832 rpm. Thus, the engine exhibited more cycle-to-cycle variation while running on ULSD#2 than JP-8. From the RHR data, the tests with ULSD#2 indicated the highest peak at the first cycle and dropped to the lowest peak at around the 20th cycle. Beyond 20 cycles, the combustion stabilized and heat release rate increased to attain a maximum at the 140th cycle. The initial decrease in heat release was associated with a larger ignition delay. Meanwhile, the exact opposite behavior was observed for JP-8 fuel. The first cycle had the lowest heat release after which the heat release improved till the 200th cycle. For both fuels, a reduction in NTC combustion resulted in a smoother and earlier heat release. Finally, it was observed that the chemical ignition delay was greater than the physical ignition delay and exerted a stronger influence on the engine stability at low temperatures. It was concluded that the higher CN of JP-8 enabled the engine to experience easier cold start events.

In the same year, Szedlmayer et al. [109] studied the effects of fuel aromatic content on the combustion of a UAV engine operating on JP-8. Four fuel samples were prepared with an aromatic content of 4.3%, 8.9%, 13.7%, and 24% while the engine load was set at 0%, 30%, 50%, and 100%. In addition, a pre-injection event was set for all operating set points except at the 100% load condition. From the in-

cylinder pressure data, there was inconclusive evidence on the impact of aromatic content on engine performance. Likewise, aromatic content did not affect the heat release rates. Furthermore, the engine performance parameters like fuel consumption, IMEP, and ISFC showed no specific trends related to aromatic content. In conclusion, the authors suggested realistic altitude test conditions to quantify the effects of aromatic content on engine performance.

In the same year, Kim et al. [110] conducted tests at the Air Force Research Laboratory to understand the effects of altitude on the performance of a CI engine. The engine used was an in-line multi-cylinder, 4-stroke, direct-injection, turbocharged, CI engine in a test facility capable of independent temperature and pressure control inside the chamber up to 30,000 feet (9 km) and temperature range from -40 to 30°C. The fuels tested were derived from JP-8 with a CN of 35.2 (CN35), 41.0 (CN40), and 47.6 (JP-8). From the test results at sea level, 18,000 feet, and 25,000 feet, the CN40 fuel indicated an earlier combustion and lower pressure as compared to CN35 fuel for the same fuel injection timing. For the same reason, an increased ignition delay for the CN35 fuel allowed more time for mixing resulting in a larger premix burn event. However, engine performance was severely impacted, leading to a 40% drop in performance at higher altitude conditions. Based on their results, the authors highlighted the importance of CN and ignition quality for high altitude performance.

Summary of Conventional Jet Fuel

The SFFP directive was devised by the U.S. DoD in 1988 to minimize logistical costs and improve wartime readiness of air force bases, particularly in northern Europe. As a result, all power generators, ground support, and infantry vehicles were mandated to operate on JP-5 or JP-8 instead of DF2. In addition, it was decided that the conversion of DF2 to jet propellants be achieved without any extensive modifications to existing CI engines. Consequently, several preliminary research studies were conducted at SwRI and TARDEC to ascertain the use of JP-8 in CI engines. Mostly, they reported a 5 to 10% drop in

power caused by poor fueling, lower CN, and leakages from the fuel pump clearances. In particular, the low fuel viscosity affected parameters like fuel penetration and spray angles, possibly causing quenching on the cylinder walls. On the other hand, the low CN led to a greater ignition delay and a higher premixed burn event that could cause structural engine damage. Moreover, the reduced volumetric energy of jet propellants resulted in a power reduction as compared to DF2 fuels. During this study, they concluded that the Stanadyne rotary fuel pumps were prone to failure caused by the lack of lubrication by jet propellants. However, it was also found that a higher level of atomization improved combustion efficiency and reduced PM. Overall, their conclusions indicated satisfactory engine performance with both JP-5 and JP-8, subsequently leading to successful combat missions during the Gulf wars.

As the use of JP-5 and JP-8 became widespread with both NATO and U.S. forces, researchers began conducting studies to optimize CI engines employing these fuels. With advancement in technologies, these studies highlighted the use of high-pressure electronic fuel injection, cetane additives, blending with other fuels, multiple injection events, and other modifications to improve performance and reduce emissions. For example, while a high rail pressure improved atomization, a low viscosity tended to quench the flame on the cylinder walls; hence, causing an exponential increase in unburnt products of combustion. With the start of the Air Force Smart Operations for the 21st Century (AFSO21) program in 2009, the U.S. Air Force converted all military bases to operate solely on Jet-A. As a result, new impetus was given to analyze CI engines operating on commercially available Jet-A. Based on research conducted, the similarities between JP-8 and Jet-A revealed analogous results obtained with JP-8 in the years leading to the SFFP.

Despite nearly four decades of research investigating the use of jet propellants in CI engines, the absence of CN specifications and high variability in fuel composition has made it impossible to accurately predict engine performance. This stems from the fact that jet fuel manufacturers tailor fuel properties,

rather than fuel compositions to achieve the final hydrocarbon product. Most importantly, since gas turbines have a continuous flame, the need for a CN rating is irrelevant. In the literature surveyed, the CN varied from 25 to 60 and accurate measurements of CN are only possible through an expensive setup called the ignition quality tester that is impossible to install on the battlefield. Since CI combustion is heavily dependent on CN number, vehicle operation can be adversely affected, compromising war readiness. In addition, emissions would be difficult to control with a change in autoignition characteristics. For example, delayed ignition can cause a high rate of heat release, increasing NO_x, while the short duration of combustion could reduce combustion efficiency. Therefore, a suggestion moving forward is for jet fuel manufacturers to conform to a particular fuel composition and CN threshold.

In summary, the CI engine tests featuring aviation fuels for the SFFP can be evaluated as pre-1988 and post-1988, the year the SFFP directive was mandated. During the pre-SFFP period, the negative effects of jet fuels were a result of mechanical fuel injection and limited advances in metallurgy and manufacturing techniques. As a result, a drop in fuel viscosity increased fuel leakages and wear on the fuel injection system. Also, the decrease in volumetric energy density after switching to JP-8 reduced engine power by 5-10% and increased BSFC. Meanwhile, the introduction of modern manufacturing and electronic fuel injection during the 1990s reduced the intensity of the effects of low viscosity and density, but did not better the engine performance compared to ULSD#2. Based on the research articles reviewed, the parameters affecting emissions and fuel consumption are listed as arrows in Table 3. The property column is indicative of the increasing or decreasing magnitude of the parameter under consideration compared to ULSD#2.

Table 3: Estimated correlations based on literature review of conventional jet fuels vs ULSD#2 in CI engines

Property	NO_x	CO	HC/PM	BSFC
Density ↓	↓	↑	↑	↑
Viscosity ↓	↑	↓	↓	↓
CN ↓	↑	↑	↑	↑
HV ↑	↑	↓	↓	↓
Volatility ↑	↑	↓	↓	↓

Fischer-Tropsch Jet Fuels

Feedstocks like coal, biomass, and natural gas can be converted to liquid fuels using direct liquefaction or the Fischer-Tropsch Synthesis (FTS) catalytic process. With respect to direct liquefaction, since it involves pressures over 100 bar, temperatures exceeding 250^{o}C, and an external supply of hydrogen gas, this process is uneconomical [111]. Meanwhile, the more cost-effective, indirect coal-to-liquid (CTL) fuel production through the FTS process pioneered by German scientists Franz Fischer and Hans Tropsch in 1923 [112] became widespread as an alternative source of fuel for the German military during World War II. Since the early 1950s, South Africa through the South Africa Synthetic Oil Liquid (Sasol) Limited company has used FTS technology extensively to produce diesel and jet fuel for domestic consumption from their vast reserves of coal to offset imports of crude oil [113]. Towards the late 1990s, both the U.S. and NATO military conducted extensive tests on different aircraft to certify the Sasol sourced CTL and gas-to-liquid (GTL) jet fuel for military use. Based on these tests, a synthetic turbine fuel was certified by the British Aviation Turbine Fuel Defense Standard 91-91 in 1999 [114]. As a result, jet fuel produced through the FTS procedure was the first pathway to be approved by the American Standard of Testing and Materials (ASTM) for use in commercial and military aircraft.

With a well-established military and civilian market for the fuel, the FTS methodology is a mature technology that begins with the gasification of coal or biomass or steam reforming of natural gas into syngas. This derived syngas is a mixture of hydrogen (H_2) and carbon monoxide (CO) that is purified, filtered, and enriched before it is passed through a catalytic reactor. Inside the reactor, syngas is converted over a bed of iron, cobalt, or ruthenium catalysts to yield different hydrocarbon chains. On the surface of these catalysts, a chain growth process occurs as H_2 is added, CO is dissociated, and a new methylene (CH_2) bond is created to act as the building block for the next set of chain reactions. Of all catalysts, iron is popular because of its low cost, its ability to catalyze the water gas shift reaction, and offer a wider range of hydrocarbon chains [115]. Meanwhile, cobalt is another catalyst option given its high activity and selectivity for producing long chain straight hydrocarbons [116].

The resultant synthetic crude generated from this process is then cracked and separated to produce a range of highly tailored chemical products. Based on the operating temperature, pressure, and syngas composition, it is possible to control the output carbon numbers to yield a synthetic kerosene suitable for aviation [24]. Typically, the liquid yield is nearly 70% of the dry weight of coal with overall thermal efficiencies between 60 to 70% [117]. Here, it is important to mention that the feedstock itself could have different outcomes to produce jet fuel in terms of efficiency, although the principle reactions governing the FTS procedure remain the same. For example, using natural gas as the feedstock exhibits environmental advantages in terms of net emissions and yields a higher ratio of H_2/CO than using coal. On the other hand, biomass as a feedstock potentially results in a better gasification efficiency than both coal and natural gas due to a higher reactivity; however, there can be catalyst fouling problems due to the presence of sodium, potassium, and other substances in plant matter [117]. Overall, the basic reactions of the FTS process are listed as follows:

$(2n + 1)H_2 + nCO \rightarrow nH_2O + C_nH_{2n+2}$	(alkanes/paraffins)	(1)
$2nH_2 + nCO \rightarrow nH_2O + C_nH_{2n}$	(alkenes/olefins)	(2)

Commercially available fully synthetic jet fuel (FSJF) derived from coal is a mixture of a varying proportion of hydrocarbons where isoparaffinic kerosene (IPK) is usually considered the main component. Typically, the low temperature FTS process yields long-chain n-alkanes with a high cetane number (CN), subsequently ideal for CI combustion [118]. However, to tailor the jet fuel for volatility, the alkanes are oligomerized followed by hydrotreating and distillation to produce to branched alkanes, primarily mono- and di-methyl substituted, and subsequently separated into the desired distillation range [119]. As a result, the properties favoring CI combustion (e.g., CN) are lost as isoparaffins and aromatics; hence, the resultant jet fuels have higher activation energies for combustion [118]. Additionally, heavy naphtha kerosene (containing about 10% aromatics, light distillate #1, with about 24% aromatics, and naphtha #2, containing about 39% aromatics) makes up the remainder of the stream [120]. This variability in the percentage of aromatics is of interest for engine performance and emissions due to the high ratio of carbon to hydrogen atoms. On the other hand, synthetic jet fuel derived from natural gas is said to have enhanced combustion properties since the fuel is mainly composed of n-alkanes and iso-alkanes that results in a lower density but higher autoignition properties as compared to jet fuels derived from crude oil or coal [121]. However, both types of FTS fuels have gained significance for the U.S. military as they tend to burn clean and produce 2.4% less CO_2, 50 to 90% less soot, and almost no sulfur [122]. Moreover, they are stable across a wide range of operating temperatures, ideal for the extreme conditions required to certify military vehicles under the single fuel forward policy (SFFP) [123].

Considering the relevance of this topic to the U.S. DoD, the Syntroleum Corporation was the first U.S. manufacturer of FTS jet fuels derived from natural gas, to primarily cater to the requirements of the USAF. Their initial tests on gas turbine engines used 'S-8' and 'S-5' synthetic jet fuels produced using Syntroleum's patented GTL technology. This technology uses air instead of pure oxygen to catalytically convert the natural gas to syngas in an efficient process called as auto-thermal reforming [124]. Additionally, a low temperature cobalt catalysis process was used to achieve higher selectivity and greater yields of hydrocarbons with lower net carbon emissions [125]. In addition, the H_2/CO ratio of the syngas is close to the ideally desired 2:1 for the FTS technique.

Overall, the use of synthetic jet fuels for aviation has increased significantly in the past few decades. However, because of the pertinence of the SFFP, it is important to understand how these fuels influence the CI engine combustion process. As a result, the following section provides a chronological overview of CI engine tests with synthetic aviation fuels. For brevity, aviation fuels from Syntroleum Corporation are abbreviated as S-5 and S-8; whereas, fuels from Sasol Limited are referred to as synthetic paraffinic kerosene (SPK). The summaries represent the engine specifications, test conditions, and results relevant to the SFFP. Most importantly, since synthetic aviation fuels have a composition, viscosity, density, and bulk modulus different from ULSD#2 and JP-8, the factors affecting engine performance, emissions, and fuel injection are discussed in detail.

Literature Review of FT Jet Fuels

The first study of a synthetic aviation fuel in a CI engine was conducted by Frame and Blanks [126] at the Southwest Research Institute (SwRI) in 2003. They studied the exhaust emissions from a 6.5 L, indirect injection (IDI), and V-8 configuration turbocharged unit from a High-Mobility Multipurpose Wheeled Vehicle (HMMWV), fitted with a mechanical fuel injection system. The fuel was derived from natural gas and is referenced as S-5. They used the heavy duty EPA Federal Test Procedure (FTP) and San Antonio

Transit (SAT) transient cycles to analyze tailpipe exhaust emissions. Overall, their tests revealed a decrease in PM, NO_x, CO, HC, and CO_2 emissions as compared to ULSD#2 by nearly 10%. Furthermore, their BSFC was slightly reduced for the alternative fuel.

In 2004, Frame et al. [127] report the exhaust emissions from a military engine operated using S-5 fuel from the Syntroleum Corporation. The engine was a new 6.5 L, V-8 configuration turbocharged unit from a HMMWV while the testing was performed in accordance with the FTP and SAT test cycles. Their test results indicated the benefits of using S-5 fuels to reduce emissions. Firstly, the higher CN of S-5 results in a smaller premix burn than ULSD#2 that reduces the formation of NO_x. In addition, the absence of aromatics in the fuel reduced the flame temperature to further lower levels of NO_x. Next, the reduced density and viscosity resulted in decreased PM emissions as the atomization of fuel was increased and the mixture within the combustion chamber became more homogenized. Lastly, the S-5 fuel demonstrated a lower lubricity that could damage the fuel pump over prolonged use. As a result, a lubricity improver was recommended for military ground equipment where diesel fuel is substituted with S-5.

In a comprehensive report presented to the U.S. Army in 2007, Frame et al. [128] document exhaustive HMMWV engine tests with an alternative S-8 jet fuel. The first section highlights the importance of additives to improve the lubricity of the alternative jet fuel. Then, the second section indicates the compatibility of viton, butadiene, nitrile, and flurosilicone rubbers found in injection pumps with the low aromatic fuel. In the report, four different engine injection systems were used: Stanadyne rotary pump from a HMMWV engine, a Bosch inline pump from a Cummins 6CTA 8.3 engine, a unit injector from a Detroit Diesel Corporation (DDC) 8V92T engine, and hydraulically actuated electronic injector for the Caterpillar 3116 and 3126B engines. The nitrile rubber seals are deemed most susceptible to failure

while the flurosilicone seals showed no disintegration when switching from JP-8 to S-8. The second section in their report illustrated the cold start capability with S-8 in a HMMWV IDI engine. Here, the higher CN of S-8 enabled a faster cold start as compared to ULSD#2 and cranked without the need for glow plugs. In addition, the smoke formation at the tailpipe was reduced for the S-8 fuel. Finally, HC emissions were found to be significantly lower. In general, this manuscript was important in helping certify synthetic jet fuel for the SFFP.

In 2008, Alvarez and Frame [129] compared performance, fuel economy, and emissions of three military tactical generators running on S-8 fuel. Their Tactical Quiet and MEP 803A generators were first operated on ULSD#2 for 100 hours and then switched to a 50-50 blend of JP-8 and S-8 for 450 hours of operation. Furthermore, their 10 kW-60 Hz generator was operated for 1000 hours with S-8 fuel. Their endurance tests revealed no drop in performance except for a change in emission levels associated with a change in fuel. Due to its low aromatic character and higher CN, there was a drop in both NO_x and CO emissions with the S-8 fuel. Meanwhile, the emissions with the blend of JP-8 and S-8 were between levels of S-8 and ULSD#2. Lastly, a visual inspection of the pump did not reveal any wear associated with the lower viscosity fuels.

In the same year, Schulman and Frame [130] conducted durability tests with S-8 fuel in a Caterpillar C7 engine used in most medium tactical vehicles of the U.S. Army. The engine was tested using a 420-hour Tactical Wheeled Vehicle test cycle that simulated 40000 hours of ground operations. Overall, engine performance remained constant for JP-8, S-8, and blends of JP-8/S-8. However, a decrease in the volumetric energy density of these fuels caused a 6% drop in performance as compared to ULSD#2. As expected with emissions, the S-8 fuel showed an 8% and 6% reduction in CO_2 and HC emissions,

respectively, as compared to both JP-8; whereas, the NO_x levels remained nearly same for all fuels tested. Again, fuel pump inspections indicated no wear caused by the synthetic fuels.

In a study conducted by the U.S. Army Tank Automotive Research, Development & Engineering Center (TARDEC) at SwRI in 2009, Hansen and Frame [131] evaluated a HMMWV engine with ULSD, JP-8, S-8, and a 50-50 blend of JP-8 and S-8. The test involved a 100-mile track within the SwRI campus and the data were recorded using mobile instrumentation fitted inside the vehicle. In addition, the test engine was the same turbocharged IDI V-8 engine with a mechanical rotary fuel pump as described in a previous paragraph. Most importantly, the tests were performed alternatively by loading and unloading the vehicle to demonstrate fueling with a payload. In general, use of the S-8 fuel resulted in a lower fuel economy compared to ULSD#2 and JP-8, as volumetric energy density is reduced. However, emissions for the S-8 fuel were the lowest of all fuels as the CN was the highest and atomization was vastly better; hence, promoting complete combustion and reduced NO_x formation. Finally, no fuel pump wear was observed after analyzing the components after completing the tests with the S-8 fuel.

In 2010, Hoogterp-Decker and Schihl [132] investigated the benefits and risks associated with the use of synthetic fuels in CI engines for the TARDEC program. The authors tested ULSD#2, JP-8, SPK and a 50-50 blend of JP-8 and SPK fuel in an AVL single cylinder research engine and two heavy duty military diesel engines (General Engine Products (GEP) 6.5 L and Cummins VTA 903). The military engines were subjected to 400 hours of NATO evaluation test cycles and were tested at full load recorded at 60%, 75%, and 100% of rated speed. Furthermore, the research engine was evaluated at full-load conditions at speeds ranging from 1250 to 2200 rpm. They found that all three engines had a loss in power with the JP-8 and S-8 fuels compared to the baseline ULSD#2. This loss in power is a result of a lower volumetric energy density and variances in the fuel injection process caused by differences in fuel density and

viscosity. Furthermore, the ignition delay increased with the use of the low CN and less volatile S-8 fuel that resulted in a large premix burn phase. As a result, the S-8 burned more fuel during the premix phase with a lowered injection velocity, resulting in a short mixing controlled diffusion phase. Lastly, S-8 had a lower fuel consumption that resulted in reduced exhaust temperatures, an important factor considering the low thermal signature required on the battlefield. As a conclusion, the authors suggest using different injection strategies based on a closed-loop control of sensors.

In the same year, Wadumesthrige et al. [80] verified the long-term performance and durability of a CI engine running on a GTL fuel (S-8) for a trailer-hauled generator unit capable of providing electrical power, heating and cooling, purified water, communication, and lighting. The tests consisted of a 240-hour endurance test: about 8 hours per day at 60% of full capacity and transient load testing of 20, 30, and 40 kW for a 2-hour runtime. When compared to baseline ULSD#2 tests, no wear or performance degradation was observed during the endurance tests. Furthermore, the S-8 fuel provided a lower BSFC and higher thermal efficiency, which can be attributed to the lower density and higher heating value of S-8; hence, a lower quantity of fuel was injected into the engine per cycle. Additionally, ULSD#2 has a higher bulk modulus than S-8, causing a faster pressure pulse and a subsequent advance in fuel injection. For the same engine, the advance in pressure buildup within the fuel system resulted in a longer injection duration. In addition, the lowered viscosity of S-8 resulted in better atomization of fuel and facilitated a more complete combustion process. Moreover, the higher CN of S-8 aids in autoignition and enables a greater amount of expansion work. With respect to emissions, the smoke opacity was lower for S-8 owing to factors like a reduced aromatic content, lower boiling point, and higher atomization. Finally, the authors discussed the instabilities in generator output caused by injection pump leakages caused by a premature nozzle closure and a reduced fuel injection level that required frequent correction by the engine governor. They highlight the construction of the Stanadyne pump,

which is a back-leak less design where the clearances between the nozzle needle guide and the body are not calibrated for the low viscosity of S-8 fuel and might end up causing fueling problems.

In 2011, Brandt et al. [82] conducted performance and endurance tests on an engine fueled with a FTS fuel derived from natural gas (SPK), a blend of this FTS fuel and JP-8, JP-8, and ULSD#2. The engine was a commercially available Ford 6.7L engine in a V8 configuration that is direct injected, turbo-charged, inter-cooled, and employed a fuel lubricated high pressure common rail injection pump with piezo-electric fuel injectors. The test followed the 210-hour Tactical Wheeled Vehicle Cycle prescribed by U.S. Army in addition to pre-test and post-test performance checks for power degradation. In spite of the deviation in the FTS fuel properties from ULSD#2, the engine performed as expected without any hardware failures. However, there was a loss in power of approximately 1 to 2% over each of the pre- and post-engine tests as an increase in temperature reduced the viscosity of fuel. Next, the engine emissions were normalized with respect to ULSD#2 over the pre, post, and endurance tests. The SPK fuel showed nearly 10% lower NO_x and 14% less CO generation over ULSD#2. This reduction in NO_x is likely the result of lower in-cylinder temperatures, changes to combustion phasing, and a smaller premix burn; whereas, the reduction in CO emissions is linked to a more complete combustion process through improved fuel atomization. Finally, an analysis of the engine components indicated no viscosity-related wear on both injector and pump parts for the tests with the SPK fuel.

In the same year, Subramanian and Ciatti [133] conducted a study on a low CN isoparaffinic kerosene (IPK, CN = 39) fuel and regular gasoline to explore low temperature combustion (LTC) regimes to control emissions. They used a modern, four-cylinder, 1.9 L GM CI engine fitted with a variable vane turbocharger, EGR port, and a Bosch electronic injection system. Furthermore, a split injection strategy was employed to achieve LTC via partially premixed combustion. The tests indicated a reduction in BSFC

and NO_x emissions for IPK as compared to diesel fuel due to the reduced CN and cooled EGR lowering cylinder temperatures. On the contrary, HC and CO emissions were higher for the IPK fuel since it increased the ignition delay resulting in a later combustion event. Furthermore, at low load conditions, IPK provided higher self-ignition temperatures that avoided the diffusion burn phase resulting in lessened PM emissions. In addition, use of EGR affected the split injection process by reducing the amount of oxygen available for the second combustion event. Finally, the main observation of the heat release calculations indicated that split injection with two separate heat release events decreased NO_x emissions.

Again in 2011, Claus et al. [134] at TARDEC determined the durability effects of SPK in a Detroit Diesel/MTU 8V92TA, two-stroke engine. The tests were conducted in accordance with the 400-hour NATO AEP-5 test certification with ULSD#2, JP-8, and a 50-50 blend of JP-8 and SPK. The only inference from this test is that no major performance degradation is noticed with JP-8 or SPK fuels. A minor loss in power was an outcome of the lower mass density of the synthetic fuel as compared to JP-8. Additionally, engine power loss could be due to a buildup of fuel and oil near the fuel injector as additives in ULSD#2 that act as detergents and fuel dispersants are absent in jet fuels.

The following year, Jayakumar et al. [135], determined the effect of inlet temperatures ranging from $30^{o}C$ to $110^{o}C$ on the autoignition of fuels with different CN and volatility. Additionally, they identify the processes that lead to LTC and the negative temperature coefficient (NTC) regime including the subsequent autoignition of fuel. Here, ULSD#2 was the main fuel while two different JP-8 fuel blends were tested (CN = 44 and CN = 31) along with a SPK fuel derived from natural gas. The engine is a high compression, directly injected, single cylinder unit, fitted with a solenoid operated injector. Based on experimental results, the JP-8 fuel with the lowest CN had the highest ignition delay; whereas, the SPK

fuel had the lowest ignition delay. As a result, this fuel experienced both LTC and NTC combustion. Additionally, LTC and NTC conditions were prevalent at low load conditions; whereas, at high load and high intake temperatures, both these regimes disappeared. Next, the rate of heat release (RHR) indicated a smaller peak of the SPK fuel as compared to ULSD#2 since its higher volatility and CN enhanced liquid fuel evaporation and accelerated autoignition reactions. In addition, the SPK fuel's 7% greater heating value (while being 12% lighter) resulted in a larger RHR over ULSD#2. Lastly, authors presented a STAR-CD Computational Fluid Dynamics (CFD) simulation on the spray behavior of fuel to understand the processes that trail the fuel injection. The simulation results based on a surrogate fuel described the direct relation between formation of different species of combustion with respect to the intake temperature and ignition delay. Furthermore, the simulation showed that formaldehyde is a strong precursor to the NTC combustion regime. To conclude, the model established the effects of intake temperature on the duration and magnitude of the LTC and NTC combustion zones in accordance with experimental data.

In 2012, Jayakumar et al. [135] investigated the effects of boost pressure and inlet air temperature on autoignition via CFD simulations and subsequent experiments. The fuels used in this study were ULSD#2 (CN = 45), SPK (CN = 61), and two different batches of JP-8 (with CN = 25 and 49). The single-cylinder engine had a high compression ratio and was direct-injected (DI) as equipped with a solenoid injector operated by a Bosch ECU. Combustion experiments revealed the effects the influence of volatility, CN, heating value, and density of the test fuels on ignition delay. In specific, the ignition delay was reduced with an increase in boost pressure because of enhanced spray evaporation and turbulent mixing. Furthermore, boosting the intake pressure introduced more oxygen into the combustion chamber subsequently augmenting turbulence that enhanced mixing and atomization, leading to a further decrease in ignition delay. In addition, growing the boost pressure reduced spray penetration length

that prevented fuel from reaching the walls; hence, enhancing chemical reactions. Moreover, the higher volatility of the SPK fuel reduced the time between the start of injection and the initial exothermic reactions that precede combustion. However, its CN negatively influenced the RHR as its earlier combustion resulted in a lower peak heat release rate as compared to the other fuels tested. For similar reasons discussed with respect to boost pressure, a high intake temperature resulted in a reduction in ignition delay. The experimental results also indicated a strong correlation between the physical ignition delay and fuel volatility, while CN strongly influenced the chemical delay and autoignition reactions. Finally, these authors present a brief CFD study of the fuels in the same engine and point out the influence of combustion intermediates that affect the autoignition reactions. The CFD outcomes highlighted the formation of certain products (e.g., formaldehyde) that tend to eliminate LTC and the NTC regime of combustion. Here, as the reaction of formaldehyde proceeded, the oxidation reaction rates were found to increase sharply. Finally, the model indicated similarities between the effects of increased boost pressure and increased air intake temperature on the reduction of ignition delay and elimination of LTC and NTC combustion zones.

Again in 2012, Schihl et al. [136] studied the ignition behavior of a low CN IPK fuel from Sasol in a single cylinder AVL 521 engine via a single-injection event. The experimental engine had a hydraulically actuated electronic unit injector (HEUI) fuel injection system set at 1900 bar and was tested with ULSD#2, JP-8, IPK, and a 50-50 blend of IPK and JP-8 at speeds between 1250 and 2250 rpm. The tests were performed in two sets: the first with high, medium, and low load conditions and the second employing a closed loop air induction system with varying charge densities. As expected, the IPK fuel had poor low speed and low load combustion performance and grew the ignition delay by nearly 30% as compared to JP-8. Furthermore, the ignition delay showed a strong correlation with bulk cylinder temperatures lower than 800 K. Additionally, the longer ignition delay of IPK led to near misfiring

conditions along with a prolonged rate of heat release. In addition, a 10 to 20% longer ignition delay is observed for the IPK fuel at medium to high loads with respect to JP-8. Meanwhile, the 50-50 blend of IPK and JP-8 considerably reduced the ignition delay as compared to neat IPK. At higher loads and speeds, IPK showed no anomalies at different charge densities as compared to the other fuels tested at ignition temperatures around 850 K; whereas, testing at temperatures below 800 K has a slight ignition delay. As a result, IPK displayed around a 20% variance of ignition in comparison to the baseline fuels and to the blend of JP-8 and IPK at bulk ignition temperatures and pressures of less than 800 K and 60 bar, respectively. For the density experiments at temperatures above 950 K, ignition delay showed a lower variance with cylinder pressure. Finally, it was stated that modern injection systems would help to eliminate the effects of ignition delay caused by the obsolete HEUI injection system.

In an effort to qualify the use of alternative jet fuels in ground support vehicles for the U.S. Army, Muzzell et al. [137] present a report on the use of synthetic jet fuels as diesel substitutes on the battlefield. The report contains descriptions of seven stages of demonstrating technology readiness levels of the fuels. Stages five to seven are the focus of this review as it established the performance of CI engines with different blends of alternative fuels. In their report, the engines selected included a GEP 6.5L Turbo, Caterpillar C7, DDC/MTU 8V92T, Cummins VTA-903T, Navistar MaxxForce 9.3D, and Ford 6.7L “Scorpion” Powerstroke. These engines had either a Stanadyne rotary injector or a high-pressure common rail system. Furthermore, the engines were subjected to a 400-hour NATO test or a 210-hour U.S. Army Tactical Wheeled Vehicle endurance drive cycle. Besides, the tests featured seven MEP generator sets ranging from 2 kW to 100 kW that are evaluated based on the PM-Mobile Electric Power certification. Furthermore, stages six and seven evaluated the performance of nine different tactical vehicles and eight ground support equipment for real time performance. In addition, the operating parameters for each test were set for ambient or desert conditions. The outcome of all the

dynamometer tests indicated that the engines and fuel injection systems were compatible with the synthetic aviation fuels without any durability issues. At a maximum, the reduced viscosity and bulk modulus along with the lower volumetric energy density of these fuels resulted in a 2 to 7% power loss over the different test scenarios. Moreover, the test track engine performance results indicated a 7.8% uphill and 17.7% downhill reduction in acceleration for HMMWV vehicles with a payload, operating on SPK/JP-8 blends as compared to JP-8 fuel. As in the previous case, the lower volumetric energy density and bulk modulus of SPK resulted in this loss of performance under strained operating conditions.

In 2014, Gowdagiri et al. [138] carried out measurements of ignition delay, CO and NO_x emissions in a mechanically-injected, Yanmar L100D single cylinder CI engine with an EGR port. The tests were performed at 25%, 50%, and 75% engine loads. The fuels highlighted in this review include standard diesel fuel, a hydroprocessed jet fuel from camelina (HRJ-5), and a GTL fuel (S-8) along with standard JP-5 and Jet-A. The test results illustrated that ignition delay decreases with growing Derived Cetane Number (DCN) by about 15% for DCNs from approximately 40 to 80, which is a strong function of the physical delay caused by the mechanical injection system. Moreover, BSFC increases with a decrease in DCN due to a reduction in expansion work as the ignition is delayed into the expansion stroke. Furthermore, CO emissions correlate with DCN as a lower ignition delay allows more time for the unburned fuel to complete combustion. Finally, NO_x emissions were dependent on an increasing H/C ratio in the S-8 fuel that resulted in a lower adiabatic flame temperature, subsequently enhancing thermal NO_x formation kinetics.

Later in 2014, Zheng et al. [139] highlighted the effects of using different concentrations of CN improver 2-ethylhexyl nitrate (2-EHN) in a high speed, single cylinder DI engine fueled with Sasol IPK. The fuels tested included IPK plus a 0.1% CN improver (DCN = 37.9) called Sasol0.1 and a 0.4% CN improver (DCN

= 41.5) called Sasol0.4. During their tests, the injection pressures were set to 400, 600, and 800 bar. Overall, the tests revealed a nonlinear relationship between the ignition delay and 2-EHN percentage as evident in the RHR. In specific, the RHR peaks increased by adding the improver but the degree of reduction in ignition delay decreased with the rise in additive. They found that IPK without an additive has a 5% drop in indicated thermal efficiency with respect to Sasol0.4. Furthermore, neat IPK has the largest premix burn phase and ignition delay along with the largest NTC of the three test fuels. Additionally, the effect of the CN improver on ignition delay is more prominent at low injection pressures and temperatures. Moreover, the CN additive accelerated endothermic reactions during the pre-combustion phase and reduced the NTC rate. Furthermore, CO and HC emissions were reduced by the improver that was postulated to reduce overlean mixtures while enhancing oxidation reactions. However, PM emissions grew with the addition of the CN additive as it decreased the ignition delay, subsequently reducing the level of premixed burn while augmenting the diffusion burn phase. Typically, since Sasol fuel has a long ignition delay, its greater volatility results in overlean mixtures with equivalence ratios not in the range for soot formation; hence, PM emissions are expected to be reduced. Instead, with the addition of the CN improver, the reduction in ignition delay grew local equivalence ratios as the mixing time prior to autoignition is reduced; thus, promoting greater PM emissions. However, NO_x emissions increased since the additive grew the rate of autoignition reactions that overshadowed the effect of reducing the premixed combustion fraction. As a result, irrespective of injection pressures, NO_x emissions increased with CN additive because it augmented the RHR promoting more constant volume combustion.

In 2015, Schihl et al. [140] extended their previous work to determine the effect of using low CN synthetic jet fuels in military CI engines. In these experiments, the authors tested 25, 50, and 75% blends of CTL and JP-8 and compared the results with tests taken with neat CTL, JP-8, and ULSD#2 fuels. The

engine setup and representative tests are the same as listed in their previous work [136]. Under high load conditions, little variance in ignition delay was observed during all test conditions. However, at lower engine speeds, the authors observed a negative performance of CTL fuels with its reduced volumetric energy density being the main factor. At medium loads, the CTL fuels exhibited a greater ignition delay with respect to the other fuels tested at lower speeds, as well as a more optimal combustion phasing than baseline ULSD#2. This was likely caused by the lower mass of injection per stroke for the CTL fuel. At lower load conditions, the CTL blends performed similar to ULSD#2 while the effects of decreased CN became apparent as the percentage of CTL in the blends grew. Furthermore, neat CTL showed almost misfiring conditions at low speeds without the use of multiple injection events. Overall, the volatility and volumetric energy density of CTL affected the performance and thermal efficiency of the engine. Finally, mean ignition charge densities were impacted at low load and low speed operations where the mean ignition temperatures were lower than 750 K, subsequently resulting in a highly delayed combustion event. This resulted in steep cylinder pressure rise rates, possibly exceeding safe design limits.

In 2015, Soloiu et al. [141] investigated reactivity controlled compression ignition (RCCI) combustion employing the direct injection of S-8 and port fuel injection (PFI) of n-butanol. The engine was a single cylinder, naturally aspirated research unit with a mechanical fuel pump for the direct injection process. The tests were performed with ULSD#2, neat S-8, a 50/50 blend ULSD#2 and PFI n-butanol by mass, and a 50/50 blend of S-8 with PFI n-butanol by mass. As expected from the lower volumetric energy density of S-8, its injection event was longer in comparison to ULSD#2. Moreover, the peak pressures were reduced for the higher CN S-8 fuel as less time is available for mixing due to a decrease in ignition delay causing a smaller premixed combustion phase and more pronounced diffusion burn. Overall, the combustion phasing of blends of S-8 and n-butanol were between that of ULSD#2 and neat S-8. With

respect to emissions, the smaller premix event with S-8 lowered in-cylinder temperatures, which reduced NO_x formation by over 30% as compared to ULSD#2. On the other hand, PM emissions increased almost three times due to the growth of the diffusion burn duration. However, the oxygenated n-butanol injection for RCCI combustion reduced soot formation by nearly 66% as compared to ULSD#2. Meanwhile, the subsequent over-leaning with RCCI combustion led to a spike in CO and HC emissions.

In 2016, Soloiu et al. [142] investigated pre-mixed charge compression ignition (PCCI) using S-8 and n-butanol. The experiments were conducted using 65% by mass PFI n-butanol and 35% by mass S-8 direct injection while employing 35% EGR. The test engine was a naturally aspirated, four-stroke, liquid cooled engine fitted with a plunger type mechanical fuel injection system modified to offer port fuel injection and direct injection. The experiments were carried out at a constant speed of 1500 rpm and varying loads of 1, 3, and 5 bar BMEP. The low fuel viscosity of S-8 resulted in a delay in the injection process while its reduced volumetric energy density caused a longer duration of injection. Furthermore, it was found that PCCI enabled simultaneous reduction of NO_x and soot at 1 and 3 bar BMEP. In specific, at 1 bar, NO_x decreased by 82% while soot formation was reduced by 46% as compared to baseline ULSD#2 tests. Similarly, at 3 BMEP, soot formation decreased by 18% while NO_x emissions reduced by nearly 92%, as compared to conventional CI combustion. Here, this reduction in NO_x emissions can be explained by S-8's higher CN number, which resulted in a shorter ignition delay and lessened pre-mixed combustion phase. Further, at lower loads, soot emissions were reduced in the presence of EGR due to the addition of an oxygenated fuel and leaner air fuel mixtures. However, at a higher load of 5 bar BMEP, the classical NO_x-soot tradeoff became evident, as NO_x decreased by 97% with the presence of 35% EGR. In addition, the addition of a low-reactivity fuel like n-butanol created a heat sink within the combustion chamber, subsequently increasing the difference between bulk cylinder temperature and

local combustion temperatures. When testing CI baseline conditions, since soot is formed in fuel rich zones, ULSD#2 displayed lower amounts of soot than neat S-8 since it had a reduced diffusion burn phase. Whereas, comparing ULSD#2 against S-8 in PCCI conditions found that high rates of EGR and near-stoichiometric air fuel mixtures at high loads beyond the smoke limit resulted in a 500% increase in soot. However, HC and CO emissions increase with dual fuel combustion as some of the port injected n-butanol either escapes through the open exhaust valve due to valve overlap or is forced into the cylinder crevices during compression. Therefore, to take advantage of the reduction in NO_x with PCCI combustion, the authors proposed supercharging and optimizing fuel injection events to mitigate the excessive formation of soot and HC/CO emissions.

In 2017, Soloiu et al. [143] conducted tests of ULSD#2 blended with SPK derived from natural gas. The test engine was a single cylinder, naturally aspirated, IDI engine. Here, ULSD#2 was the base fuel for comparison, while a blend of 20% SPK and 80% ULSD#2 along with neat SPK were studied. The heat release analysis indicated that ULSD#2 had higher peak RHR than SPK and its blends. Furthermore, SPK and its blends had a shorter ignition delay due to its greater CN advancing combustion and decreasing the level of air fuel mixing; hence, a lower premix burn phase. The results of the SPK and ULSD#2 blend emissions analysis revealed reduced NO_x at low loads, increased NO_x at medium loads, and similar NO_x levels at high loads with respect to ULSD#2. Additionally, neat SPK demonstrated reduced NO_x at low loads. Furthermore, soot emissions are reduced for SPK and its blends due to a lower sulphur and aromatic content, subsequently improving atomization and volatility. They did find high levels of HCs for SPK (28% greater than ULSD#2) due to leakages in the fuel pump caused by its low viscosity. Moreover, SPK and its blends demonstrated a decreased thermal efficiency since these fuels had a reduced higher heating value as compared to ULSD#2. Finally, mechanical efficiency increased for SPK because of a reduction in heat flux with the increase in the work transferred to the engine in contrast to ULSD#2.

In the same year, Soloiu et al. [144] conducted an experimental investigation on the combustion and emissions characteristics of n-butanol/GTL and n-butanol/ULSD#2 blends (n-butanol blended in both cases as 25% and 50% by mass) in a single-cylinder experimental CI engine. The engine was run with 15% EGR and a boost pressure of 1.2 bar. The authors reported that GTL's lower viscosity and density caused the injector to be open longer, subsequently delaying the fuel injection process. For these same reasons, the spray penetration of GTL was lower than ULSD#2. Next, the higher CN of GTL resulted in a lower peak pressure and a longer diffusion burn phase across all loads as compared to ULSD#2. With regards to emissions, the GTL fuel showed an increase in soot emissions by nearly 250% over ULSD#2 at full load due to its considerably longer diffusion burn phase. Meanwhile, its lowered peak pressures and the absence of aromatics reduced NO_x levels by over 36% as compared to ULSD. Furthermore, the GTL fuel grew both HC and CO emissions for the same reasons as the increase in PM. However, for fuel blends with a higher proportion of GTL fuel, its higher energy content and uniform combustion phasing resulted in a greater thermal efficiency. Additionally, the shorter ignition delay leads to lesser accumulation of fuel during combustion which tends to reduce in-cylinder temperatures and peak pressure during the premix burn that leads to lower heat losses to the cylinder walls and an overall improvement in thermal efficiency.

In a final study in 2017, Soloiu et al. [145] investigated the performance of an experimental CI engine when fueled with a blend of 80% ULSD#2 and 20% CTL jet fuel. The engine was equipped with an electronic fuel injection system, 15% EGR, and supercharging. In addition, the injection system had two set points, 800 bar and 1200 bar. Comparing the performance of ULSD#2 and the 80-20 blend, the lower CN CTL fuel grew the ignition delay which increased the premix burn phase since the fuel has more time to mix with the inducted air. When the injection pressure was increased, the pressure peak grew due to an enhanced atomization. Furthermore, the higher energy content of the CTL fuel resulted in a

decreased BSFC. As a result of this decreased level of fueling with CTL and its blends, both NO_x and soot emissions decreased for the high-pressure condition as lower in-cylinder temperatures and leaner mixtures were observed.

Summary of FT Jet Fuels

From the literature review, the CTL fuel tests in CI engines have brought to light the influence of CN on combustion. Of importance, jet fuel manufacturers do not need to comply with CN rating regulations since jet fuel burns in a continuous flame that does not require good autoignition characteristics. Here, the presence of isoparaffinic components, cycloparaffins, and naphthalenes in this fuel results in a low CN, which affects engine performance. As a result, CTL fuels typically result in a delayed ignition process that might result in unstable engine operation. Furthermore, this longer ignition delay leads to a greater premix burn, which increases the peak RHR that could potentially damage engine components. Subsequently, this often generates greater in-cylinder pressures and temperatures; hence, NO_x emissions grow in comparison to JP-8. Next, the effects of low viscosity and high volatility lead to better atomization and evaporation, increasing the premix phase of combustion. Furthermore, a lower H/C ratio reduces combustion efficiency and increases the adiabatic flame temperature. Meanwhile, the low density of CTL fuels results in a drop in the volumetric energy density, which serves to decrease the amount of fuel burnt and reduces premix burn. As a result, if the CN is sufficiently low, both premix burn and NO_x levels increase compared to JP-8 and ULSD#2. Next, a reduced diffusion burn with delayed combustion event, reduces PM, CO, and HC emissions. In addition, the low aromatic content of CTL fuel prevents the formation of polycyclic hydrocarbons acting as precursors to the formation of soot. Finally, as CN delays the initial phase of combustion, this results in a greater constant volume-like combustion event that serves to reduce BSFC. However, a lesser volumetric energy density results in greater fuel

consumption. Another factor working against CTL fuel is the global effort to reduce the usage of coal and fuel manufacturers have turned to natural gas as a feedstock to decrease their carbon emissions.

As a result, GTL fuels have gained popularity due to reduced emissions, convenient transportation, and a reduced cost of production. Moreover, the steam reforming process used to produce GTL fuel yields syngas with a higher H_2/CO ratio. Typically, the CTL process produces syngas with a H_2/CO ratio of 0.7 and relies on the water gas shift to increase the hydrogen content in the syngas stream. This results in a more energy intensive process while simultaneously raising GHG emissions. On the other hand, the GTL pathway yields syngas that is closer to the stoichiometric value of 2.2 through steam reforming of natural gas [146]. Hence, the reasons for the higher quality syngas stem from enhanced selectivity through the use of cobalt catalyst and higher energy content (H/C ratio) of natural gas. From a point of view of IC engines, GTL fuels predominantly consist of straight chain paraffins, which results in a relatively high CN and heat of combustion as compared to ULSD#2, CTL, and JP-8. Subsequently, this enables a shorter ignition delay that decreases premix burn while augmenting the diffusion burn phase; hence, reducing the cylinder pressure rise that lowers cylinder temperatures [147]. Furthermore, the effects of a lower viscosity benefit the atomization and evaporation processes to create a homogenous air-fuel mixture. Therefore, reduced levels of thermal NO_x are seen for GTL fuels as compared to CTL or Jet-A fuels. As a result, one would expect higher PM emissions with a greater duration of combustion. However, the absence of aromatics prevented the formation of PAHs that act as precursors to the formation of PM. Furthermore, the higher heating value of GTL fuel results in a lower BSFC as compared to CTL and Jet-A. Moreover, GTL fuel has better thermal stability than other alternative fuels; hence, this generates a more predictable engine performance over the fuel's lifetime. Overall, GTL tests in CI engines show combustion characteristics exactly opposite to those of low CN CTL fuels, leading to better engine performance, lower BSFC, and reduced levels of PM emissions.

In addition, the properties of CTL and GTL fuels have resulted in a few issues with respect to the fuel injection system. As stated, their reduced bulk modulus, viscosity, and density can influence optimal fuel injection events and result in unsatisfactory engine performance. Furthermore, their lower viscosity can induce fuel leakage and slippage past pump clearances while potentially causing poor lubricity. As a result, with modern common rail injection systems operating at pressures close to 2000 bar, fuel systems could catastrophically fail with inadequate lubrication. Furthermore, its lower viscosity reduces the fuel penetration within the cylinder and increases the angle of spray, affecting the physical portion of ignition delay. These events could disturb the air-fuel mixing in the cylinder, leading to more heterogeneous combustion than desired. However, improvements in metallurgy and manufacturing processes along with the introduction of higher speed sensors and controls have helped tackle this issue.

Overall, the U.S. DoD has simultaneously undertaken efforts to reduce dependency on foreign oil and promote the use of alternative fuels. Since the technology to produce CTL and GTL fuels is mature, this allows for competitive pricing with conventional petroleum derived jet fuels. In addition, with their tailored compositions and fuel properties, these fuels can provide better thermal stability in harsh environments associated with combat. As a result, as the price of crude oil increases, both CTL and GTL fuels will assume a larger share in the U.S. military inventory, subsequently requiring continued research on the subject.

To summarize the CTL and GTL fuels, the coal gasification and steam reforming pathways for coal and natural gas respectively have reached technological maturity in terms of energy utilization and product yield. However, the more paraffinic GTL jet fuels show better CI engine performance than CTL jet fuels, ULSD#2 and conventional Jet-A/JP-8. Primarily, the higher CN of GTL fuels reduces ignition delay, premix burn that results in a more gradual and longer heat release event with lowered NO_x emissions compared

to CTL fuels. In fact, GTL fuels have exhibited the simultaneous reduction of NO_x and PM. Furthermore, the adoption of GTL technology has been more widespread as the costs associated with extracting and transporting natural gas are lower than coal. Based on the research articles reviewed, the parameters affecting emissions and fuel consumption of CTL and GTL jet fuels are listed as arrows in Table 4 and Table 5 respectively. The property column is indicative of the increasing or decreasing magnitude of the parameter under consideration compared to Jet-A.

Table 4: Estimated correlations based on literature review of CTL jet fuels in CI engines vs Jet-A/JP-8

Property	NO_x	CO	HC/PM	BSFC
Density ↓	↓	↑	↑	↑
Viscosity ↓	↑	↓	↓	↓
CN ↓	↓	↓	↓	↓
HV ↑	↓	↓	↓	↓
Volatility ↓	↓	↑	↑	↑

Table 5: Estimated correlations based on literature review of GTL jet fuels in CI engines vs Jet-A/JP-8

Property	NO_x	CO	HC/PM	BSFC
Density ↓	↓	↑	↑	↑
Viscosity ↓	↑	↓	↓	↓
CN ↑	↓	↓	↓	↓
HV ↓	↑	↑	↑	↑
Volatility ↓	↓	↑	↑	↑

Hydroprocessed Esters and Fatty Acid (HEFA) Jet Fuels

In the past decade, HEFA based jet fuels have been produced from feedstocks like camelina, jatropha, algae oils, animal fats, and waste cooking oils to prevent competition for cultivable land with food crops. Although these fuels include distinct chemical pathways for production, intermediate compounds like triglycerides and free fatty acids (FFA) are the common building blocks necessary to produce synthetic aviation fuels. Of note, HEFA jet fuels are also referred to as hydroprocessed and renewable jet (HRJ) or hydrotreated vegetable oil (HVO) jet fuels. In addition, a HEFA jet fuel produced through Syntroleum Corporation's Bio-Synfining™ process is commonly referred to as R-8.

Currently, the large-scale production of HRJ jet fuel represents a mature technology, where Honeywell and Syntroleum Corporations [148] remain the dominant mass producers. These companies implement a process called hydrogenation represented in Figure 3, which involves saturation of the double bond through the catalytic addition of hydrogen in a reaction controlled environment to yield intermediates like triglycerides [149]. To begin with, the oils are catalytically hydrogenated to convert liquid phase unsaturated FFAs into saturated FFAs with the addition of hydrogen. After the molecules are saturated, the addition of hydrogen results in the conversion of glycerol to propane, in the presence of a catalyst. Subsequently, the propane molecule is cut to produce three moles of FFA per mole of triglycerides. Further, the carboxyl acid species attached to the FFA is removed to form straight chain hydrocarbons based on the selectivity of the process. In the last stages, the process consists of any of three steps; i.e., decarboxylation, decarbonylation, or hydro-deoxygenation. The decarboxylation process removes oxygen in the form of carbon dioxide while the decarbonylation step removes oxygen as carbon monoxide and hydro-deoxygenation displaces the oxygen in the water. The subsequent process involves the hydrotreating and hydro-isomerization of paraffins that yields a synthetic jet fuel, meeting ASTM

D7566 standards (as of 2011) for cold flow and high flash point [150]. Here, the resultant fuel is an SPK with carbon chains ranging from C_9 to C_{15} [148] and the composition varies significantly with each proprietary bio-refining process and feedstock.

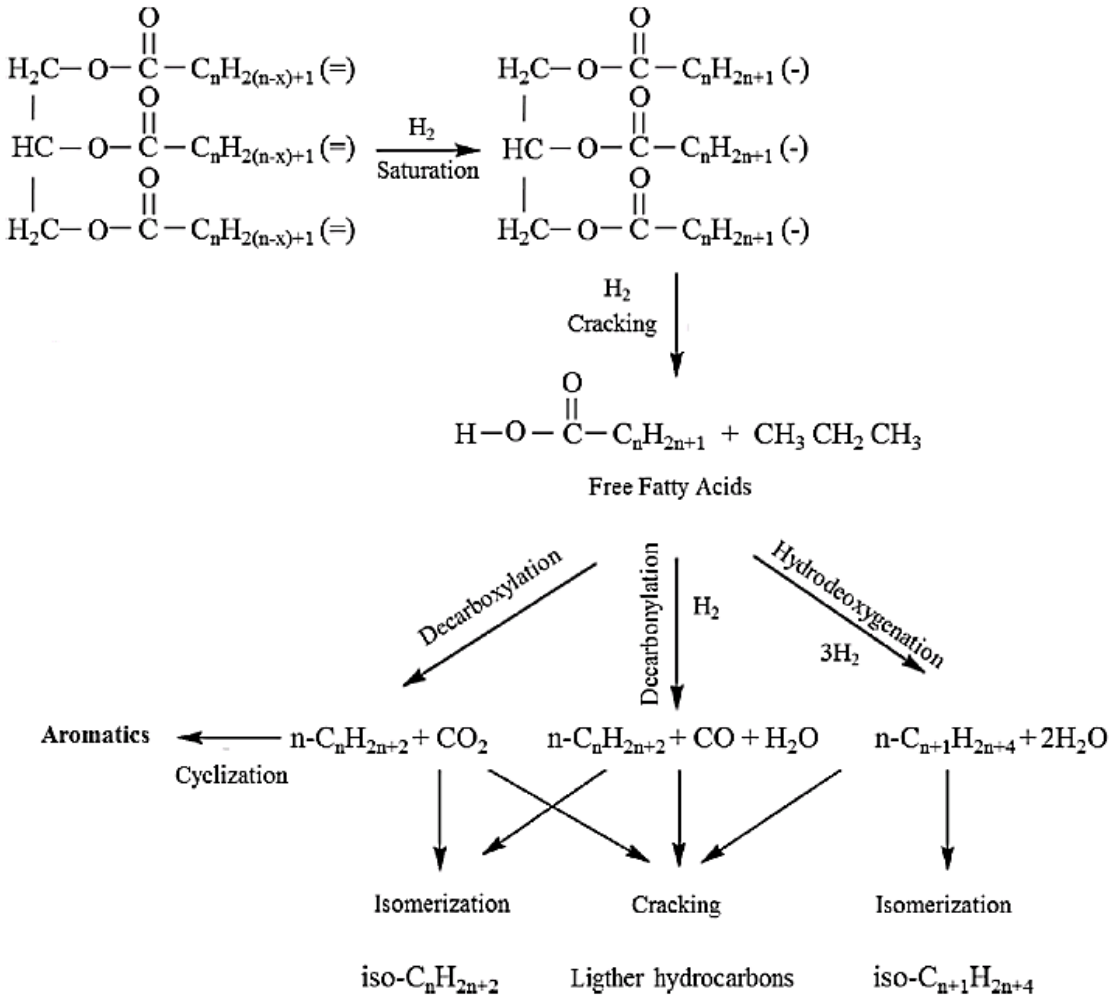

Figure 3: Catalytic conversion of vegetable oils or animal fats to light hydrocarbons via hydro-treatment [151]

Another process to manufacture jet fuel from plant-based oils is called through catalytic hydrothermolysis (CH). Jet fuel derived through the CH process complies with ASTM standards and has been approved for military use. Additionally, the CH process utilizes high-temperature water that results in minimal formation of gaseous products or biochar [152]. Most importantly, CH reduces hydrogen

consumption by 74% and CO_2 generation by 65% as compared to other HEFA processes [153]. This methodology consists of cracking, hydrolysis, decarboxylation, isomerization, and cyclization to convert triglycerides into a mixture of straight, branched, and cyclic hydrocarbons [154]. These reactions take place in a reactor maintained between temperatures ranging from 450 to 475^{o}C and a pressure of 210 bar, in the presence of water and a catalyst [155]. Next, the reactions result in a mixture of carboxylic acids, oxygenated species, and unsaturated molecules sent for decarboxylation and hydrotreating to remove the unsaturation and oxygen content. At the final step, hydrocarbons ranging from C_6 to C_{28} are discharged for fractional distillation to yield diesel, naphtha, or jet fuel.

Overall, fuels manufactured through HRJ processes often yield hydrocarbons with a higher CN along with lower aromatics and sulphur content as compared to JP-8 or Jet-A [156]. Yet, these jet fuels have seen relatively slow adoption as compared to Fischer Tropsch (FT) fuels since the land use change factor has considerably affected their socio-economic aspects. Additionally, the limited scale up factor required for mass production of HRJ fuels have resulted in higher costs per gallon of fuel as compared to FT fuels [157]. Nevertheless, HEFA fuels remain in contention to replace fossil-fuel derived jet fuels in the near future as some pathways can reduce life cycle emissions by over 95% in comparison to Jet-A [158]. In addition, hydro-processing of oils can be integrated into existing petroleum refineries as the processes to catalytically crack and synthesize jet fuel are similar [159]. Furthermore, advances in the design of catalysts have reduced the energy consumption and improved the selectivity required to produce high quality hydrocarbons with tailored fuel properties for aviation [151]. As a result, these fuels remain important in consideration for the SFFP and the following section summarizes recent research where HRJ fuels have been utilized in CI engines.

Literature review of HEFA jet fuels

Shortly after HRJ fuels were certified for use in gas turbines in 2011, Hamilton et al. [160] tested a HRJ fuel derived from hydrotreated camelina vegetable oil. They performed tests with JP-5 and HRJ fuel in a HMMWV vehicle including an AM GEP 6.5 L turbocharged V8 engine with a mechanical fuel injection system. As expected, the higher CN of HRJ fuel resulted in a 2% to 5% decrease in ignition delay over the load range as compared to a baseline JP-5 fuel. Accordingly, JP-5 was found to have larger combustion duration than the HRJ fuel. Here, the reduced ignition delay affected premixing and slowed down the initial kinetic reactions for combustion to proceed. However, because of its longer ignition delay, the peak combustion pressure was larger for JP-5 than the HRJ fuel. Comparing the brake specific performance of both engines, the higher density of JP-5 resulted in better combustion phasing and 7% more power than engine operation with HRJ fuel. Moreover, the BSFC of the HRJ fuel was 2% to 4% higher than tests with JP-5 as the shorter combustion period and lower peak pressures reduced engine piston work. To conclude, CO_2 emissions for HRJ fuel tests represented 2% to 6% lower levels than that of JP-5 as its higher H/C ratio results in less CO_2 generated per fuel molecule combusted.

In the following year, Cowart et al. [161] performed an experimental study on the ignition delay of a renewable hydrotreated jet fuel derived from camelina in a HMMWV engine featuring comparable conditions described in the previous paragraph [160]. Concurrently, the authors presented a chemical kinetic model to estimate engine performance with a surrogate fuel. Based on the results of the experiments, BMEP and engine power utilizing the HRJ fuel was 10% lower than ULSD#2 due to the reduced density of the jet fuel. Furthermore, the higher CN of this renewable fuel decreased the ignition delay; however, it resulted in a more uniform combustion phasing as compared to ULSD#2. The second section of their efforts described a model of the physical and chemical delay of the HRJ fuel. Overall, their simulations were successful in predicting the dependency of load and speed on ignition delay.

In 2012, Hansen et al. [162] conducted a generator durability test according to the MIL-STD-705c standard using a blend of 50-50 JP-8 and HRJ fuel. Their study represented a joint effort between Southwest Research Institute (SwRI) and U.S. Army TARDEC Fuels and Lubricants Research Facility and merely presented an overview of generator performance, without any qualitative analysis. In all, 14 models of engine-generator pairs were tested: Yanmar L48 and L70, Onan DN4M, Isuzu C240, Yanmar 4TNV84T-BGGE, John Deere 4039T, and Caterpillar 3126B. The authors did not observe any fuel related engine or pump failures during the tests.

An analogous study was performed by Yost and Brandt [82] at the SwRI in the same year, with a 50-50 blend of JP-8 and HRJ. The engine was a 6.7L V8 turbocharged engine with a modern high-pressure (2000 bar) fuel injection system commonly used for light infantry military vehicles. Additionally, the engine was examined in accordance with a 420-hour tactical wheeled vehicle cycle engine endurance test cycle. Results from the tests indicated a 5.9% decrease in power at ambient conditions and a 4.6% reduction at elevated temperature conditions, caused by reduced fuel delivery at full load. This was more than double the power reduction observed with ULSD#2 and JP-8. Moreover, NO_x emissions were lower for the HRJ fuel as its premixed burn phase was reduced due to a decrease in ignition delay. In addition, the higher volatility of the HRJ fuel reduced THC and CO emissions throughout the load range since atomization around the injector nozzle was enhanced. Here, the CO emissions of the HRJ fuel were also thought to decrease due to an alteration of combustion phasing caused by differences in viscosity and density that affected the quantity of fuel injected into the cylinder. Furthermore, factors like the hydrogen/carbon atom ratio (H/C), aromatics content (mass and volume), olefins content, bulk modulus, and saturation content affected emissions. To further elucidate the interdependencies between the parameters, the authors presented the different correlations. For example, H/C ratio and degree of saturation were correlated directly but were inversely proportional to the aromatic and olefin content.

Overall, HC emissions indicated a distinct inverse relationship between H/C ratio and saturation content. In addition, the bulk modulus demonstrated an inverse relation with H/C ratio and saturation. Hence, at medium loads, NO_x emissions decreased; whereas, HC emissions increased at full load as the saturation of the molecule increases for the HRJ fuel. On the contrary, at higher loads, CO emissions increase while HC emissions decrease with an increase in the H/C ratio and saturation of the molecule. Overall, the engine performance utilizing jet fuels was deemed adequate, except for the changes in emissions profiles due to the differences in fuel properties.

In a study conducted by TARDEC, Jackman et al. [163] tested two Navistar CI engines in accordance with the NATO 400 hr durability test. The fuels selected were JP-8 and a 50-50 blend of JP-8 and HRJ fuel. The two inline-6 9.3 L engines were outfitted with a hydraulically assisted injection system, typically utilized on Mine-Resistant Ambush Protected vehicles. One engine was examined utilizing JP-8 fuel while the other was tested with the renewable fuel blend. Across the entire test envelop, the engine power output for the HRJ blend did not fall below 95% of the rated load with JP-8. This decrease in power was attributed to the reduced volumetric energy of the HRJ fuel blend in comparison to JP-8. Moreover, a teardown of the renewable fuel blend engine did not indicate any fuel related damage.

The following year, Cowart et al. [164] endeavored to determine the parameters required to certify new renewable fuels in military CI engines. They referenced previous data based on results of extensive tests on a HMMWV engine fueled with neat HRJ. They proposed that engine performance with alternative fuels be evaluated based on a maximum difference in ignition delay of $\pm$ 20%, an angle of peak combustion pressure between 4^{o} to 18^{o} after top dead center (ATDC), and a maximum rate of heat release of $\pm$ 15% when compared with JP-5 as a baseline fuel. For the tests conducted on the HMMWV engine, the ignition delay for the HRJ fuel is found to be 6% shorter as compared to JP-5; hence it remained within the acceptable range. Meanwhile, the angle of peak combustion varied between 6^{o} and

10.5^{o} ATDC, again within the window of acceptance for an alternative fuel. Finally, the rate of heat release is 2.9% lower for HRJ fuel as compared to JP-5, which was deemed within safe operating limits.

In 2015, Mangus et al. [41] conducted performance and emissions analyses of ULSD#2, Jet-A, and blends of a HEFA based jet fuel (R-8) and Jet-A in a single cylinder CI engine with electronically controlled fuel injection. Unnormalized combustion results indicated that as the R-8 blend level increased, combustion advanced closer to TDC because of a higher CN in spite of the greater viscosity of R-8 and poorer atomization of fuel. However, when R-8 percentage increased in the blend with Jet-A, the decrease in volumetric fuel energy and increase in viscosity reduced peak cylinder pressures as compared to ULSD#2 due to a reduced premixed burn phase. In addition, the larger CN of R-8 had a more dramatic combustion phasing effect, which was subsequently nullified by normalizing the injection timing. Next, a heat release analysis indicated that the injection events of blends of R-8 and Jet-A were longer than that of neat Jet-A due to R-8's higher viscosity. Additionally, average in-cylinder temperatures for low loads decreased with the greater blends of R-8 due to a longer fuel injection process with R-8's reduced heating value and lower density playing a significant factor. Under high load conditions, the in-cylinder temperature grew as the diffusion burn phase increased due to this lengthened fuel injection process. Considering emissions, a reduction in premix burn with greater blend percentages of R-8 resulted in a more gradual heat release, reducing thermal NO_x emissions. Besides, prompt NO emissions were reduced due to the molecular structure of R-8. Furthermore, CO emissions decreased as R-8 has a higher CN and subsequently burns more readily than Jet-A or ULSD#2. At lower loads, R-8 exhibited greater PM emissions due to a greater viscosity and larger particle size. Whereas at higher loads, a larger in-cylinder temperature coupled with a longer diffusion burn increased combustion efficiency and reduced PM emissions for R-8. When analyzing BSFC, R-8 and blends of R-8 and Jet-A had lower fuel consumption than ULSD#2 due to R-8 having greater mass-based energy content.

In 2015, Neal and Rothamer [165] measured the effects of a transient jet fuel spray on jet development and combustion in a CI-DI optically accessible engine. The fuel injection parameters of jet penetration, jet dispersion angle, lift-off length, and liquid length were measured for variations in injection pressure, fuel type, intake temperature, and ambient cylinder conditions. Additionally, the fuels used were ULSD#2, JP-8, and tallow derived HRJ fuel. Next, the Bosch injection system was electronically actuated featuring a six holed nozzle from a Stanadyne injector. Furthermore, the optical setup consisted of a high-speed imaging system designed for OH chemiluminescence along with vapor and liquid shadowgraphy. For these experiments, results from the combustion tests agreed with data acquired through constant volume combustion chambers. Firstly, liquid penetration into the combustion chamber grew without an appreciable change in the quasi-steady regime of injection as the fuel pressure was increased. In addition, an injection pressure increase resulted in a premature lift-off length that shortened the ignition delay. Moreover, the intake air temperature did not affect the jet penetration length, but an increased density of the intake fuel charge affected the liquid and penetration length proportionately while reducing the lift-off length. Subsequently, it was observed that fuels with a lower volatility generated a shorter jet penetration, but overall combustion and heat release was affected by the higher CN of the HRJ jet fuel as compared to both ULSD#2 and JP-8. On the contrary, transient injection conditions resulted in non-linear jet behavior. Furthermore, the transient rate of injection resulted in a change in fuel mass injected, which affected the engine output.

In an effort to certify a new catalytic, hydrothermally converted fuel from Chevron (CHCJ-5), McDaniel et al. [166] performed a couple engine tests in 2016. The first engine under consideration was an indirect injection, Waukesha Diesel Cooperative Fuels Research (DCFR) engine with a mechanical fuel injection system. The second engine was a Yanmar L100V engine with direct mechanical injection while the third engine was a 6.5 L, V-8, turbocharged HMMWV CI engine with a mechanical fuel injector. In addition,

steady state tests were conducted at 25%, 60%, and 90% of maximum rated load. Based on the ignition delay, maximum rate of heat release, and combustion phasing diagrams, all engines showed a variability of around 10 to 15% using CHCJ-5 as compared to a baseline JP-5 fuel. Next, the RHR showed a 10 to 15% decrease in heat release for the CHCJ-5 fuel as its higher CN led to a shorter ignition delay and a smaller premix burn. Moreover, the crank angle of peak pressure was reduced slightly for the CHCJ-5 fuel as the duration of the fuel injection process grew. Finally, the cold start event was studied and the higher CN of CHCJ-5 allowed an earlier start-up as compared to JP-5.

Summary of HEFA Jet Fuels

To meet the goals of net carbon reduction for the U.S. military and transition away from foreign oil dependency, biologically based jet fuels have seen increased usage in the last decade. Based on a literature review, HEFA fuels have demonstrated adequate performance in CI engines as compared to JP-8 and ULSD#2, without the need for engine modifications. However, establishing a general trend between all tests is not possible as each fuel from various feedstocks possess different characteristics and properties. For most part, the higher CN imparted by the presence of straight chain paraffins results in a slightly earlier ignition process. Furthermore, this quicker ignition leads to a smaller premix burn, resulting in lower in-cylinder pressures and reduced levels of thermal NO_x as compared to JP-8. In addition, the absence of aromatics and improved atomization when a lower viscosity is present might result in lower PM emissions as compared to JP-8. However, the reduced volumetric energy of this fuel results in a reduction in engine BMEP and possible increase in BSFC. Moreover, a high H/C ratio for paraffinic fuels produces less CO_2 than ULSD#2 and JP-8 and can result in net-zero emissions if the feedstock does not compete with land for food crop. Next, the low fuel viscosity of this fuel affects parameters like jet penetration, liquid length, jet dispersion angle, and liftoff length, possibly causing inefficiencies during the fuel atomization process subsequently affecting the physical ignition delay.

Finally, research studies conducted at SwRI and TARDEC focus mainly on the overall engine performance under endurance tests cycles to estimate the durability of engines during combat. Their results reveal a marginal loss in power associated utilizing HEFA fuels as compared to JP-8 while establishing the compatibility of low lubricity fuels on engine components like injection pumps and fuel injectors. In addition, engine teardowns do not indicate anomalous events of combustion (ex. accumulation of carbon, blow-by, etc.) that could possibly damage engine components.

Primarily, oils derived from biomass are hydrogenated to form free fatty acids which are hydro-oxygenated to yield bio-crude. Alternatively, a new pathway in catalytic hydrothermolysis has offered higher oil yields than traditional hydrogenation. Next, the HEFA fuel tests have indicated strong dependency on feedstocks. For example, the tallow derived R-8 fuel shows improved engine performance and reduced NO_x and PM emissions over Jet-A, JP-8, and ULSD#2 due to a CN that is close to 70. As reference, the relationship between the different fuel properties of high CN HEFA jet fuels is summarized in Table 6. In summary, the use of jet fuels derived from biomass sources have not reached full potential due to small scale production and land use factor of feedstocks.

Table 6: Estimated correlations based on literature review of HEFA jet fuel in CI engines vs Jet-A/JP-8

Property	NO_x	CO	HC/PM	BSFC
Density ↓	↓	↑	↑	↑
Viscosity ↓	↑	↓	↓	↓
CN ↑	↓	↓	↓	↓
HV ↑	↑	↓	↓	↓
Volatility ↓	↓	↑	↑	↑

ATJ Fuel

The well-established ethanol industry for renewable transportation fuel in the U.S. has been the driving force behind exploring alternative jet fuels via alcohol-processing pathways. Backed by a record corn production, U.S. ethanol production has touched nearly 18 billion gallons in 2018 [167] and continues to grow by five percent every year. With decades of advancements in bio-crude synthesis, the technological maturity of alcohol conversion processes, presents a cost-effective solution to achieve carbon-neutral emissions for jet fuel production. As the USAF evaluated biomass based alternative jet fuels to eliminate the dependence on foreign oil and reduce carbon footprint for the operational fleet, alcohol to jet (ATJ) fuel assumed significance for the single fuel policy. While ethanol is the most widely used intermediate for the synthesis of ATJ fuel, ATJ fuels can also be derived from methanol, butanol, isobutanol, propanol, and other long chain fatty alcohols using various biochemical and thermochemical conversion paths and feedstocks. Currently, ATJ fuel is produced on a commercial scale from biomass feedstocks like fermentable sugars such as sugar cane and sugar beet, hydrolyzed grain starch from wheat or corn, hydrolyzed polysaccharides from lignocellulosic biomass, or wood sent through thermochemical conversion [154]. Mostly, ATJ production includes a three-step process, viz. alcohol dehydration, oligomerization, and hydrogenation, as illustrated in Figure 4. Besides the three-step process, the Ziegler one step and two-step process using complex catalysis are being used for commercial ATJ fuel production by the US Navy [154],[168]. Among recent breakthroughs in cost-effective ATJ production, LanzaTech has developed gas fermentation processes using acetogenic bacteria to convert waste gases from steel mills to ethanol, a primer for ATJ fuel [169]. On similar lines, Gevo Inc. has formulated their high-butanol yielding Gevo Integrated Fermentation Technology (GIFT) to produce jet fuel using yeast strains via fermentation of sugars [170]. Lately, higher alcohols, especially butanol has gained significance as an intermediate for the ATJ pathway as butanol offers a higher energy

density and lower water solubility than ethanol [168]. The lower affinity of butanol with water reduces the corrosion in pipes and other fuel handling equipment [171]. Also, butanol dehydrates and oligomerizes at a lower temperature than ethanol, resulting in higher yields and lesser energy utilized per gallon of fuel produced [168]. In 2016, based on prior successful testing in commercial and military aircraft, ASTM approved a 50 percent blend of synthetic isoparaffinic kerosene produced from an ethanol or isobutanol intermediate for use in aviation turbines. The recommended fuel properties have been listed in appendix A for reference. Since then, more than ten companies have been producing ATJ fuel for commercialization, each having their own proprietary fuel formulation process. As a result, the properties of fuels may vary, leading to additional problems if ATJ fuels were to be used for the single fuel concept. However, the low CN of jet fuels derived from alcohols is the primary cause of concern for the U.S. military using these fuels [172]. The low CN intensifies the existing negative effects of lowered viscosity by increasing ignition delay, increasing premix burn that result in higher NO_x formation [147]. Hence, the current studies on ATJ fuel aim at determining the optimal blends of ATJ and Jet-A or JP-8 that can be used in CI engines without the need for extensive engine modifications.

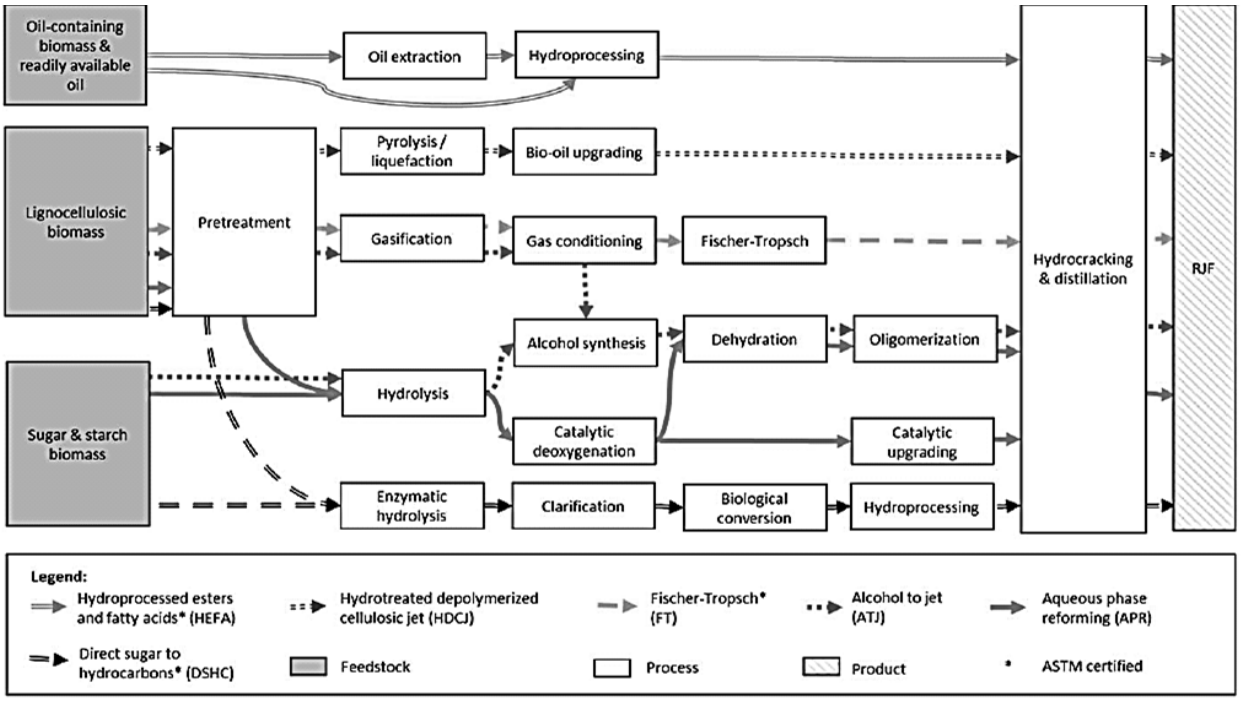

Figure 4: Commercially operating renewable jet fuel pathway summary via different thermochemical and biochemical processes with different biomass feedstocks [173]

Literature Review of ATJ Fuel

In 2014, Brandt et al. [174] performed an engine performance, emission and fuel system durability test on a 4.5 L, inline, four-stroke, turbocharged, mechanically injected John Deere 404HF280 engine. The fuel was limited to a blend of 25% ATJ and 75% JP-8 to maintain a minimum CN of 40 and was compared with neat JP-8 serving as the baseline fuel. Additionally, the test methodology followed a 210-hour tactical wheel cycle certification required for battlefield worthiness in an ambient environment and desert-like conditions. The tests did not indicate a significant difference in engine power for all the fuels and different test conditions. The fuels performed similarly for the ambient conditions while there was a noticeable power drop caused by the higher temperatures impacting the viscosity of the fuel in the desert condition test. When studying emissions at ambient pre-testing conditions, the THC emissions showed a slight decrease at higher loads in the case of the blended fuel because of higher cylinder

temperatures in the case of the fuel blend. In desert conditions, the increased ATJ fuel slippage in the pump caused by lower fuel viscosity lead to pressure imbalances in the pump, discharging excess fuel, increasing THC particularly at medium engine loads. Further, CO emissions follow similar trends as THC emissions. Moving on, NO_x emissions decrease for ambient test conditions as the load increases and are lower for the ATJ blend. For post-testing conditions, identical trends are observed as seen in the pre-testing conditions. Beyond pump wear associated with the Stanadyne injection systems, the ATJ fuel showed no performance deficiencies compared to the JP-8 fuelled test.

In 2015, Dickerson et al. [175] studied the performance of multiple diesel engines running on a low cetane ATJ and standard JP-5 in blends of 20, 30 and 40% ATJ by volume. The ATJ fuel was derived from branched butanol using a biomass feedstock that is later converted to an isoparaffinic jet fuel via reforming and hydrotreating. The mechanically injected engines selected for the study included two directly injected Yanmar Diesels and one indirectly injected Waukesha CFR diesel. The test results revealed an increase in cold-start misfires as the blends of ATJ fuel increased, likely caused by the low CN of the fuel. Additionally, the low CN and low kinetic reactivity also increased ignition delay, start time and time to rate speed as the percentage of ATJ fuel in the fuel blends increased. The start of injection was delayed for all engines as an increase in ATJ fuel content reduced the overall bulk modulus of the fuel. However, the increased ignition delay promoted enhanced premix time in the case of the IDI CFR engine while cooler in-cylinder temperatures, extended the diffusion burn in the case of the Yanmar CI engines. Since the effects of ATJ fuel were significant for the 40% ATJ blend, the authors determined a 30 percent ATJ blend in JP-5 as optimized for stable combustion characteristics.

In the same year, Yost and Frame [176] from the SwRI presented an interim report for the U.S. Army TARDEC program to determine the CN range for a blend of ATJ and JP-8. The engine was a 6.5 L, V8 turbocharged indirect diesel engine fitted with a Stanadyne Pump Line Nozzle (PLN) mechanical fuel

injection system. The test was carried out over the 13-Mode European Stationary Cycle (ESC) using 15, 35 and 50% ATJ in JP-8 fuel with 44.2, 36.4 and 32.0 CN respectively. The authors found a slight increase in engine torque at full load conditions with the 15 percent blend as it has the highest CN. The higher CN promoted better combustion and a shorter ignition delay. Considering emissions, HC and CO emissions increased with an increase in ATJ fuel percentage, likely caused by the greater proportion aromatics, viscosity and fuel density in blends. NO_x emissions were highest for the 3% blend as the ignition delay causes higher premix burn and higher in-cylinder temperatures. Ideally, NO_x emissions increase with ignition delay; however, the longer ignition delays promoted late combustion in regimes of lower in-cylinder temperatures. The most important observation is that the low CN promoted excessive heat release rates, which could damage internal engine components in the long run.

Again in 2015, Brandt et al. [177] undertook a second study on the engine performance, fuel system durability, and exhaust emissions of a Caterpillar C7 and a GEP 6.5L engine fuelled with a blend of 25% ATJ and 75% commercially available Jet-A to maintain the CN at 40 for stable engine operation. The Caterpillar engine was a 7.2 L, turbocharged, inline six-cylinder engine utilizing a hydraulically actuated electronic fuel injection system. The GEP 6.5L engine was the same engine described in the study performed by Yost and Frame [176]. The testing procedure included a pre and post-combustion analysis in addition to a 210-hour durability test, each carried out at ambient and desert operating conditions. During testing, the C7 engine experienced non-fuel related loss of power and data collection was suspended while in the case of the GEP engine, the Stanadyne pump failed for unknown reasons, preventing the desert condition operating tests. From the in-cylinder test data for the successful part of the experiment, the apparent heat release rate in the pre-combustion chamber at high power condition indicated an increased ignition delay associated with the lower bulk modulus and CN for the 25 percent ATJ blend. For similar reasons, the peak pressure is higher for ULSD#2 given the high energy content and

ignition quality. Similar trends were observed in the pre-combustion chamber results in the peak torque condition. During the 210-hour test, only a slight decrease in engine torque was observed for the 25% ATJ blend compared to ULSD#2. With respect to emissions, CO and PM formation were reduced in the case of the ATJ fuel because of a larger diffusion burn and a lower percentage of aromatics in the fuel. NO_x formation was highest for the pre-test condition for the 25 percent ATJ blend, likely caused by higher residual gas temperatures. Overall, the ATJ blend did not significantly affect the functioning of the engine, both in terms of power and emissions and was deemed suitable for use.

In a final study on ATJ fuel at SWRI in 2016, Hansen et al. [178] tested a mobile 30 kW generator paired to a Cummins 3.3L QSB engine. The engine featured a turbocharger and a high pressure common rail, electronically controlled, fuel injection system. As with the previous studies by the SWRI research group, the fuel selected is a blend of 25% ATJ and 75% commercially sourced Jet-A. The test included a maximum power test, a high-altitude test, hot condition test, high temperature test, cold battery start test, extreme cold battery start test, and a 500 hr durability test prescribed by the MIL-STD-705C standard. The engine performed without any noticeable decline in power or fuelling issues, except at the altitude test of 10000 ft, where a faulty testing procedure was identified and rectified for future reference. This study did not present any quantitative results to make sufficient inferences.

Summary of ATJ Fuels

Of late, the rapid growth in corn production has made ATJ fuel the foundation for the U.S. military to transition away from foreign oil to offset GHGs for transportation. Only recently, companies like LanzaTech and Gevo have made several breakthroughs to scale-up the production of aviation fuels from alcohols. Their fuel has been successfully tested at SwRI, indicating no significant degradation in engine performance. As with all aviation fuels, the low viscosity and density of ATJ fuel improves atomization and mixing that positively affects the physical ignition delay. On the other hand, the reduced viscosity

during desert test conditions led to fuel slippage and eventual flooding of the engine. Furthermore, a low CN below 30 is a cause for concern. Consequently, the increase in ignition delay raises NO_x emissions because of a higher premix burn phase. For the same reason, engine operation becomes unstable as blends of ATJ fuel increase beyond 30%, which is the recommended blend percentage of ATJ with JP-8. Furthermore, current laboratory-based production techniques for the fuel have not been able to standardize the levels of aromatic content that can affect both emissions and power output. As a result, more research is required to establish ATJ fuels for the SFFP to lower GHG emissions while considering its competition with food crops that could lead to an increase in land use factor; hence, growing their indirect emissions.

In conclusion, the pathways of ATJ fuels have been developing rapidly due to advances in bio-engineering where methods of gas fermentation (LanzaTech) and Gevo Integrated Fermentation Technology (Gevo) have been successfully implemented to commercial and military aviation. However, the low CN (CN < 30) has restricted the widespread use of ATJ fuel for the SFFP. All CI engine tests have indicated unstable engine operation, lower power generation and increased levels of NO_x compared to Jet-A, JP-8, and ULSD#2. Based on the literature review, the different properties have been summarized in Table 7.

Table 7: Estimated correlations based on literature review of ATJ jet fuel in CI engines vs Jet-A/JP-8

Property	NO_x	CO	HC/PM	BSFC
Density ↓	↓	↑	↑	↑
Viscosity ↑	↓	↑	↑	↑
CN ↓	↑	↑	↑	↑
HV ↓	↓	↑	↑	↑
Volatility ↓	↓	↑	↑	↑

Sugar to Jet (STJ) Fuel

Advancements in bio-catalysis, bioprocessing, and bio-refining have led to less intensive and environmentally benign techniques to utilize plant matter for jet fuel. One of these recent developments, the conversion of sugar to jet fuels, has been used to produce second-generation biofuels for the aviation industry. Typically, plant sugars have carbon chains in the C_5 to C_6 range as compared to C_{15} to C_{16} for vegetable oils. Hence, biofuel manufacturers have focused mainly on high oil yielding seeds since they can generate a jet fuel closer in character to petroleum jet fuel. However, purely in terms of net weight, the amount of cellulosic biomass available for bioprocessing far exceeds the amount of oilseeds accessible. Thus, scientists have proposed using sugar-based pathways for jet fuel production to take advantage of this large content of cellulosic biomass. Here, the feedstock for catalytic upgrading of sugars to hydrocarbons can include sugars and sugar intermediates like sucrose from sugarcane, corn sugar from corn starch, lignocellulosic sugars from hydrolysis of hemicellulose and cellulose [154]. Furthermore, the use of municipal waste, crop waste, construction waste, weeds, and dead forest wood as feedstock prevents the need to use cultivable land that may otherwise increase indirect emissions and create conflicts with food crops. Moreover, enzymatic reactions pose no risks to the environment since no harmful byproducts are formed in the biofuel manufacturing process. As a result, jet fuels from sugars have recently assumed importance as airlines look to incorporate alternative fuels to reduce carbon emissions.

Currently, two manufacturers have developed commercial-level technologies to convert sugars to jet fuels. Virent Inc. upgrades sugars to hydrocarbons through their BioForming process that consists of Aqueous Phase Reforming (APR) and catalytic processing. Here, biomass feedstock is converted to soluble carbohydrate streams via enzymatic hydrolysis of lignocellulosic biomass to form sugars [154].

After pretreatment, the sugars are purified by hydrolysis before being sent to the APR reactor for conversion into polyhydric alcohols or short-chain oxygenates. These alcohols are converted into alkenes via acid condensation, aldol condensation, and dehydration or hydro-dehydration. Finally, the alkenes from the APR reactor and alcohol conversions are hydrotreated to form jet fuels.

Meanwhile, Amyris Inc. developed a direct sugar to hydrocarbon process via microbial fermentation. In this process, a specially engineered yeast microbe catalyzes and ferments sugar to form a compound called farnesene. This 15-carbon molecule compound is of similar density to some of the petroleum hydrocarbons and synthetic isoparaffinic kerosene used in jet fuel [26]. Subsequently, farnesene is purified and hydroprocessed to form farnesane jet fuel, a sesquiterpene where the dodecane base chain has substituted methyl groups. Since they have obtained up to a 97% recovery of pure farnesane, the resulting jet fuel is of high quality and comprises nearly 99.5% of a C15 isoparaffin [179]. Backed by several tests in gas turbine engines, Amyris' sugar derived jet fuel was approved for use as a drop-in fuel for Jet-A in June 2014, as prescribed by the ASTM D7566 standard [180].

Currently, sugar-to-jet fuels are mostly in the research and development stage, where the efforts are focused on increasing the yield from non-food, crop-based feedstocks using better catalysts and enzymes. However, given the potential of this fuel, it is important to understand its prospective impact as part of the SFFP. Hence, the following section provides a brief overview of the few studies performed using farnesane in CI engines.

Literature review of SIP fuels

In 2014, Millo et al. [181] investigated the performance of 30% by volume blends of farnesane with ULSD#2 (F30). The engine tested was a four-cylinder, inline turbocharged unit with EGR and common rail fuel injection. The engine was tested under seven different part load points based on the New European

Driving Cycle by normalizing fuel injection to have a similar BMEP to compensate for the difference in fuel properties. For a preliminary full load test, a 2% reduction in brake torque was observed for the F30 blend in comparison to neat ULSD#2, due to its lower volumetric energy density. At part load operation, no significant variations in engine performance and BSFC were observed with both fuels. Considering emissions, both CO and HC emissions were reduced as the higher CN and volatility of F30 ensured better combustion, particularly at low and medium loads. Moreover, PM emissions at medium and high loads were found to decrease since farnesene is a respectively pure fuel (i.e., 99.5% C15 chain alkane) without the aromatics typically responsible for PM production. This was contrary to the usual scenario where a higher CN fuel results in a longer diffusion burn and increased PM emissions. In addition, NO_x emissions were found to be comparable to the ULSD#2 tests. Finally, their extended investigation while changing EGR rates indicated soot-NO_x and brake specific CO-NO_x tradeoffs that highlighted the possibility of an additional reduction in emissions through ECU recalibration.

In 2015, Groendyk and Rothamer [182] studied the effects of fuel properties on the autoignition of farnesane in a CI engine as a drop in replacement for ULSD#2. They primarily focused on the influences of fuel volatility and the narrow boiling point of single component biofuels like farnesane. Although the authors used nine different blends of fuel for the analysis, this review is limited to the 70-30 blend of farnesane and heptamethylnonane (HMN). The test was performed on a Caterpillar B15 engine with a solenoid-operated Bosch common rail injector. In addition, three injection pressures (50, 100, 150 MPa) were used for the analysis and the injection timing was normalized to compensate for the difference in fuel properties. Here, test results indicated a drop in cylinder temperature with the binary fuel blend as compared to ULSD#2 since fuels with a higher CN (i.e., farnesane) tend to have a reduced premix burn phase as ignition delay is reduced. For the same reason, the heat release was lower for the fuel blend in comparison to ULSD#2. With respect to pollutant formation, reduced HC emissions were found as

improved volatility and atomization cancelled out the effects of an increase in CN that grew the combustion duration. On the other hand, NO_x and CO emissions did not indicate any significant variations between ULSD#2 and the binary fuel mixture while considering fuel properties. Furthermore, PM emissions were significantly lower since (as indicated prior) farnesane is a single component alkane with no aromatics. Overall, the authors suggest that the CN rating of the fuel is the only important parameter to determine fuel behavior beyond physical fuel properties.

Recently in 2018, Soriano et al. [183] focused on the performance and emissions of a modern CI engine fueled with a sugar-derived jet biofuel. The engine was a four-cylinder, four-stroke, turbocharged, intercooled unit, fitted with a diesel oxidation catalyst and electronically operated common-rail fuel injection system with a pre-injection event. Two different test conditions were used to test the engine; New European Driving Cycle and Worldwide Harmonized Light Duty Vehicles test cycle. Furthermore, four fuels were tested including ULSD#2, Fischer-Tropsch based GTL fuel, a blend of 72% soybean and 28% palm biodiesel, and farnesane. Based on the engine tests at low loads, the authors found that farnesane's BSFC was higher than the GTL fuel. In addition, the brake thermal efficiency was found to be the lowest for the GTL fuel while the thermal efficiencies were similar for ULSD#2, biodiesel blends, and farnesane. Overall, both the BSFC and brake thermal efficiency were tied to the heating value of the fuels. Meanwhile, THC emissions decreased for biodiesel because of the additional oxygen atom present in its molecular makeup. Moreover, THC emissions fell for both paraffinic fuels (GTL and farnesane) due to the absence of aromatic compounds. In general, since farnesane is a pure compound and has a faster evaporation rate, this generated a better atomization process; hence, it lowered emission levels as compared to all other fuels. Next, a higher CN and H/C ratio for the paraffinic fuels resulted in lower adiabatic flame temperatures that reduced NO_x emissions. Moving on, the Particle Number Concentration (PNC) was predominantly dependent on the engine load in addition to the parameters of

premix burn, CN, and air-fuel ratio that favored the accumulation mode over nucleus mode for the formation of PM. Further, as farnesane was a single component hydrocarbon without pollutants like sulfur, PNC was lower than both GTL and ULSD#2. In addition, it was determined that the lower THC emissions of this fuel decreased the potential of particle formation and growth through hydrocarbon condensation or adsorption. Moreover, the higher volatility and smaller chain length of farnesane resulted in a lower PNC and subsequently lesser PM formation than all the fuels tested. As a result, farnesane had reduced pollutant emissions with a slightly improved engine performance; hence, justifying it a feasible alternative jet fuel.

Summary of SIP fuels

Farnesane is a relatively new biofuel that has recently been approved for use in aviation gas turbines. Until now, only Amyris and Virent have been producing farnesane jet fuel for a few select airlines and test results directly pertinent to the SFFP have not been investigated. However, independent researchers have indicated that farnesane, in general, has a positive effect on CI engine performance and emissions. One reason is that the fuel is a single-component compound (C15 alkane); hence, it has predictable fuel properties. Particularly, the CN is higher than ULSD#2, giving it respectively good cold start and thermal properties. Moreover, its lower viscosity improves the atomization process and its higher volatility increases evaporation; hence, resulting in overall better air-fuel mixing. These combined components result in a reduced ignition delay, subsequently decreasing the premix burn event as early ignition results in less fuel entrained for the autoignition reactions. This results in lower in-cylinder temperatures and a reduced RHR, which reduces the formation of thermal NO_x. Furthermore, the enhanced atomization provided by this fuel results in a more homogenous mixture that prevents the formation of pockets of fuel rich zones and accumulation of hydrocarbons in crevices. As a result, HC

and CO emissions are reduced as compared to ULSD#2. Finally, the absence of aromatics in the fuel averts the formation of soot particles, in spite of its slightly longer diffusion burn phase.

Although there might be a clear advantage in using single component fuels in CI engines, there have been respectively slow advancements with respect to the wide scale production of farnesane. Since sugarcane continues to be the main feedstock, there are higher indirect emissions with an increase in land use factor. Current efforts are investigating the production this fuel using waste biomass and other biodegradable matter to take advantage of the cellulosic sugar content. Simultaneously, research has targeted the development of new microbes and catalysts that reduce the energy requirement for bio-synthesis and grow the overall yield from the raw feedstock. Overall, as the production of non-food crop farnesane improves, additional research will be needed to certify it as a potential option for the SFFP. As an overview, a summary of the respective farnesane fuel properties have been tabulated in Table 8.

Table 8: Estimated correlations based on literature review of Farnesane jet fuel in CI engines vs Jet-A/JP-8

Property	NO_x	CO	HC/PM	BSFC
Density ↑	↑	↓	↓	↓
Viscosity ↑	↓	↑	↑	↑
CN ↑	↓	↓	↓	↓
HV ↔	↔	↔	↔	↔
Volatility ↓	↓	↑	↑	↑

Conclusion

A chronological review of aviation fuels used in CI engines for the SFFP indicates how the change in fuel physical properties and chemical composition of these fuels affect engine performance and emissions. Typically, aviation fuels have lower viscosities that improve atomization and facilitate a more

homogenous fuel-air mixture. In addition, this reduced fuel viscosity influences fuel injection, especially mechanical fuel injection systems where the decreased volumetric density results in a lower power output. In addition, the depressed viscosity caused wear in older engines with mechanical fuel injection pumps. However, the advanced metallurgy employed in newer engines with electronic fuel injection systems do not show issues with either fuel injection or lubrication. Based on the review, research on CI engines fuelled with JP-8, Jet-A, or JP-5 fuels have shown a slight decrease in power output due to the lower volumetric energy density of aviation fuels. However, the main cause of concern is the variability in CN caused by the absence of a CN standard that affects combustion phasing. For most cases, the CN for JP-8 was found to be less than ULSD#2, resulting in delayed ignition and an increase in NO_x emissions. As a result, JP-8 fuels need a CN improver to ensure reliable engine operation.

Like JP-8, CTL fuels have a lower CN than ULSD#2 that can lead to unstable engine operation and higher NO_x emissions. On the contrary, GTL fuels have shown superior performance and lowered emissions in CI engines as the fuel mainly includes straight long chain paraffins that imparts a greater LHV. In addition, GTL fuels lack aromatics; hence, improved engine performance and diminished emissions are seen. Next, HEFA fuels can be produced from biomass waste and animal fats that reduces net GHG emissions. These fuels have a higher LHV and show similar combustion characteristics as GTL fuels. However, the vast variability in feedstock sources can lead to inconsistent fuel properties that could affect engine performance. Moving on, production of ATJ fuels has gained momentum with the increase in ethanol production from corn. However, these fuels have a CN lower than 30; hence, blends up to 30% are permissible without affecting engine performance and increasing emissions. Finally, sugar-based jet fuels are composed mainly of a single component called farnesane that leads to predictable engine performance and emissions. Since most sugar-based fuels are produced from sugarcane, a rise in production could increase the land use factor and intensify indirect emissions. As a result, new

biocatalysts are being developed to increase yield of hydrocarbon generation from raw feedstock. To sum up, the variability in fuel properties and particularly CN has prevented the widespread convincing use of all aviation fuels in CI engines for the SFFP. Moreover, fixed standards for CN in fuels and fuel blends would be important to closely match engine performance with ULSD#2. For newly formulated biofuels, precautions must be exercised in preventing indirect emissions due to the land use factor.

Overall, the review suggests that the CN is the most important parameter that determines the blend ratios between Jet-A or JP-8 and any alternative fuel under consideration. Since gas turbine combustors have a constant flame, the need for good autoignition characteristics is irrelevant, negating the need for any CN specification. Furthermore, this absence of CN regulations has resulted in a large variation of CN of jet fuels from different manufactures ($29 < CN < 70$) [140]. As a result, the review papers that tested low CN fuels reported high ignition delay, reduced power delivery, increased fuel consumption, higher combustion pressures and temperatures, and a high level of NO_x emissions over ULSD#2. Furthermore, the engine combustion had elevated levels of vibration and noise that could be detrimental for overseas covert military operations. In conclusion, CN regulations are essential for the SFFP as the problems associated with a variation in CN will only be exasperated with the induction of newly formulated alternative jet fuels in the near future.

Chapter 3: Performance and Emissions of Synthetic Paraffinic Jet Fuel in a Single Cylinder Compression Ignition Engine

Abstract

To minimize operational costs for the U.S. military, the use of alternative aviation fuels in compression ignition (CI) engines was mandated by the U.S. Department of Defense (DOD) via the Single Forward Fuel Policy (SFFP). Consequently, engines designed to run on diesel fuels were made to operate on aviation fuels without the need for any extensive modifications. As a result, the difference in physical and chemical properties of diesel and aviation fuels resulted in certain issues with respect to combustion. With the formulation of clean-burning synthetic aviation fuels from coal via the Fischer Tropsch synthesis, Sasol's coal to liquid (CTL) jet fuel is being studied here for feasibility in military CI engines for the SFFP. In this study, a single cylinder, direct injected engine equipped with electronic fuel injection is used to evaluate engine performance and emissions using ULSD#2, Jet A, and Sasol's CTL fuel. Here, Sasol CTL is added to Jet A to create 5%, 10%, 20%, and 50% blends by volume. Based on the results, the 5%, 10%, and 20% blends indicated marginally superior performance to ULSD#2 due to increased homogeneity. However, for the 50% blend, it was suspected that a combination of high compression ratio, lower cetane number, and temperature-reduced viscosity inhibited combustion. Emissions-wise, particulate matter levels were noticeably reduced due to the absence of aromatic hydrocarbons in the CTL fuel while nitrogen oxide (NO_x), carbon monoxide (CO), and total hydrocarbon (THC) levels were identical for each of the tests.

Introduction

Historically, diesel has been the go-to battlefield fuel since compression ignition (CI) engines offer high reliability and rugged construction. Additionally, CI engines have greater torque and mileage as compared to gasoline engines, essential for operating heavily loaded armored vehicles. However, during the cold war within the colder climates of northern Europe, diesel-fueled CI engines in North Atlantic Treaty Organization (NATO) battle tanks and other ground support vehicles were plagued by waxing and subsequent fuel filter failures. As a stopgap measure to stabilize the cold flow properties of the fuel, NATO forces began blending standard ultra-low sulfur diesel (ULSD #2) fuel with jet propellant # 8 (JP-8). Since JP-8 is a middle-distillate with additives (e.g., antioxidant, static dissipater, and anti-corrosion) and lubricity improvers, it offered more stability as compared to other aviation fuels in extreme weather conditions associated with combat [184]. Subsequently, two separate fuel supply chains presented logistical problems and escalated operational costs. As a result, the United States (U.S.) Department of Defense (DoD) issued a directive in 1988 called the single forward fuel policy (SFFP), where JP-8 was selected as the fuel for all military vehicles with CI engines [185]. With a lower cloud point and higher volatility compared to standard ULSD #2, JP-8 eliminated issues associated with low temperature operations and could be used as-is in CI engines without requiring modification. Nonetheless, as JP-8 has different physical and chemical properties compared to ULSD #2, the performance of military vehicles could be adversely affected in the long run.

For example, during the first Gulf War in 1990, ground vehicles operating in the extreme heat and sandy conditions in Iraq were reported to have hot start issues and fuel injection failures with JP-8. It was later found that lubricity was severely compromised when ULSD #2 was replaced with JP-8 and its decreased viscosity in hot climates fell below recommended standards [186]. As a result, this paved the way for

fuel research by the military to ensure optimal performance of engines, from both a strategic and economic perspective. For older engines, subsequent JP-8 testing found issues with respect to the lubricity of fuel, spray formation, auto-ignition, and part load operation [103]. Moreover, the inclusion of modern technologies like exhaust recirculation valves, variable vane turbo charging, modern piston designs, high pressure injection systems, variable valve timing, multiple injection events, etc., further complicate the use of JP-8 in engines designed to operate solely on ULSD #2. In addition, there has been a recent thrust by the DoD to utilize alternative and renewable jet fuels to alleviate concerns brought about by volatile fuel costs and political instability in oil-rich Middle East countries [187].

One possible solution is to use the conversion of coal to a liquid fuel through a process called Fischer-Tropsch Synthesis [188]. In specific, several chemical engineering corporations have used this technology to take advantage of regions with high coal reserves by producing synthetic fuel from coal to primarily offset imports of crude oil. Namely, South Africa was the first country to take advantage of abundant coal feedstocks and adopt coal to liquid (CTL) jet fuel for their domestic airline use. Citing advantages of CTL sourced jet fuel, the Aviation Fuels Committee of the United Kingdom (UK) approved Sasol's synthetic CTL fuel for military and civilian use in 1999. With the formal induction of alternative jet fuels in the UK aviation sector, the U.S. began testing several different aircraft to certify the CTL as a drop-in alternative jet fuel. In 2008, the UK Ministry of Defense, through the Defense Standard DEFSTAN 91-91, approved Sasol's CTL fuel for commercial use in all aircraft. Subsequently, the American Society for Testing and Standards (ASTM) included the Sasol CTL fuel in its ASTM D1655 specifications based on the DEFSTAN 91-91. Later, in 2016, the ASTM D7566 standard was formulated to describe the specifications of jet fuel derived from several non-conventional sources including coal.

Although it takes more than a ton of coal to produce one barrel of synthetic fuel [189] that potentially releases two times more carbon dioxide (CO_2) without carbon capture and storage (CCS) [190, 191], the

CTL pathway is the currently largest source of alternative jet fuels. With U.S. defense forces alone utilizing close to 85 million barrels of fuel in 2017 [192] and researchers predicting that alternative jet fuel production will exceed a billion barrels annually by 2030 [193], it is important to investigate the potential of CTL for the SFFP policy. Moreover, the advancement of CCS technology might place the energy intensive CTL process on par with conventional petroleum fuels [194]. This might be advantageous for the U.S. that is estimated to have nearly 270 billion tons of coal reserves and recovering only 15% of this amount using sustainable technologies for liquid fuel production would yield three to four million barrels per day for the next 90 years; hence, supplementing DoD's requirements with synthetic fuels [189]. In addition, Elia et al. [195] illustrates that it might be possible to produce enough synthetic fuel to meet the entire demand for U.S. domestic transportation fuels using coal, biomass, and natural gas feedstocks. Finally, the economic viability of synthetic fuels becomes positive when crude oil exceeds $50 per barrel [196], which has been the case in the last two decades.

As a result of the potential of CTL fuels for the SFFP, this effort presents the combustion analysis of a representative CTL fuel produced at the Secunda Plant in Sasolburg, South Africa. First, a description of the CTL fuel fabrication process is presented along with a literature understanding of its potential impact when used in CI engines. Then, the experimental setup and test conditions required to measure the performance and emissions from the engine are described in detail. Accordingly, standard Jet-A procured from the local municipal airport is blended with the CTL fuel in ratios of 5%, 10%, 20%, and 50% volumetrically, after which the fuel properties are determined in the ASTM laboratory at the University of Kansas. Furthermore, the methodology to identify the fuel is discussed in depth. Next, the fuel injection is adjusted so that the location of peak pressure matches for the different test conditions and blends. After acquiring and collating data to post process the results, a discussion and inferences are presented along with plots of in-cylinder pressure, heat release, and in-cylinder temperatures. Finally, to

conclude the study, brake specific emission results from the Fourier Transform Infrared Spectroscopy (FTIR) emission analyzer are discussed in detail to highlight the combustion efficiency of the engine with respect to each of the blends tested.

Synthetic Jet Fuel Composition and Impact on Engine Operation

The Secunda plant produces a fully synthetic jet fuel (FSJF) as a mixture of different streams of hydrocarbons distilled from synthetic crude derived from coal as the primary feedstock. The process starts with gasification of coal to yield a mixture of hydrogen (H_2) and carbon monoxide (CO), called syngas. The syngas is cleaned to remove CO_2 and other impurities and is further enriched before undergoing several catalytic reactions to yield a mixture of different long-chain paraffinic hydrocarbons. These Fischer-Tropsch reactions take place in a high temperature and high-pressure reactor over an iron catalyst via indirect liquefaction where the reactor parameters and composition of syngas determine the length of the hydrocarbon chains [197, 198]. These chains are cracked using conventional refining processes to yield different distillates and the basic reactions [188] of this process are listed as follows:

$(2n + 1)H_2 + nCO \rightarrow nH_2O + C_nH_{2n+2}$	(alkanes/paraffins)	(1)
$2nH_2 + nCO \rightarrow nH_2O + C_nH_{2n}$	(alkenes/olefins)	(2)

Since FSJF is a mixture of different distillates of hydrocarbons through dissimilar process streams, it is not possible to present an accurate composition of a FSJF.

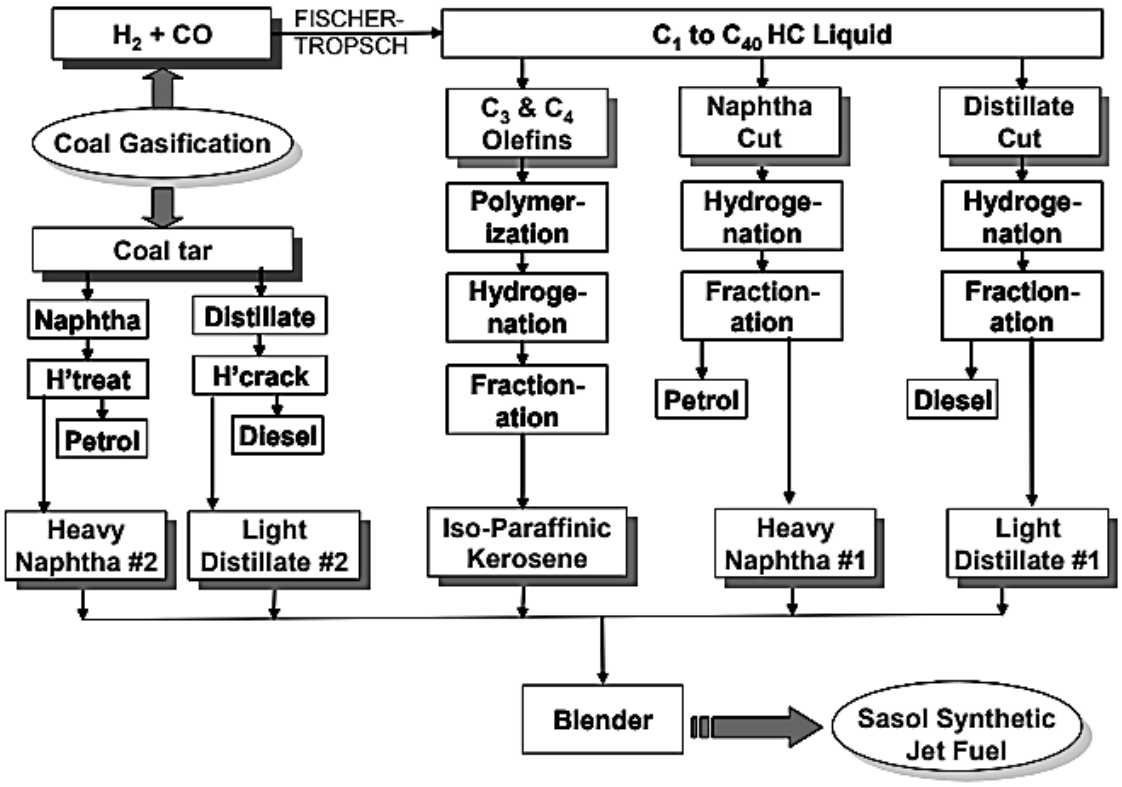

Figure 5: Production streams of fully synthetic coal to jet fuel at Sasol [199]

Here, Figure 5 indicates the various distillation streams emanating in FSJF. In this illustration, FSJF is a mixture of a varying proportion of hydrocarbons where isoparaffinic kerosene (IPK) is considered the main component. Typically, the low temperature Fischer-Tropsch process yields long-chain n-alkanes with a high cetane rating, ideal for CI combustion [118]. However, to tailor the jet fuel for volatility, the alkanes are oligomerized followed by hydrotreating and distillation to produce to branched alkanes, primarily mono- and di-methyl substituted, and subsequently separated into the desired distillation range [119]. As a result, the properties favoring CI combustion (e.g., cetane number) are lost as isoparaffins and aromatics; hence, the resultant jet fuels have higher activation energies for combustion [118]. Additionally, heavy naphtha kerosene (containing about ten percent aromatics, light distillate #1,

with about 24 percent aromatics, and naphtha #2, containing about 39 percent aromatics) makes up the remainder of the stream [120].

The classified composition of the FSJF makes it impossible to predict the behavior of the fuel, particularly when analyzing nonlinear combustion in CI engines. In addition, changes in feedstock characteristics may impart different properties to the fuel. However, common properties reported in the literature include low aromatic content, density, and viscosity as compared to conventional jet fuel [199] that has similar performance to JP-8 with negligible differences in performance and emissions, particularly at high loads [85]. For comparison to FSJF, conventional Jet-A fuel is a hydrocarbon mixture containing around 38.8 percent paraffins, 26.9 percent monocycloparaffins, 11.2 percent dicycloparaffins, 16.1 percent alkylbenzenes, 3.7 percent indanes and tetralins along with 3.3 percent naphthalenes [200]. Thus, the differences in fuel compositions with respect to ULSD #2 lead to deviations in properties of Jet-A and CTL FSJF from ULSD #2, that cause combustion instabilities when used in CI engines.

Of interest, the (typically) lowered proportion of aromatics in FSJF is of particular interest as certain elastomeric components like seals and O-rings need this component to swell and expand for protection against fuel leaks [201]. Additionally, as jet fuel is less dense and viscous, the reduced lubricity of FSJF promotes wear on mechanical components [202]. Furthermore, this low viscosity fuel might slip past pump and injector clearances and result in unwanted fuel injection events; hence, potentially resulting in a reduced pressure in the fuel rail. Moreover, as fuel is normally volumetrically metered into the engine, a change in viscosity affects the fuel injectors and the subsequent quantity of fuel entering the cylinder. In addition, the lower percentage of straight chain paraffins and higher content of cycloparaffins in jet fuels as compared to ULSD #2 results in a fuel with a reduced cetane number that negatively influences ignition delay [203]. To further illustrate the effects of cetane number on

combustion of Sasol's FSJF, Schihl et al. [41] discuss how the absence of a cetane specification for jet fuel results in issues associated with delayed ignition and heat release that could result in abnormal engine performance and emissions. In another article, Laura and Schihl [132] highlight issues with blending two low ignition quality fuels that severely impact the functionality of an engine. Here, an excessive ignition delay could result in high pressure rise rates causing structural and thermal damage of engines. Moreover, Schihl et al. [140] indicate a drop in part load performance of a CI engine and misfire by the use of a CTL fuel. A subsequent research effort by Schihl et al. [136] further elaborated that the low ignition quality of Fisher-Tropsch jet fuels resulted in a 20% increase in ignition delay and lengthy heat release events. To study the effects of a low cetane number, Zheng et al. perform an engine study using Sasol CTL fuel with a cetane improver. Their results reveal a non-linear decrease in ignition delay and high in-cylinder temperatures, subsequently increasing NO_x emissions. In other non-engine combustion studies, FSJF has been shown to burn clean, producing 50-90% lower PM emissions and no sulfur emissions when compared to standard petroleum-based jet fuels [204-206]. This is attributed to the absence or lowered percentage of aromatic compounds or polyaromatic hydrocarbons (PAH) that are precursors of soot formation [207]. However, while the reduction of NO_x and PM with the higher volatility and subsequently lower premix burn of JP-8 has been extensively documented [70, 71, 63, 81, 78], there is a dearth of information on the emission profiles of blends of Jet-A and Sasol's FSJF in CI engines, presenting another incentive for the current study.

Due to an increase in production and adoption of alternative jet fuels to reduce the carbon footprint, research on alternative jet fuels used in CI engines for the SFFP is of high importance. Additionally, modern engines with electronically controlled injection systems present challenges as fuel injection pressures have gone beyond 100 MPa, which could lead to complete system failure if they operate beyond the design limits. As a result, the combined effect of low viscosity and density need to be

evaluated based on engine performance as changes in physical properties of fuels alter the fuel quantities metered into the engine. Further, stringent emissions regulations adopted by the U.S. DoD necessitate evaluation of alternative fuels that burn with reduced amounts of NO_x and PM. Overall, the complex mixture of hydrocarbons distilled from the synthetic crude, the absence of aromatics, and the lack of regulations to specify a standard for the cetane number of jet fuels [208] are the main incentives for this study.

Experimental Setup

The research engine under consideration is a single-cylinder CI Yanmar L100V that was retrofitted with an electronic fuel injection system to emulate a modern CI production engine. For this study, forced induction and exhaust gas recirculation are omitted to reduce the complexity of the analysis. Of interest, engine specifications are listed in Table 18 in Appendix A for further reference. In addition, the complete experimental setup with the emission analyzing equipment, sensors, and automated data acquisition systems are described in detail by Langness et al. [209]. For accurate load measurements and steady state operation, the engine is paired to an alternating current Dyne Systems regenerative dynamometer with an Interlock V OCS controller to govern the engine speed. A FUTEK (Model # TRS-605) transducer measures engine brake torque that is fitted with a coupling between the shafts of the dynamometer and the engine. This torque transducer is rated to 200 N-m with an error of ±0.2% at full load during torque peaks. The fuel injector, which is a piezoelectric fuel injector (Model #044510183) sourced from a 1.3 L Fiat Punto, is controlled by a Bosch MS 15.1 electronic control unit (ECU). Although the ECU allows a maximum of five injections per thermodynamic cycle with injection sweeps at a resolution of 0.2^{o} per crank revolution, the current analysis is limited to a single injection event per thermodynamic cycle. Here, the controlling Bosch Modas Sport software is operated to ensure peak pressure combustion timing at the same crank angle location for all fuels and fuel-blends tested based on load (i.e.,

combustion normalization). Furthermore, the Bosch fuel rail (Model # 261-B1-135-201) can be pressurized up to 200 MPa using a Bosch CP3.2 high pressure pump. However, for the current study, the injection pressure is set at 40.0 ($\pm$0.5) MPa to prevent excessive pressure rise, in case the fuel has higher reactivity than ULSD #2. The fuel pump is driven by an externally connected 0.5 HP Leeson motor (Model #C42D17FK1C), which is coupled to a Toledo speed reduction box (Model # M164-A7H). As a result, the external motor avoids parasitic power draw from the engine. An Emerson Elite Coriolis mass flow meter (Model # CMF-010M) measures the fuel density and flow rate from a gravity-fed tank. This device has a flow measurement accuracy of $\pm$0.1% and a density accuracy of ±0.5 kg/m^3 of the flow rate.

An Omega differential pressure transducer (Model # PX277-30D5V, accuracy $\pm$1% of range) and a Merriam laminar flow element (Model #50MW20-2, accuracy ± 0.72% to ± 0.86% of reading) measures engine intake air flow rates. Next, ambient air conditions are found using an Omega pressure sensor (Model #EWS-BP-A, accuracy ±1% of full scale) and another Omega sensor (Model #EWS-RH) records air temperature and relative humidity. The relative humidity sensor has a humidity measuring accuracy that ranges from 3 to 4% of the range while the temperature accuracy is 1.4°C to 1.7°C across the full scale. Then, the air moves into a 30-gallon plenum to reduce oscillatory effects. A separate Omega pressure transducer (Model # PX329, $\pm$0.25% static accuracy) and an Omega thermocouple (Model #TC-K-NPT) are located in this plenum to measure the temperature of the air entering the cylinder. Furthermore, a Kistler encoder (Model # 2614B1) attached to the flywheel and a Kistler piezoelectric pressure transducer (Model # 6052C) installed directly in the cylinder head are part of the high-speed in-cylinder pressure measurement system. This transducer has a full range of 0 to 250 bar with an error of 0.5% at full scale. A Kistler signal converter (Model # 2614B2) receives signals from the encoder to register a digital crank output every 0.2^o crank rotation. The fuel injection system is coupled to a National

Instruments multifunction PCI I/O module (Model # 7843) that is interfaced with a LabVIEW routine for data sampling.

Finally, the emission measuring system consists of an AVL SESAM Fourier Transform Infrared Spectroscopy (FTIR) emissions analyzer (Model # 2030HY) to monitor gaseous emissions. Additionally, the system is equipped with a Magnos106 oxygen sensor (accuracy $\pm$0.05%) to measure diatomic gaseous species and an AVL Smoke Meter (Model # 415SE, detection limit - 0.02 mg/m^3) to find particulate emissions. Data acquisition is managed by a National Instruments (NI) systems real-time controller (model# cRIO-9014) that is interfaced with a modular LabVIEW routine developed in-house. Different modules allow for the collection of low (10 Hz) and high-speed (43 kHz) data from the engine.

Test Methodology

The dynamometer and LabVIEW program that connects to the Bosch ECU is configured to provide five load set points at 0.5 N·m, 4.5 N·m, 9.0 N·m, 13.5 N·m, and 18 N·m; i.e., effectively zero load to full load. Further, the engine operates at an intermediate speed of 1800 rpm to avoid mechanical and vibrational stresses associated with higher speeds. Additionally, tests at 1800 rpm provide a good blend of premix and diffusion burn for the single cylinder engine. The engine is initially calibrated with ULSD #2 at standard injection timings as the baseline fuel against which all fuels are tested. Next, the S0 blend is tested to determine variations against ULSD #2. The blend ratios selected for the analysis are abbreviated as S0, S5, S10, S20, S50, and S100 for brevity where S0 represents a neat Jet-A fuel, S5 represents a blend of 5% FSJF and 95% Jet-A by volume and so on. At this stage, the injection is normalized if needed to remove the influence of ignition delay and match the peak in-cylinder pressure with respect to the crank angle [41]. Subsequently, the remaining fuel blends are tested by first normalizing the fuel injection and then allowing enough time for steady state conditions and residual

fuel from the previous tests to burn off. Steady state conditions are reached when the exhaust temperature changes less than one percent per minute. The high-speed computer saves data for 60 thermodynamic cycles after steady state conditions are reached, while the emissions analyzer records data every second for five minutes [41]. A post processing MATLAB program developed by a previous student [36] filters the data from the computers to provide cycle-averaged values and standard deviations of the different parameters measured, which are automatically saved in an Excel file.

Fuel Analysis and Preparation

As described earlier, the Sasol FSJF is a synthetic 'drop-in' fuel approved by the ASTM for commercial aviation. The sample tested at the University of Kansas was stored in a fuel bunker for roughly four years before performing tests (Note: contamination tests are presented later) for the analysis presented in this report. Here, the unknown composition of the FSJF warrants laboratory tests to determine the basic physical characteristics of the fuel blends that could help predict combustion trends. The ASTM laboratory at the University of Kansas is equipped with the Koehler KV4000 Series Digital Constant Temperature Kinematic Viscosity Bath (ASTM D445) for measuring the kinematic viscosity, 6200 PARR Bomb Calorimeter (ASTM D240) for measuring energy content, Anton Paar 5000M DMA Density meter (ASTM D4052) for measuring the density, and a Paclp Optidist distillation unit (ASTM D86) to calculate the calculated cetane index (CCI). A table of the blended fuel properties is provided in Table 9. Since the laboratory is not equipped with a cetane engine or an ignition quality tester, the CCI is estimated using ASTM D4737 standard that describes an empirically-derived, four-variable equation. [210]. This standard is particularly suited for fuels that do not have a cetane improver and have CN values between 32.5 and 56.5 and is useful for predicting a trend in the actual CN. Additionally, the ASTM D4737 utilizes the fuel distillation temperatures obtained from the ASTM D86 method to estimate the CCI.

Table 9: Physical properties of blends of Jet-A and Sasol FSJF from ASTM laboratory tests

Blend → Property ↓	S0	S5	S10	S20	S50	S100	ULSD #2
Kinematic Viscosity (mm^2/s)	1.333 ±0.018	1.346 ±0.028	1.349 ±0.017	1.361 ±0.074	1.410 ±0.018	1.489 ±0.082	2.570 ±0.015
Density (kg/m^3)	791.93 ±0.277	792.59 ±0.118	793.56 ±1.144	795.42 ±0. 968	800.22 ±0.130	808.65 ±0.244	837.58 ±0.1269
LHV (MJ/kg)	46.11 ±0.019	45.45 ±0.081	45.95 ±0.369	46.22 ±0.456	46.54 ±0.985	46.77 ±1.025	45.58 ±0.081
LHV (MJ/m^3)	36518.09 ±15.640	36019.85 ±64.358	36465.52 ±292.902	36762.16 ±362.869	37242.08 ±788.373	37819.93 ±824.822	38174.82 ±68.011
CCI	47.62 ±0.196	46.90 ±0.195	46.33 ±0.194	45.37 ±0.192	43.85 ±0.182	39.43 ±0.181	48.71 ±0.122

To conduct the tests on the single cylinder engine, the FSJF is blended volumetrically with standard Jet-A and held in different fuel tanks for convenience to swap out fuels while testing. The injection sweeps controlled by the Bosch Modas Sport software for the entire tests are indicated in Table 10. In addition, this table indicates the absence of the adjusted blend of S20 at full load, which will be explained in the sections that follow.

Table 10: Injection timing for the adjusted and unadjusted test conditions for blends of Jet-A and Sasol FSJF

Blend → Load (N·m) ↓	S0 (ms)	S5 (ms)	S10 (ms)	S20 (ms)	S20 (adjusted) (ms)	ULSD #2 (ms)
0.5	12.5	12.5	12.5	12.5	13.0	12.5
4.5	12.5	12.5	12.5	12.5	12.8	12.5
9.0	11.0	11.0	11.0	11.0	11.3	11.0
13.5	10.0	10.0	10.0	10.0	10.3	10.0
18.0	11.0	11.0	11.0	11.0	-	11.0

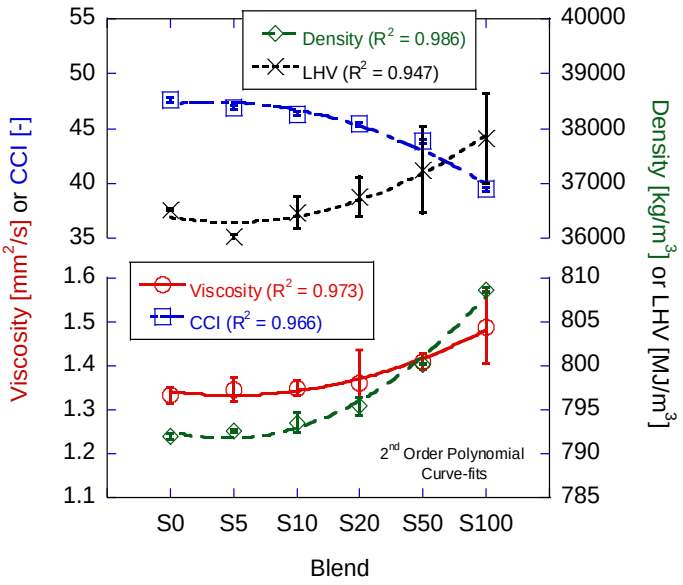

Figure 6: Curve-fits depicting trends of different fuel properties

Determination of Jet Fuel

As the properties of CTL and GTL fuels overlap, it can be confusing to correlate fuel composition with engine performance and emissions. Hence, an important part of this study was to identify the fuel since the sample provided by Sasol could have been derived from either coal or natural gas. For this, a sample of Sasol CTL was injected into the Agilent 5977A Gas Chromatography/Mass Spectrometry (GC/MS) machine that helped identify the important constituents of fuel. The plot depicted in Figure 6 was obtained through the Agilent MassHunter data acquisition software.

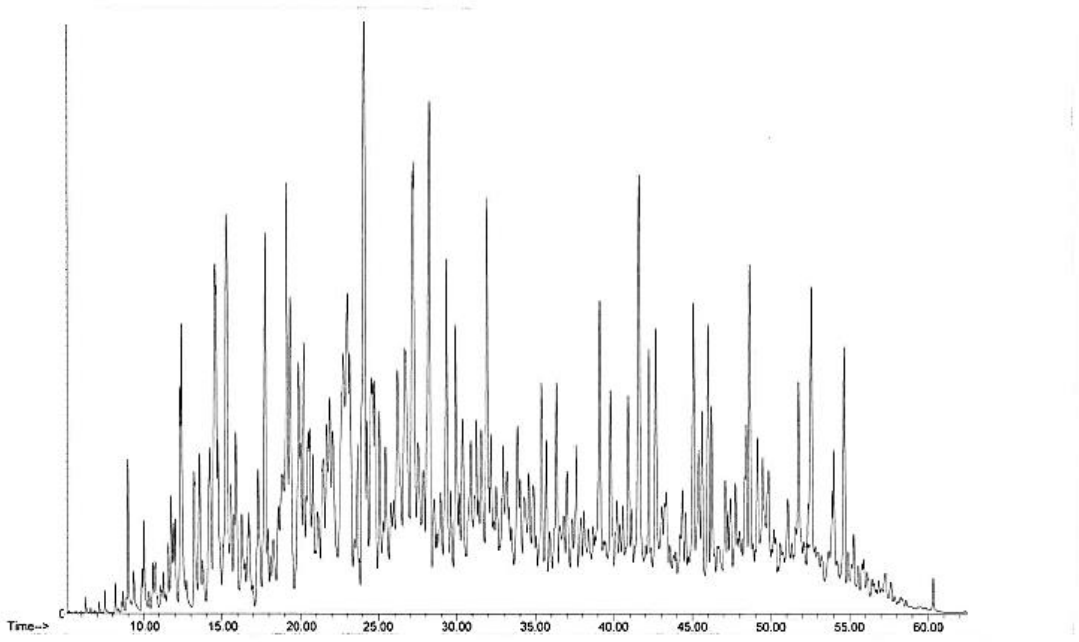

Figure 7: Gas Chromatograph and Mass Spectrograph of CTL fuel obtained from the Chemical/Environmental Engineering Department at the University of Kansas

On closer observation, the peaks in Figure 6 are consistent with a similar CG/MS plot corresponding to a low cetane number Sasol IPK fuel in a recent publication portrayed in Figure 7 [211]. A comparison of both figures indicated earlier peaks with a mixed proportion of naphthalenes, alkanes, cycloalkanes, and a small fraction of aromatics, typical of CTL fuels with higher volatility. On the contrary, natural gas derived hydrocarbons have a larger proportion of straight chain alkanes that result in well-defined peaks in the GC/MS with a lower retention time (Shell SPK, Figure 7). As a result, it was determined that the fuel was a mixture of coal derived hydrocarbons and not natural gas-derived hydrocarbons.

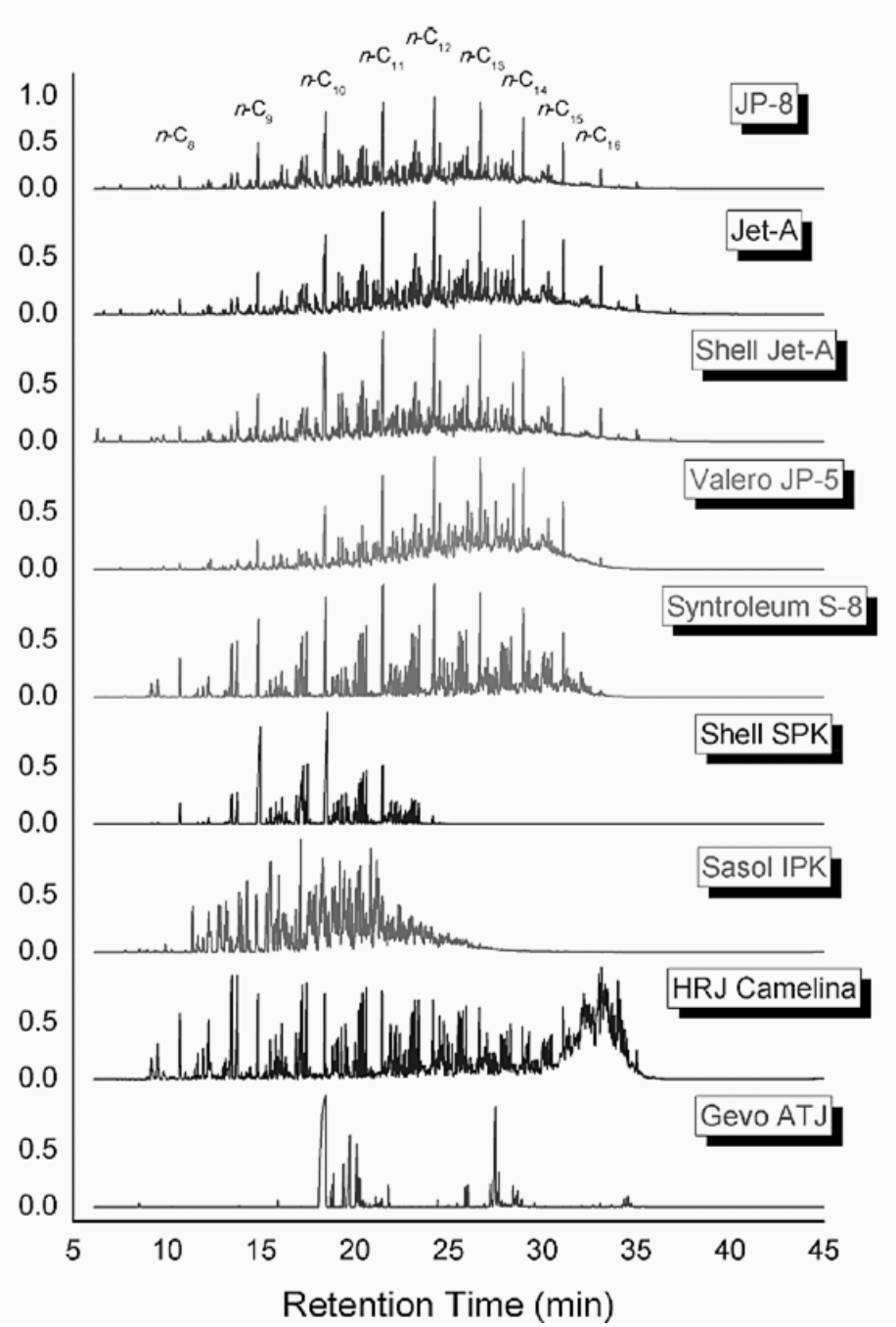

Figure 8: Normalized GC/MS plots for different aviation fuels approved for military use

Results and Discussion

The following sections describe the test engine results in detail, highlighting the potential effects of density, viscosity, and cetane number on combustion. To further elaborate on the data acquired from the engine test cell, the in-cylinder pressure, temperature, and heat release results are presented against the engine crank angle data. Additionally, the combustion efficiency, brake specific emissions, and brake specific fuel consumption are plotted with respect to engine load and blend percentage to indicate the trends related to emissions. For comparison, ULSD #2 serves as the baseline fuel to identify atypical combustion behaviors that arise from deviations in fuel properties. Furthermore, as the neat Jet-A fuel and blends of Jet-A and Sasol FSJF (S5, S10) had similar ignition delays, only the S20 blend was normalized by matching peak pressures to eliminate the effects of combustion phasing. Finally, it is important to note that combustion was unsuccessful when testing the adjusted S20 blend and the S50 blend. A hypothesis for poor combustion is discussed, followed by engine performance and emissions. Of note, the 0.5 N-m, low-load condition is not discussed in detail as the highly stochastic cycle to cycle variations typical of heterogeneous combustion introduce high uncertainties in measurements of both torque and emissions. To further elucidate the shortcomings in low-load measurements, results from a previous study indicate the difficulty in maintaining engine torque at 0.5 N-m due to fluctuation in engine torque measurements recorded by the Futek torque transducer (Model # TRS-705) [212]. However, the low load conditions are presented for additional reading based on formats followed by research relevant to CI engine combustion.

Factors Affecting Combustion

Fuel Pump and Fuel Injector Efficiency

The regimes of combustion depend largely on the performance of the fuel injection system. In the current setup, fuel is injected from a six-hole injector nozzle at a pressure of 40 ± 0.5 MPa. Although the injector can work up to 200 bar, the pressure is set at 40 bar to prevent accidents while testing new blends of fuels. The function of the fuel injector is to atomize the fuel and propagate the fuel into the cylinder to effectively utilize the air charge. Assuming ideal conditions, fuel exits the nozzle in the form of a conical jet that breaks up and atomizes due to the unstable growth of surface waves based on the surface tension of the fuel. As the jet velocity increases, the aerodynamic forces within the cylinder further increase the surface tension forces resulting in breakup of the jet into finer particles of fuel [147]. These surface tension forces are substantially influenced by the density of the charge within the cylinder and most importantly, the fuel viscosity. Since jet fuels are less viscous, the spray angle increases. This wider angle affects jet atomization, lowers mixing rates and in some cases, impinges directly on the cylinder walls. Direct impingement of fuel on cylinder walls causes increased wear and a growth in unburned components of combustion. However, a lowered viscosity raises surface tension forces, which result in better atomization and fuel break-up. Meanwhile, films of fuels with high surface tension are destroyed faster resulting in larger drops of fuel [213]. Therefore, the performance of the engine depends on the fuel injection process which in turn is a strong function of the fuel viscosity, density, and bulk modulus.

Sasol FSJF has less than half the viscosity of ULSD#2 due its differences in fuel composition (Table 9). The test engine fuel injection pump is a third generation Bosch CP 3.2 radial piston high-pressure common rail pump driven by an externally powered motor and is responsible for creating a pressure of 200 MPa

in the common rail. Researchers have repeatedly indicated that the lower viscosity of alternative kerosene-based fuels like Jet-A and Sasol FSJF detrimentally affects the functioning of the fuel pump, particularly due to pumping losses, lowering the volumetric efficiency of the pump. Typically, a finite amount of fuel can pass through the clearances between the numerous moving components of the fuel pump for lubrication. Researchers have formulated empirical and theoretical equations based on the fundamentals of fundamentals of fluid dynamics to predict the mass flow past the clearances in the pump as a function of parameters like rail pressure, average viscosity, pump speed, and geometry. Lastly, research shows that blends of ethanol and diesel result in similar viscosities as blends of Jet-A and CTL fuel. As a result, a relative comparison can be made with data obtained from researchers working on combustion of blends of ethanol and diesel, despite there being a dearth of experimental data to specifically highlight the long-term effects of using jet fuel in diesel fuel pumps.

Hot Engine Starts

The effects of low fuel viscosity of jet fuel are worsened during high engine operating temperatures. Since the test exceeded 8 hours, the engine block and components of the engine are at an elevated temperature compared to the ambient. As a result, the increase in fuel temperature results in a further drop in viscosity, increasing the hydraulic and pumping losses in the fuel pump and fuel injection system. Under standard operating conditions, ASTM D 975 mandates that ULSD#2 fuel have a kinematic viscosity range from 1.9 to 4.1 mm^2/s at 40^oC for safe engine operation [214]; whereas, aviation fuels have viscosities ranging in the 1.4 to 2.0 mm^2/s range [215]. As a result, the viscosity of the fuel could fall below 1.0 mm^2/s causing in an increase in clearances, flooding the cylinder and ceasing engine operation. Furthermore, a large reduction in fuel viscosity could lead to a wider spray angle of injected fuel with subsequent wall quenching, inhibiting combustion [147]. This problem was documented in the

alternative fuel based CI engine test conducted by Brandt et al. [174] where it was reported that the higher amounts of fuel entered the cylinders and increased THC emissions. Hence, the engine was immediately shut off to prevent hydro-locking. In a separate incident following the CTL fuel test, a fault in the FTIR laser prevented any future testing.

Low Fuel Cetane Number and Viscosity

Since Sasol produces different streams of jet fuel, there is one blend that consists of a large proportion of Sasol's isoparaffinic kerosene (IPK) that has reportedly poor autoignition characteristics [139]. Since the CCI is only an approximation of the trend of the CN, the actual fuel cetane could be much lower than what is described in Table 9. Further, the ASTM methods to determine the calculated cetane as well as derived cetane number do not correlate well when the CN is below 40 [140]. Additionally, the methods of calculated CN and derived CN could overestimate the CN by as much as 25. As a result, the autoignition quality of the fuel would drastically affect the higher blends of Jet-A and Sasol CTL and lead to unstable engine operation across the entire load range. Furthermore, the unusually high compression ratio (21.2:1) of the single cylinder research engine used for the current study compression ratio could compound the effects of lower cetane and viscosity to inhibit combustion. Generally, the high compression ratio increases the degree of atomization of fuel within the combustion chamber. However, excessively high compression ratios and lower viscosities and CCI could combine to decrease fuel penetration, widen the fuel spray and subsequently prevent combustion, particularly at higher blends.

In-Cylinder Pressure

The in-cylinder pressure curve depicts the influence of fuel properties, operational parameters, and fuel injection timing on combustion. For the current study, in-cylinder pressure data presented in Figure 9

are an average of 60 thermodynamic cycles over all test load conditions for a crank angle between 5^{o} BTDC and 20^{o} after ATDC. The rapid rise in pressure upon autoignition denoted by the deviation away from the motoring curve indicates the premix phase of combustion after an ignition delay. During this period, the fuel that was atomized and mixed during the ignition delay rapidly ignites and creates the explosive force. Thus, the rate of premixed combustion is proportional to the mass of the fuel-air mixture prepared during the ignition delay. While this premix burn effectively implies constant volume-like combustion and is desirable for engine performance, too high of a peak pressure could structurally damage the engine. In general, a greater pressure peak than ULSD#2 can denote improved combustion and atomization for the fuel under study. Moreover, in terms of emissions, higher in-cylinder pressures tend to correlate with greater temperatures (via the ideal gas law), enhanced NO_x formation, and reduced partial combustion products. Whereas, the subsequent diffusion burn (aka mixing controlled combustion) phase occurs at a slower rate where fuel that is atomized becomes ready for combustion [147]. This stage of combustion is associated with lower pressures and reduced flame temperatures that result in lower NO_x emissions and higher soot formation along with greater partial combustion products. Hence, subsequent discussions rely predominantly on pressure-crank angle data to compare engine performance and emissions for the fuels tested.

As denoted in Figure 9 at all load conditions, Jet-A and its blends with Sasol's FSJF demonstrate a greater peak pressure than ULSD#2. At low loads (Figure 9a and 9b), the minimal quantity of fuel injected into the cylinder does not result in a significant difference in the pressure profiles between the fuels. However, at medium and high loads (Figure 9c, 9d, and 9e), the in-cylinder pressure rises significantly for the blends of Jet-A and Sasol's FSJF fuel as compared to ULSD#2. This is due to primarily to the reduced viscosity of these fuels that promotes an enhanced mixing with the air in the cylinder. In particular, a decrease in fuel viscosity leads to a wider spray angle, shallower penetration depth, and

smaller droplet size. Moreover, the lower CCI of these blends allows more time for this mixing to occur with added fuel entering. These facets overcome the respectively lower density and energy content of these fuels (note: the engine injects fuel on a volumetric basis) that would otherwise suggest a less energetic combustion event.

Moving on, the addition of Sasol's FSJF fuel to Jet-A results in a higher in-cylinder pressure compared to neat Jet-A (S0). Investigating Figure 9, blend viscosity increases with CTL addition suggesting a worse mixing process. However, the CCI drops while the density and energy content increases with blend percentage. Therefore, more time is allowed for mixing while a greater level of energy is added. This lessened CCI does eventually impact the combustion event at 20% blend resulting in a slightly later rise in pressure (Figure 9c); hence, injection timing had to be adjusted to normalize the combustion event.

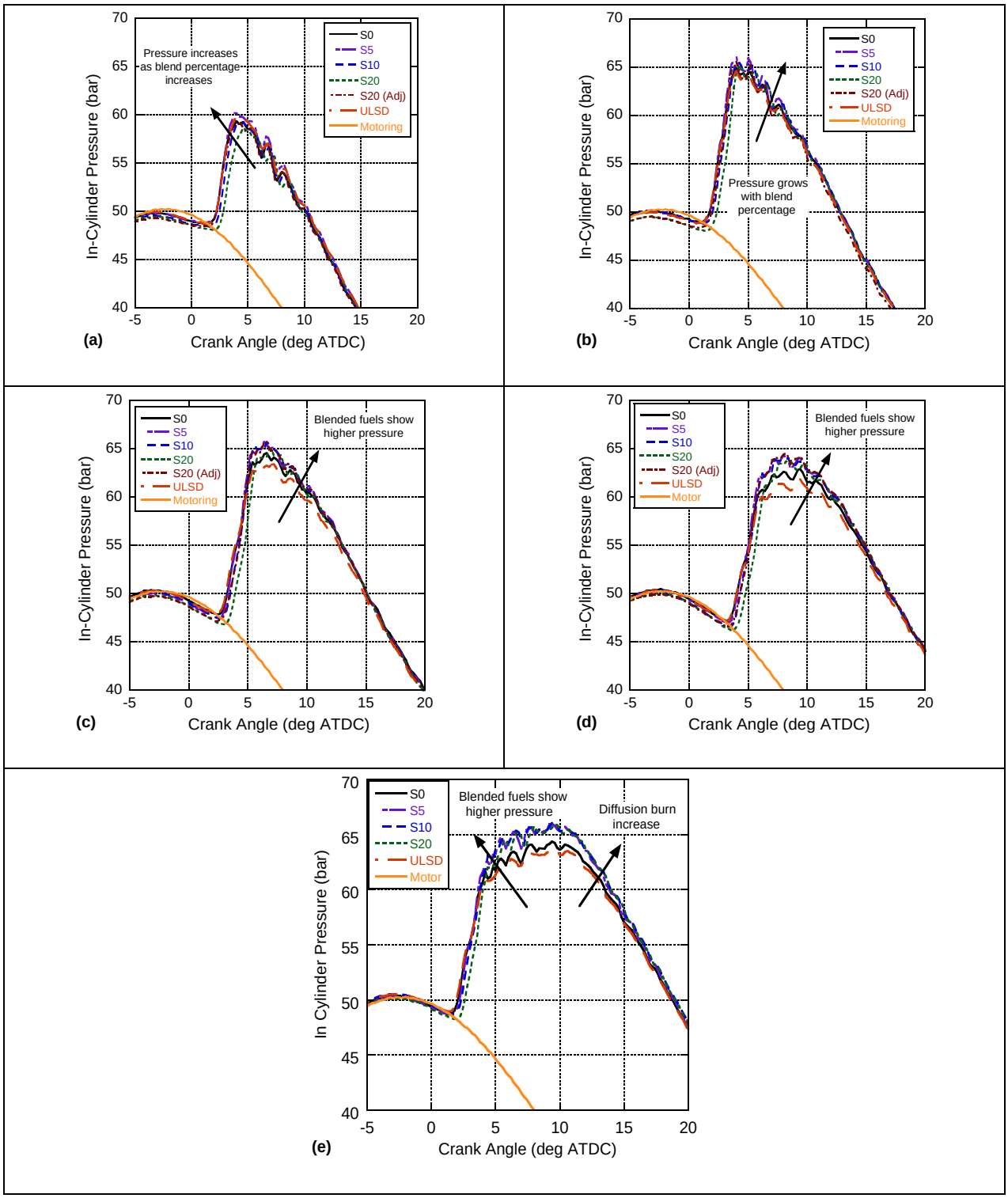

Figure 9: In-cylinder pressure vs. engine crank angle for unadjusted and adjusted fuel blends at different engine loads, (a) 0.5 N-m load, (b) 4.5 N-m load, (c) 9.0 N-m load, (d) 13.5 N-m load, and (e) 18.0 N-m load

An initial assumption upon reviewing Table 9 would be that moving to the less energetic Jet-A (S0) from ULSD#2 would increase the brake specific fuel consumption (BSFC) of the engine as additional fuel is needed to achieve the set loads. Moreover, to attain the greater pressures seen in Figure 9 might require more of this lower volumetric energy dense fuel. However, within experimental error, there is little difference in BSFC between ULSD#2, Jet-A, and the Sasol FSJF blends as shown in Figure 10. Interestingly, it appears that the enhanced mixing of the less viscous jet fuels effectively offsets their reduced energy content. Furthermore, as the blend level progresses (S0 to S20) and viscosity increases, the respective growth in energy content mostly makes up for a respectively poorer mixing event. This supports prior work that indicates efficiency is tied strongly to the generation of a homogeneous fuel-air mixture with the viscosity of the fuel playing a significant role [216]. With respect to load, the engine (generally) runs more thermodynamically efficient as the load increases; therefore, less fuel is needed to achieve the next torque set point and the BSFC decreases for all fuels. Overall, the similar BSFC levels at different blend ratios indicate that Jet-A and Sasol FSJF can be blended for military operations without a penalty for power and fuel consumption; hence, with logistical fuel costs potentially exceeding $400 per gallon [217] this is an advantageous outcome.

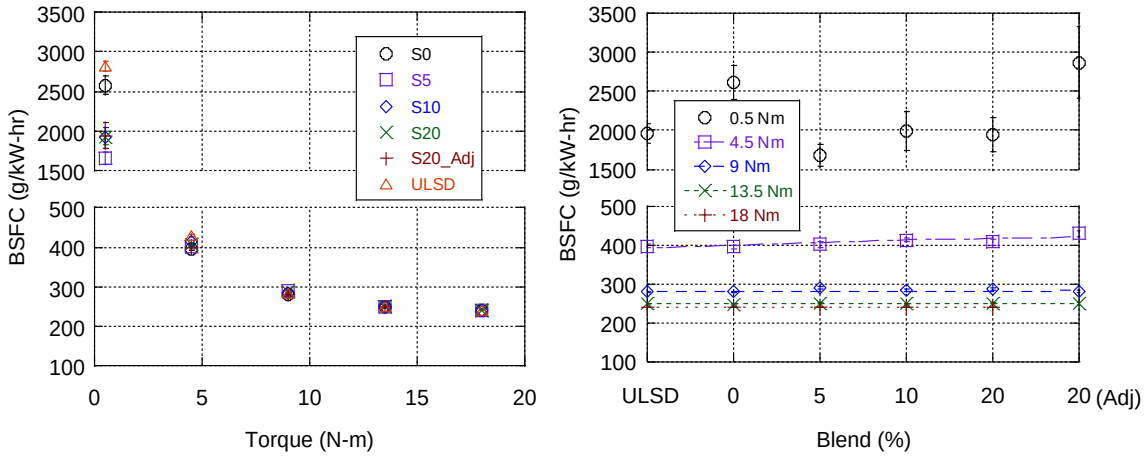

Figure 10: BSFC vs. torque (left) and blend percentage (right) for ULSD#2, Jet-A, and Jet-A/Sasol FSJF blends

Rate of Heat Release (RHR)

The rate of heat release from the burning fuel is presented as a useful method to approximate the progression of combustion resulting from the influence of fuel properties and injection timing. Moreover, heat release is an accurate depiction of combustion phasing in the cylinder, representing fuel injection, ignition delay, premixed combustion, diffusion burn, and late combustion. To model the rate of heat release (RHR), a quasi-static analysis using pressure is performed employing the first law of thermodynamics while assuming the air fuel mixture acts as an ideal gas. Here, a heat release model developed by a previous graduate student is used [37, 34].

Similar to the in-cylinder pressure plots, Jet-A and its blends with Sasol's FSJF fuel have a greater rate of heat release rate than ULSD#2 across all operating conditions. At low loads (Figures 11a and 11b), combustion is predominantly premixed where a lesser quantity of fuel injected has more time to mix homogenously. The higher heat release rate is again a function of a reduced viscosity and lower CCI enhancing atomization and mixing for these fuels while overcoming their respectively reduced energy content. At medium and high loads (Figure 11c, 11d, and 11e), the effect of CCI becomes more pronounced (i.e., growth of ignition delay at the 20% blend level) and the premixed burn phase

increases. In addition, the diffusion burn phase appears to grow slightly as the reduced viscosity of the jet fuels promotes a more homogeneous combustion process during this phase.

When Jet-A is compared to the blends of Jet-A and Sasol's FSJF fuel, the RHR is lower for the neat S0 fuel. Like the discussion involving in-cylinder pressure, the increasing viscosity of Sasol's FSJF blends reduces the homogenization of air and fuel. However, the drop in CCI with blend percentage promotes a longer mixing process while a more energetic fuel is added. As a result, the heat release rate grows with blend percentage. This is seen primarily in the premixed burn phase where the time for mixing has a greater impact on the rate of heat release; i.e., combustion during the diffusion burn phase is governed more by the rate at which fuel enters the cylinder with mixing playing a secondary role.

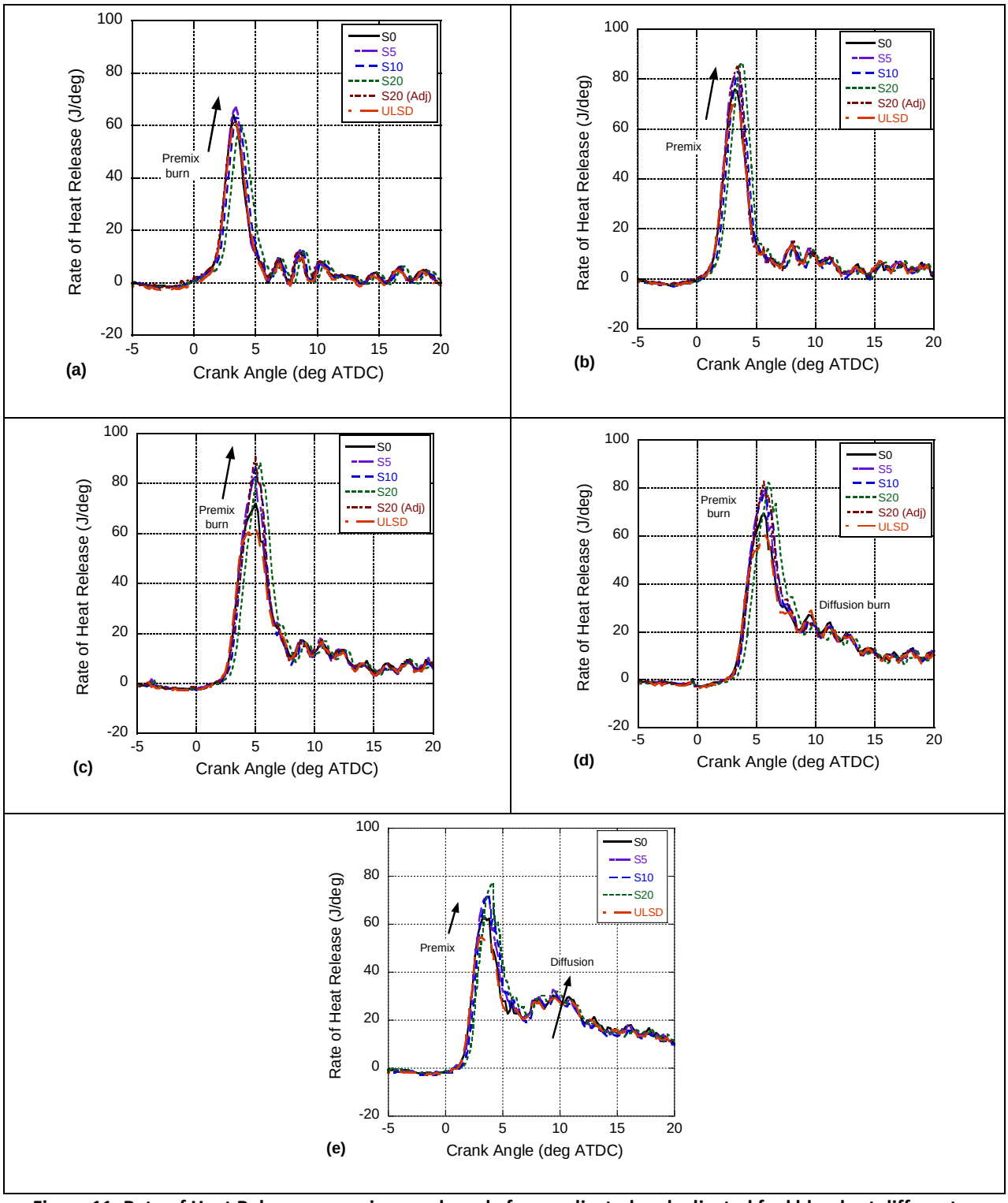

Figure 11: Rate of Heat Release vs. engine crank angle for unadjusted and adjusted fuel blends at different engine loads, (a) 0.5 N-m load, (b) 4.5 N-m load, (c) 9.0 N-m load, (d) 13.5 N-m load, and (e) 18.0 N-m load

In-Cylinder Temperature

Average global in-cylinder temperature estimates are important from the point of view of NO_x emissions. Between the thermal, prompt, and fuel bound nitrogen based kinetics for NO_x formation, the thermal route is prominent and associated with local in-cylinder temperatures exceeding 1800 K [147]. As a result, thermal NO_x emissions are of concern for CI engines and changes to the premixed burn phase can play a significant role in their formation [218].

The trends of in-cylinder temperatures in Figure 12 follow the discussion of the in-cylinder pressure and rate of heat release; i.e., temperatures of the jet fuels are greater than ULSD#2 while increasing with a growing proportion of CTL fuel in the blends with respect to S0. Next, a rise in premixed burn (S20 > S10 > S5 > S0 > ULSD#2) in Figure 12 results in larger in-cylinder temperatures during the earlier phase of combustion. Moreover, the small growth of diffusion burn (S20 > S10 ≈ S5 ≈ S0 > ULSD#2) leads to higher gas temperatures towards the end of combustion. Overall, this will result in augmented heat transfer to the cylinder walls and a respectively hotter residual gas left in the cylinder. This greater residual gas temperature is evident in Figure 12 by a larger value for temperature around TDC. Hence, moving to this CTL fuel results in a double compounding effect on temperature. Its properties will generate a more energetic heat release rate that additionally starts at a higher in-cylinder temperature due to hotter walls.

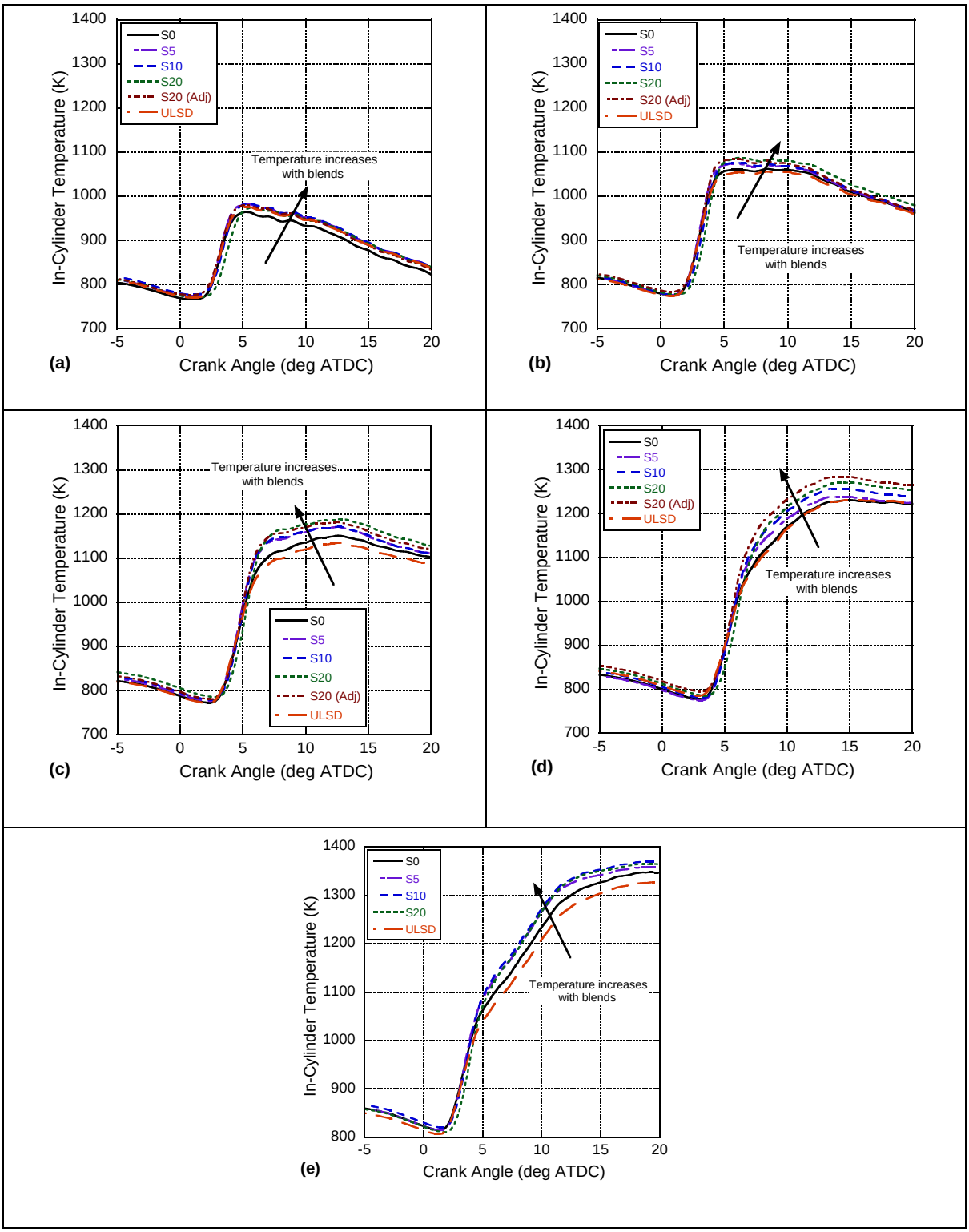

Figure 12: Rate of Heat Release vs. engine crank angle for unadjusted and adjusted fuel blends at different engine loads, (a) 0.5 N-m load, (b) 4.5 N-m load, (c) 9.0 N-m load, (d) 13.5 N-m load, and (e) 18.0 N-m load

NO_x Emissions

Compression ignition engines mainly produce nitric oxide (NO) and nitrogen dioxide (NO_2) emissions that are together expressed as nitrogen oxides (NO_x). At temperatures above 1300^{o}C, molecular nitrogen present in the air dissociates into its atomic state, which is highly reactive with multiple valence electrons and ionized states. Mostly, this atomic nitrogen is converted to NO via the extended thermal Zeldovich mechanism in near-stoichiometric and lean air fuel mixtures [147]. While NO_2 does additionally form during this process, at sustained high in-cylinder temperatures it quickly dissociates back to NO. Furthermore, the formation of NO_x is influenced by the residence time of the combustion mixture within the cylinder under high temperatures. Hence, greater in-cylinder temperatures earlier in the combustion process (i.e., pre-mixed) tends to produce more NO_x emissions.

Figure 13 highlights a decreasing trend of NO_x concentrations with respect to engine load. On an absolute basis, NO_x emissions will increase with load as the temperature grows (see Figure 12). However, the engine runs more thermodynamically efficient as the load increases and BSFC decreases (see Figure 6). Since emissions are presented on a per energy basis (g/kWh – legislated as such for stationary engines), lower NO_x emissions are seen per gram of fuel entering. In other words, as fuel efficiency grows with engine load, respectively less extra fuel is needed to achieve the next set point resulting in a lower added potential for NO_x emissions.

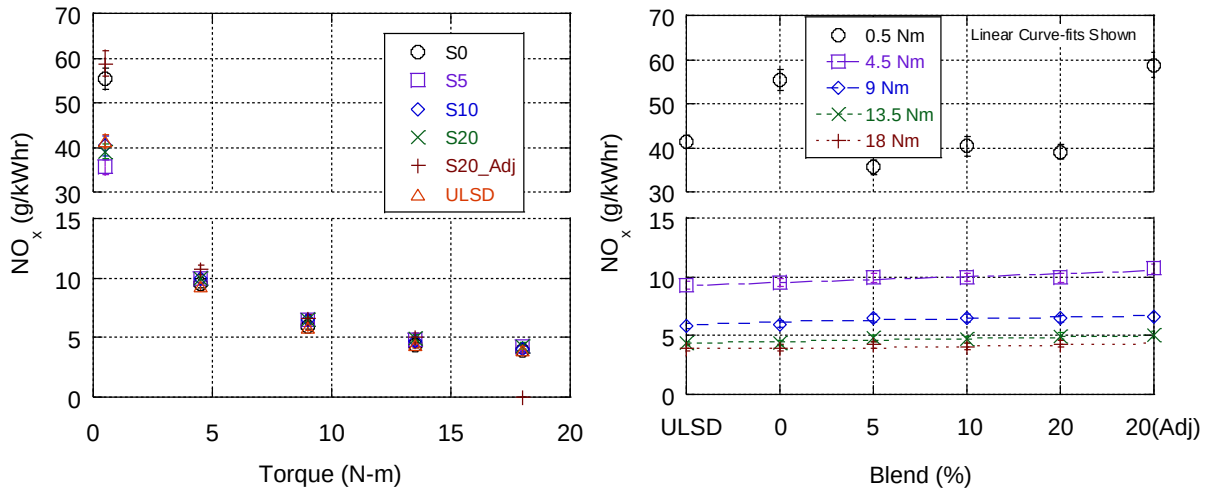

Figure 13: Brake-Specific NO_x emissions vs. (left) torque and (right) blend percentage for ULSD#2, Jet-A, and Jet-A/Sasol FSJF blends

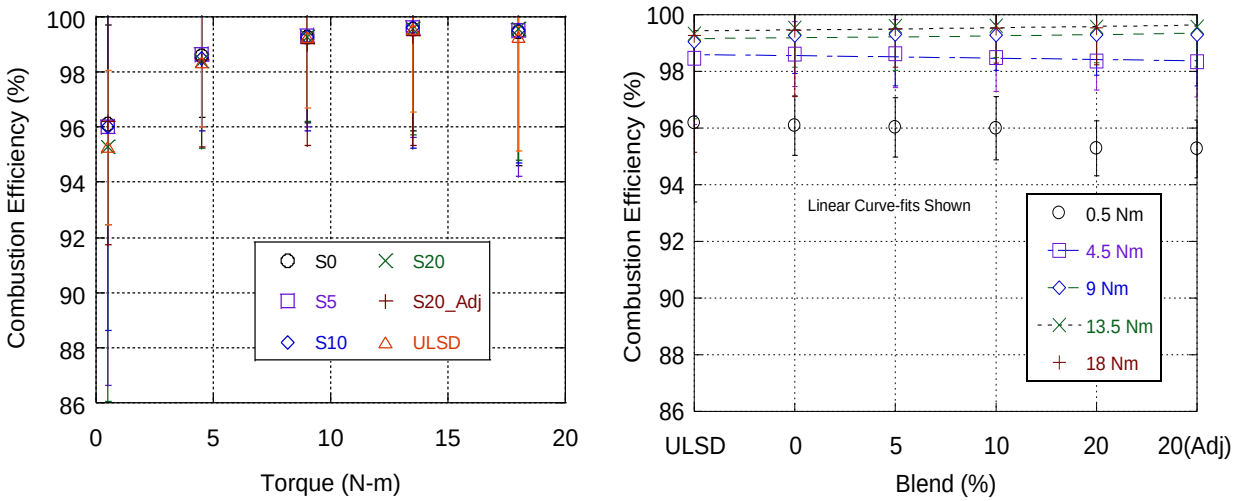

Figure 14: Combustion efficiency vs. torque (left) and blend percentage (right) for ULSD#2, Jet-A, and Jet-A/Sasol FSJF blends

In addition, Figure 13 indicates the variation in brake-specific NO_x emissions with the different blends of fuel. In contrast to ULSD#2, ignoring the respectively more variant no load situation, within experimental error S0 has similar NO_x emissions; whereas, increasing CTL blends might see a slight growth in NO_x (highlighted by the linear curve-fits in Figure 13). Interestingly, despite the distinctive rise of in-cylinder pressures, heat release rates, and temperatures of the jet fuels, NO_x concentrations do not

grow significantly. Recalling the literature review in Chapter 2, CTL fuels have a lower H/C ratio that might reduce combustion efficiency while increasing the adiabatic flame temperature (about 7.5ºC higher than Jet-A under lean conditions [219]). Investigating the combustion efficiency in Figure 14 finds that all fuels perform relatively similar within experimental error. Therefore, perhaps only an increased adiabatic flame temperature is encountered and local combustion temperatures are growing noticeably; hence, local NO_x production is similar for the jet fuels even though the global temperature is rising. It is only when the combustion process becomes respectively more energetic (e.g., S20) and a significantly greater pre-mixed burn event is encountered that this overcomes the adiabatic flame temperature effect.

CO Emissions

Carbon monoxide (CO) emissions are typically formed due to incomplete combustion in local fuel rich zones with a slow rate of oxidation reactions encountered during the expansion stoke (i.e., diffusion burn phase). In these fuel rich zones, there is insufficient oxygen for the carbon to become completely oxidized to carbon dioxide (CO_2). Moreover, as the piston expands, the temperature drops subsequently reducing the bulk gas temperature that results in a quenching of the CO oxidation process. In general, CI engines produce negligible CO emissions since excessive air is always available for reactions to complete. Furthermore, as highlighted in Figure 14, as the load increases in these engines, global temperatures rise, promoting a more effective combustion process (i.e., combustion efficiency in Figure 6 rises with load) and lower CO emissions.

Similar to the NO_x results, CO emissions in Figure 15 are largely consistent between ULSD#2, Jet-A, and its blends with Sasol's FSJF. As stated prior, both the pre-mixed and (to a significantly lesser extent) diffusion burn phases grow when moving to the jet fuels. Moreover, there are estimated reduced local temperatures and a lower H/C ratio for these jet fuels (at an equivalent BSFC) that should additionally

enhance the CO production process. Hence, more fuel-rich zones through the diffusion burn process that combust respectively colder with a greater CO potential because of more carbon bonds. However, the lower viscosity of the jet fuels promotes a more homogeneous combustion process with lower local fuel-air ratios that overcomes these aspects ending in similar CO emissions. Moreover, with an increasing FSJF blend percentage, again the respectively greater energy content of this fuel mitigates a decreasing homogeneity as the fuel viscosity grows.

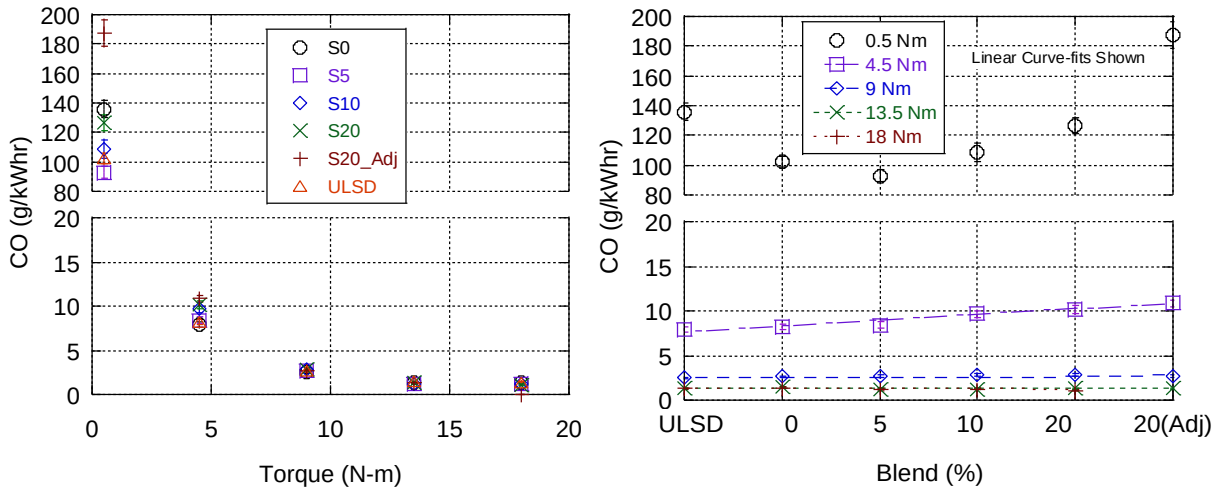

Figure 15: Brake-Specific CO emissions vs. torque (left) and blend percentage (right) for ULSD#2, Jet-A, and Jet-A/Sasol FSJF blends

Total Hydrocarbon (THC) Emissions

THC emissions are caused by incomplete fuel combustion in conditions that accentuate the heterogeneous nature of CI combustion and generally follow the same trends as CO emissions. The greater the level of the diffusion burn phase and the more heterogeneous the fuel-air mixture, the more potential there is for THC emissions. In addition, for fuels with a low CCI, overleaned zones in the flame front can grow with an increase in ignition delay and result in greater THC emissions during the premixed burn phase. However, in contrast to the CO emissions, THC emissions decrease noticeably for the jet fuels in comparison to ULSD#2 as shown in Figure 16. Here, the increased homogeneity of the jet

fuels again counters the growth of a colder and slightly larger diffusion burn process with their lower H/C ratio now providing an additional factor that reduces THC emissions. Furthermore, their reduced amount of hydrogen overcomes any possible growth in THC emissions during the premixed burn phase due to overleaning.

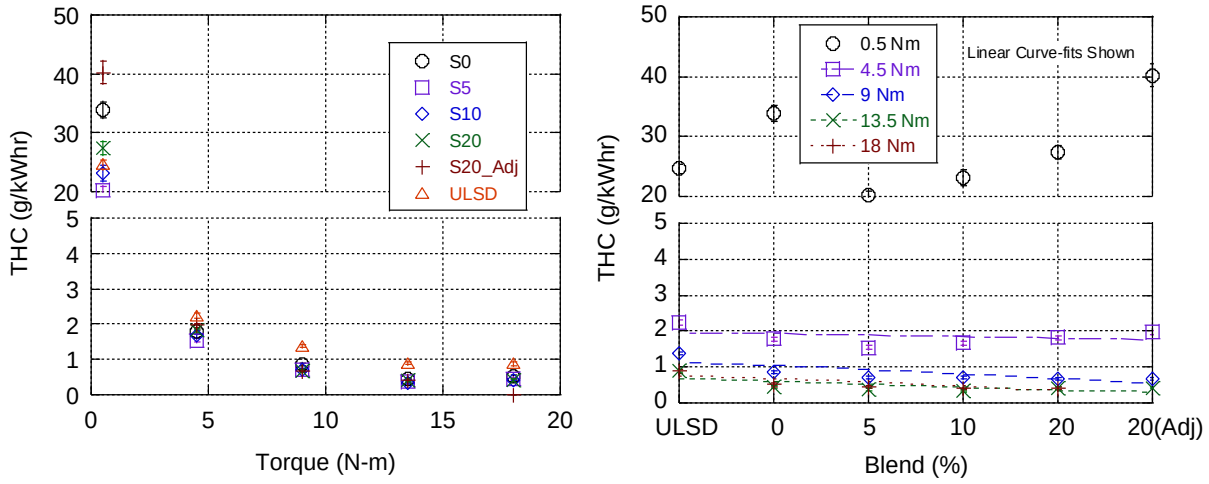

Figure 16: Brake-Specific THC emissions vs. torque (left) and blend percentage (right) for ULSD#2, Jet-A, and Jet-A/Sasol FSJF blends

Particulate Matter Emissions (PM)

A reduction in PM emissions is a primary concern for the U.S. military as $PM_{2.5}$ can damage lung tissues and cause severe health problems. Moreover, military bases are prone to elevated levels of $PM_{2.5}$, risking adverse effects on the health of military personnel [220]. PM emissions in CI engines are formed within the rich air-fuel mixtures in the combustion chamber via an agglomeration process. Among all the hydrocarbon species, aromatic compounds that form polycyclic hydrocarbons (PAH) act as precursors to the formation of PM [147]. Here, these PAH continue to grow and gain mass by addition of gas phased molecules. Then, coagulation takes place via reactive particle-particle collisions, followed by carbonization of particulate material, and, finally, the oxidation of PAHs and soot particles. Typically, at low loads, PM is formed as cooler in-cylinder temperatures prevent ideal fuel atomization that results in

larger droplets of fuel [147]. In addition, these particles are formed during the diffusion burn in rich fuel spray cores and consist of organic compounds that develop from fuel, lubricants, additives, and sulfur in the fuel.

Figure 17 indicates a rise in PM emissions with increasing load as the level of diffusion burn grows significantly. Hence, this provides more opportunity for the agglomeration of particles. In general, ULSD#2 has the greatest level of PM emissions followed by S0 and then the Sasol FSJF blends. This is mainly attributed to the aromatic content in these fuels [221]. Since Jet-A and ULSD#2 have an aromatic hydrocarbon content between 10 to 20%, their PM emissions are higher than the Sasol CTL fuel blends. Correspondingly, the absence of aromatic compounds in the Sasol CTL fuel negates the formation of the PAH precursors to the formation of soot. As a result, Figure 17 indicates a distinct drop in PM with an increasing blend of Sasol FSJF fuel. Here, it can be postulated that the effects of aromaticity in the fuel has the strongest influence on PM emissions as the other factors (i.e., greater and colder diffusion burn versus improved homogeneity) appear to largely balance themselves via the discussion surrounding CO and THC emissions.

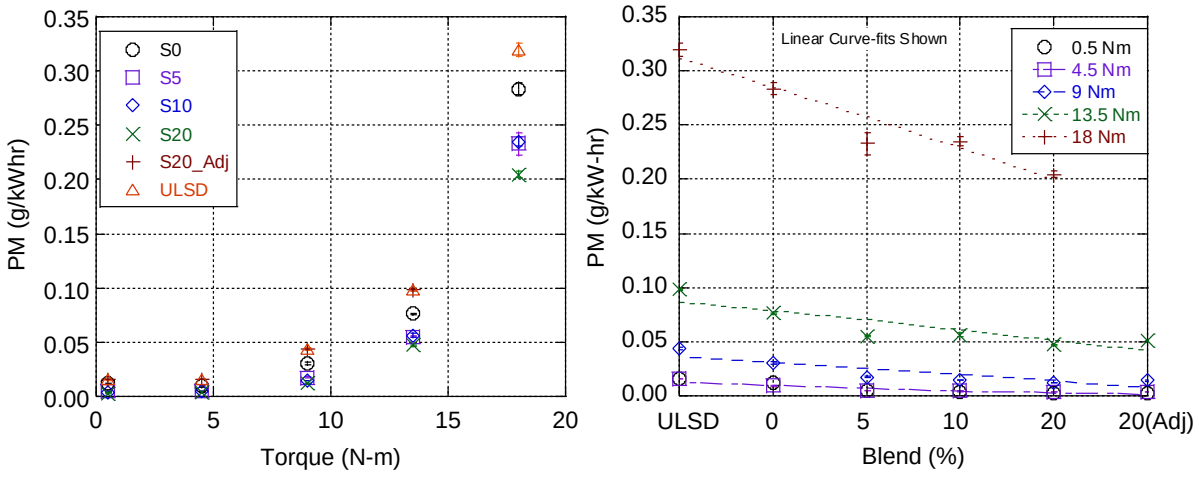

Figure 17: Brake-Specific PM Emissions vs. torque (left) and blend percentage (right) for ULSD#2, Jet-A, and Jet-A/Sasol FSJF blends

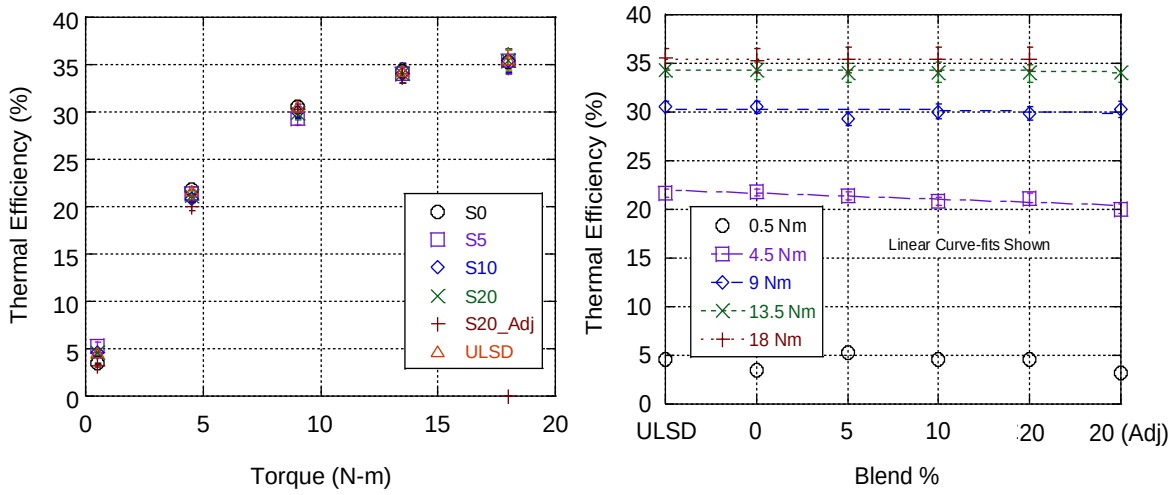

Figure 18: Thermal efficiency vs. torque (left) and blend percentage (right) for ULSD#2, Jet-A, and Jet-A/Sasol FSJF blends

By definition, thermal efficiency is the ratio of useful work produced in the thermodynamic cycle to the chemical energy released by the fuel. Hence, thermal efficiency rises with load (Figure 18) as the ratio of friction to useful brake power decreases. Further investigating Figure 18 finds that Jet-A (S0) has largely the same thermal efficiency as ULSD#2 within experimental error. Here, the level of homogeneity does increase with S0 and the in-cylinder pressure does rise; hence, thermal efficiency should be higher. However, recalling the in-cylinder temperature discussion, there is a greater level of heat transfer to the walls subsequently robbing the engine of efficiency. In addition, a hotter residual gas with S0 will reduce the ratio of specific heats of the overall mixture resulting in a less advantageous expansion phase. As a result, alike thermal efficiencies are encountered. Similar to prior stated results, as the FSJF blend level progresses growing the fuel viscosity, the added energy content largely makes up for this respectively worse mixing event and uniform thermal efficiencies are principally seen.

Moving on, Figure 19 summarizes the fuel conversion efficiency that follows similar trends as the thermal efficiency, in addition to lending credence to the BSFC results in Figure 10. Since fuel conversion efficiency is defined as the ratio between the shaft work produced by the engine and the theoretical

energy content of the fuel, the fuel conversion values increase with load. Again, with respect to the jet fuels, the corresponding changes to fuel and combustion properties (i.e., viscosity, energy content, adiabatic flame temperature) all appear to offset each other resulting in comparable fuel conversion efficiency outcomes.

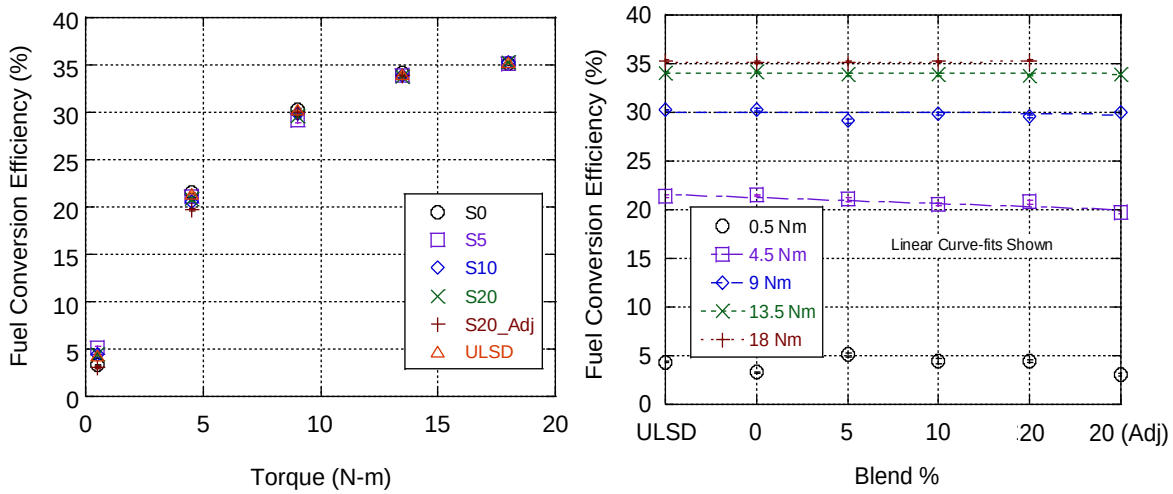

Figure 19: Fuel conversion efficiency vs. torque (left) and blend percentage (right) for ULSD#2, Jet-A, and Jet-A/Sasol FSJF blends

Conclusion

The U.S. DoD mandates the use of jet fuel in compression ignition engines in military bases to lessen the operational and logistical expenses of the U.S. military. However, the difference in physical properties and chemical compositions between jet and diesel fuels creates complications that affect engine performance by lowering power output compared to ULSD#2. As a result, additional research is needed to certify the use of aviation fuels on the battlefield to avoid compromising on war readiness of modern CI engines. Furthermore, as the U.S. military looks to reduce its dependency on foreign oil and augment petroleum-based fuels with non-petroleum fuels, CTL fuel has emerged as a viable option for the SFFP,

considering the vast reserves of coal on the U.S. mainland and highly matured status of CTL conversion technologies. Based on the literature review, the clean-burning nature and higher energy content of CTL fuels than ULSD#2 are advantageous for the U.S. military. However, the low viscosity and variability of CN of coal-derived fuels are cause for concern as both engine performance and emissions are negatively influenced without appropriate combustion strategies. Purely in relevance to the SFFP, it may be necessary to regulate the CN of jet fuels to prevent the use of fuel with CN less than 40. Else, the battlefield performance could be compromised if a military base receives a batch of low CN jet fuel. Additionally, introducing cetane additives on the battlefield is not an option as battle readiness would be adversely affected.

In the current experiment, CTL fuel from Sasol Ltd was tested in a single-cylinder, DI, CI engine that was retrofitted with an electronic fuel injection system. This engine was connected to a set of high-speed computers and sensors to record in-cylinder data and an AVL AVSM FTIR analyzer to measure multiple species of emissions. Since the FAA mandates a maximum of 50% blend for use in gas turbines, the fuel samples are prepared by adding Sasol CTL fuel to commercially available Jet-A in 5%, 10%, 20%, and 50% blends by volume, while ULSD#2 serves as a baseline fuel for comparison. Most importantly, the peak of pressure for each blend was matched with ULSD#2 to normalize combustion and eliminate the effects of combustion phasing while comparing different fuel blends.

Based on the tests, the addition of CTL fuel to Jet-A improved combustion up to the 20% blend due to the effects of improved homogeneity. Primarily, a reduction in cetane rating for the CTL fuel allows the less viscous jet fuel blends to be more premixed upon combustion. For these reasons, the jet fuel blends show higher in-cylinder pressure and temperature than ULSD#2. Next, the heat release plots indicate a slight retardation of ignition delay with the increase in percentage of CTL fuel in the blend, pointing to a growing influence of the reduced cetane rating of Sasol's CTL fuel. While testing the 50% blend,

combustion did not occur even after adjustments in injection timing as a combination of low viscosity and cetane rating is thought to have inhibited combustion. Also, the AVASM FTIR showed a large increase in THC emissions, indicating that the fuel did not ignite. One possible explanation for this is based on research conducted by Brandt et al. [174] where higher engine temperatures reduces fuel viscosity to levels below the safe operating limits. This results in increased fuel leakage past the fuel pump and injector, inhibiting combustion. Of note, a closer analysis of the ATJ fuels conducted by Dickerson et al. [175] indicates the similarities to CTL fuel. In particular, the CN number being relatively low (CN = 18) leads to misfires and unstable combustion at higher blends with JP-5/JP-8/Jet-A. Furthermore, the density, viscosity, and heating values of the ATJ fuel blends reported in the aforementioned analysis are close to the CTL fuel values determined in Table 9. Based on their study, the authors prescribed a maximum blend of 30% with Jet-A or JP-8 to achieve stable engine performance. For the same reason of low CN, the ATJ fuel-based CI combustion tests conducted at SwRI were performed using blends where the CN did not fall below 40. Thus, the similarities in fuel properties of ATJ and CTL jet fuels highlight the need for identical combustion strategies for the SFFP.

On the other hand, emission results show only marginal levels of differences between the different fuels tests. NO_x levels were slightly raised as percentages of CTL fuel in the blend increased. This was a result of the minor decrease in CN of Sasol CTL that promotes a more premixed burn. Next, the partial components of combustion show a marginal decrease compared to ULSD#2 and neat Jet-A as the improved atomization and higher LHV are beneficial for completion of chemical reactions. However, the PM levels markedly decreased with the absence of aromatics in the CTL fuel. In addition, the BSFC and thermal efficiency for all test fuels and the different fuel blends were nearly identical at medium to high load conditions.

To conclude, Sasol's CTL fuel blended with Jet-A showed an improvement in CI engine performance and similar emissions compared to ULSD#2 up to 20% blend by volume. Hence, CTL fuel can be aptly used in CI engines without affecting battlefield performance. However, beyond the 20% blend, the decrease in viscosity due to a rise in operating temperatures and the low cetane rating resulted in cylinder conditions that were below the safe limit for CI engines. Additionally, one could postulate an increase in fuel leakages past the clearance volumes in fuel injectors and pumps that hampered combustion. As suggestions to reach plausible solutions for the unsuccessful engine tests at higher blend percentages of CTL fuel, multiple injection strategies and appropriate determination of fuel composition could assist in the accurate prediction of CI combustion.

Chapter 4: Conclusion and Future Work

The combustion of alternative fuels in CI engines was studied based on the SFFP initiated by the U.S. DoD. The introduction presented an overview of how the SFFP evolved from the need to minimize operational and logistical costs of NATO forces and U.S. military stationed overseas. Subsequently, the formulation of synthetic fuels provided further impetus to reduce foreign oil dependence and advance research on newer jet fuels for the SFFP. In addition, the decision to convert all U.S. military bases to operate solely on commercial Jet-A instead of JP-8 was an inducement to study jet fuel combustion in CI engines. Currently, the thrust towards reducing carbon emissions opened several pathways for environmentally benign biosynthesized jet fuels to be used for the U.S. military. Hence, a comprehensive review featuring CI engine tests with alternative fuels approved for use by the ASTM 7566D standard was presented. With the use of fuels other than ULSD#2, the review highlighted the effect of changing fuel properties on CI engine combustion and emissions that are critical to military vehicles. To conclude the study, results from an engine test performed at the University of Kansas were discussed to compare the performance of a blend of coal-derived jet fuel and commercially available Jet-A for the SFFP. Chapter 2 provided a comprehensive review of ASTM-approved aviation fuels that have been tested in CI engines. The notion of using jet fuels in CI engines began with the use of JP-5 as early as 1965. First, studies featuring naval JP-5 fuel were evaluated extensively for engine performance where it was established that the low viscosity led to a loss in engine power and premature wear of mechanical fuel injection systems. With the introduction of the SFFP directive in 1988 by the U.S. DoD, SwRI and TARDEC were tasked with certifying the use of JP-8 in CI engines where their research focused on engine performance and fuel lubricity. Consequently, the research at SwRI and TARDEC indicated a decrease in engine power output, growing ignition delay, fuel pump leakages, rough performance, and increased emissions compared to ULSD#2. In the following years, additional research was performed on engines to

evaluate the use of modern facets of CI combustion like newly formulated fuel additives, electronic fuel injection, high pressure common rail fuel systems and multiple injection events. To be specific, the reduced volumetric energy density increased the BSFC and reduced the range of combat vehicles fitted with electronic fuel injection systems. All things considered, it was established that the low viscosity, absence of a CN rating, and high variability of fuel composition made it difficult to predict engine performance and emissions when fueled with petroleum-derived jet fuels. With the formulation of alternative fuels derived from coal and natural gas, additional research was required to certify synthetic fuels for the SFFP. Peculiarly, the CTL fuel was derived from multiple streams of light distillates that yielded fuels of varying composition that could impact the process of blending fuels to conform to regulations. Overall, CTL fuels indicated similar performance as JP-8 barring a few cases where the significantly low CN resulted in unstable engine operation, high heat release, and premix burn with a rise in NOx emissions. Meanwhile, the paraffinic GTL fuel with a higher LHV improved engine performance and reduced emissions compared to ULSD#2 and Jet-A. For both GTL and CTL fuels, the absence of aromatic hydrocarbons drastically reduced the formation of PM. However, the production of liquid fuels from natural gas is considered more profitable and less energy intensive than coal derived jet fuel, leading to a decline in CTL fuel utilization.

With large-scale bio-jet fuel production gaining importance due to an emphasis on renewable fuels, extensive tests are being undertaken to confirm the viability of using HEFA, ATJ and SIP jet fuels for the SFFP. Firstly, HEFA fuels indicated superior performance and lowered emissions compared to ULSD#2 and Jet-A or JP-8. Based on the research articles reviewed, HEFA fuels revealed identical engine performance and emissions as GTL fuel. However, the vast variation in feedstock could affect certain fuel properties. Next, the abundance of corn as a fuel crop presented an opportunity to formulate jet fuels to reduce net carbon emissions. In the limited combustion research that has been carried out

recently, CI engine tests with ATJ fuels indicated a decline in performance that limited the blend percentage to 30% by volume with JP-8 due to a notably lower cetane rating (CN < 30). Finally, advances in bio-engineering have enabled the conversion of waste cellulosic sugars to valuable hydrocarbons. Furthermore, SIP fuel showed promise as a biojet fuel because of its single-component composition (called farnesane with a significantly higher CN than ULSD#2) that enables predictable engine performance and emissions.

Collectively summarizing alternative fuels, the lowered viscosity of all jet fuels improved atomization and homogeneity, but negatively influenced factors like fuel injection, fuel cone angle and fuel jet penetration. However, the difference in chemical properties imparted a different CN to each fuel that affected the chemical delay phase during autoignition. For example, the use of CTL and ATJ fuels resulted in unstable engine operation when CN was found to be below the ASTM permissible limit of 40. The lowered CN increased premix burn (and NO_x formation) and pushed combustion into the expansion stroke, leading to a loss of useful work. On the other hand, GTL and HEFA fuels improved engine performance over ULSD#2 with a higher LHV and CN. Moreover, the lack of aromatic hydrocarbons was the leading factor in reducing the formation of PM, including fuels with higher CN that had a significantly longer diffusion burn. Overall, the absence of a CN rating and variability in chemical composition of jet fuels are the main causes of unpredictable CI engine performance and emissions.

Chapter 3 elucidated the testing and subsequent analysis of using coal-derived synthetic fuel in CI engines for the SFFP. For the study, a blend of Jet-A and Sasol's CTL fuel were tested in a single cylinder research engine in ratios of 5%, 10%, 20%, and 50% by volume. This fuel had higher energy content but a lower CN and viscosity than ULSD#2 that combined to inhibit engine operation after blends greater than 50%. For fuel blends up to 20%, no advance in injection was required, indicating that the combustion of Jet-A and CTL fuel was practically identical. Meanwhile, the heat release plots for the jet fuel tests

indicated marginally higher engine performance compared to ULSD#2 due to improved atomization and better LHV. Additionally, the emission results demonstrated identical levels of BSFC, NOx, and unburned products of hydrocarbons between the tested blends of jet fuel. This startling similarity would imply that Sasol CTL fuel can be safely blended at lower blends without a penalty in engine performance. In the long term, the combustion tests suggested that Sasol fuel can be utilized in CI engines at low blends, offering a slight improvement in power and significantly lowered PM emissions.

In conclusion, the production of CTL fuels has fallen considerably to minimize the utilization of coal as a fuel. However, recent advances in carbon capture and sequestration may lessen the impacts of GHG emissions and initiate the recuperation of CTL jet fuels. Hence, subsequent efforts should aim at establishing an appropriate fuel chemistry to understand the smaller but significant nuances of using alternative aviation fuels in CI combustion. Next, the higher compression ratio could be lowered to reveal additional facets of low CN fuel. Furthermore, the tests could point to a relationship between viscosity and cetane number that may assist in identifying optimal blend ratios for stable engine performance. Additionally, the influence of parameters like higher fuel injection pressure and EGR could extensively influence the formation of NO_x and PM. Finally, the low cetane CTL fuel can be investigated for low temperature combustion to achieve the NO_x-PM tradeoff.

References:

1. EIA, US. *Short-Term Energy Outlook (STEO)*. Department of Energy.2017.
2. NOAA. *Carbon Dioxide*. https://climate.nasa.gov/vital-signs/carbon-dioxide. 2017.
3. EPA. *Overview of Greenhouse Gases*. https://www.epa.gov/ghgemissions/overview-greenhouse-gases#carbon-dioxide. 2015.
4. Heywood, John B. *Internal combustion engine fundamentals*. McGraw-Hill. 1988.
5. EIA, US. *Monthly energy review*.2017.
6. DOD, US. *Fiscal Year 2016 Operational Energy Annual Report*.2017.
7. Blackwell, Kristine E. 2007. *The Department of Defense: Reducing Its Reliance on Fossil-Based Aviation Fuel-Issues for Congress*. 2007.
8. Act, Energy Policy. 2005. *Energy policy Act of 2005*. Washington, DC: US Congress. 2005.
9. Martel, Charles R. *Military Jet Fuels, 1944-1987*. Aero Propulsion Lab, AFWAL AFSC.1987.
10. Leonard, J T. *Generation of Electrostatic Charge in Fuel Handling Systems: A Literature Survey*.1981.
11. K.C. Bachman, W.G. Dukek and A.H. Popkin. *Aircraft Incidents Attributed to Static Electricity, 1959-1969*.1969.
12. al., Beery et. *Assessment of JP-8 as a replacement fuel for the Air Force standard jet fuel JP-4*.1975.
13. Pera, Maurice E. Le. 2005. The Reality of the Single-Fuel Concept. *Army Logistician, Life Cycle Management*.
14. J.N. Bowden, S.R. Westbrook, M.E. LePera. *A Survey of JP-8 and JP-5 Properties*.1988.

15. Montemayor, Alan F, et al. *Potential Benefits From the Use of JP-8 Fuel in Military Ground Equipment*. Southwest Research Inst., San Antonio, Tx and Belvoir Fuels and Lubricants Research Facility. 1989.

16. Likos, William E., Owens, Edwin C., and Lestz, Sidney J. *Laboratory Evaluation of MIL-T-83133 JP-8 Fuel In Army Diesel Engines* 1988.

17. W.E. Butler, Jr. R.A. Alvarez, D.M. Yost, S.R. Westbrook, J.P. Buckingham, S.J. Lestz. *Final report on field demonstration of aviation turbine fuel MIL-T-83133C grade JP-8 (NATO Code F-34) at Fort Bliss, TX*.1992.

18. Hardenberg, H. O., and F. W. Hase. *An Empirical Formula for Computing the Pressure Rise Delay of a Fuel from Its Cetane Number and from the Relevant Parameters of Direct-Injection Diesel Engines*. 1979.

19. Schihl, Peter, and Laura Hoogterp. *On the ignition and combustion variances of jet propellant-8 and diesel fuel in military diesel engines*. US Army Tank Automative Research Developement and Engineering Center. 2008.

20. Mattie, David R, and Teresa R Sterner. *Past, present and emerging toxicity issues for jet fuel*. Toxicology and applied pharmacology, 2011. 254.2: p. 127-132.

21. Alm, Alvin L, and Richard H Truly. *More Capable Warfighting Through Reduced Fuel Burden*. 1998. p.

22. Dimotakis, Paul, et al. *Reducing DoD fossil-fuel dependence*. MITRE CORP MCLEAN VA JASON PROGRAM OFFICE. 2006.

23. Moore, Richard H, et al. *Biofuel blending reduces particle emissions from aircraft engines at cruise conditions*. Nature, 2017. 543.7645: p. 411-415.

24. Blakey, Simon, et al. *Aviation gas turbine alternative fuels: A review*. Proceedings of the combustion institute, 2011. 33.2: p. 2863-2885.

25. El Takriti, Sammy, et al. *MITIGATING INTERNATIONAL AVIATION EMISSIONS*. 2017. p.

26. Radich, Tony. *The Flight Paths for Biojet Fuel*. 2015.

27. IATA. *2036 Forecast Reveals Air Passengers Will Nearly Double to 7.8 Billion*. http://www.iata.org/pressroom/pr/Pages/2017-10-24-01.aspx. 2017.

28. Vann, Lance A. *Feasibility of JP-8 to Jet a Fuel Conversion at US Military Facilities*. Air Force Institute of Technology. 2008.

29. DLA, USAF and. *The Air Force Fuel Conversion Program*.2017.

30. Howards, S. *Airport-Based Alternative Fuel Vehicle Fleets*. National Renewable Energy Lab., Golden, CO (US). 2001.

31. Donohoo-Vallett, Pearl Elizabeth. *Scaling Air quality effects from alternative jet fuel in aircraft and ground support equipment*. 2010.

32. Miller, B., et al., *Guidelines for Integrating Alternative Jet Fuel Into the Airport Setting*. Transportation Research Board.2012.

33. Langness, Chenaniah, et al. *Construction, Instrumentation, and Implementation of a Low Cost, Single-Cylinder Compression Ignition Engine Test Cell*. 2014.

34. Mattson, Jonathan M. S., and Christopher Depcik. *Emissions–calibrated equilibrium heat release model for direct injection compression ignition engines*. Fuel, 2014. 117.Part B: p. 1096-1110.

35. Mattson, Jonathan, et al. *Second-Law Heat Release Modeling of a Compression Ignition Engine Fueled With Blends of Palm Biodiesel*. Journal of Engineering for Gas Turbines and Power, 2016. 138.9: p. 091502-091502-10.

36. Langness, C. *Effects of Natural Gas Constituents on Engine Performance, Emissions, and Combustion in Compressed Natural Gas-Assisted Diesel Combustion*. KU ScholarWorks. 2014.

37. Mattson, Jonathan MS, and Christopher Depcik. *First and second law heat release analysis in a single cylinder engine*. SAE International Journal of Engines, 2016. 9.1: p. 536-545.

38. Mattson, Jonathan Michael Stearns. *Power, Efficiency, and Emissions Optimization of a Single Cylinder Direct-Injected Diesel Engine for Testing of Alternative Fuels through Heat Release Modeling*. 2013.

39. Hileman, James I., et al. *Energy Content and Alternative Jet Fuel Viability*. Journal of Propulsion and Power, 2010. 26.6: p. 1184-1196.

40. Mangus, Michael, and Christopher Depcik. *Comparison of ULSD, used cooking oil biodiesel, and JP-8 performance and emissions in a single-cylinder compression-ignition engine*. SAE International Journal of Fuels and Lubricants, 2012. 5.3: p. 1382-1394.

41. Mangus, Michael, et al. *Performance and Emissions Characteristics of Hydroprocessed Renewable Jet Fuel Blends in a Single-Cylinder Compression Ignition Engine with Electronically Controlled Fuel Injection*. Combustion Science and Technology, 2015. 187.6: p. 857-873.

42. EIA, US. *U.S. Kerosene-Type Jet Fuel Wholesale/Resale Price by Refiners*. 2019.

43. Schmitigal, Joel, and Jill Tebbe. *JP-8 and other Military Fuels*. Tank and Automotive Research Development and Engineering Center (TARDEC). 2011.

44. Edwards, James T. 2017. *Reference jet fuels for combustion testing*. 55th AIAA Aerospace Sciences Meeting. 2017.

45. Shafer, Linda, et al. *Chemical Class Composition of Commercial Jet Fuels and Other Specialty Kerosene Fuels*.

46. Weir, Donald G. *Strategic Implications for a Single-Fuel Concept*. Army War College. 1996.

47. Wise, WW, and JJ Wise. *Substitution of JP-5 for Diesel Fuels Ashore*. US Naval Civil Engineering Laboratory Technical Note N-660, Port Hueneme, CA, 1965. p.

48. Wise, Judith J, and Sheldon Phelps. *Heavy Equipment Operators Evaluation: JP-5 vs DF-2*. NAval Civil Engineering Lab. 1965.

49. Watson, William W. *The Use of JP-5 Aviation Turbine Fuel in Large-Bore, Low-Speed Diesel Engines*. U.S. Naval Civil Engineering Laboratory. 1965.

50. Lestz, S.J. *Comparison of DF-2 and JP-5 in GMC Detroit -Diesel 6V-53T Performance Evaluation*. US Marine Corps. 1972.

51. Marvin, FR. *Performance Curves, DDA Engines, JP-4, JP-5 and No. 2 Diesel Fuel*. Letter to Headquarters US Marine Corps, 1974. p.

52. Moon, Richard B. *Evaluation of JP-5 Turbine Fuel in the Single Cylinder Cue 1790 Diesel Engine*. Southwest Research Institute (SwRI). 1979.

53. Lee, J.R. *JP-5 Fuel Compatibility Test (400-Hour Mission Profile)*. Teledyne Continental Motors, General Products Division 1979.

54. Bowden, JN, et al. *Military Fuels Refined from Paraho-II Shale Oil*. Southwest Research Institute (SwRI). 1981.

55. Montemayor, AF, et al. *Fuel Property Effects on Diesel Engine and Gas Turbine Combustor Performance*. Southwest Research Institute (SwRI). 1981.

56. Montemayor, Alan F, and Edwin C Owens. *Comparison of 6.2 L Arctic and Standard Fuel Injection Pumps Using JP-8 Fuel*. Southwest Research Institute (SwRI). 1986.

57. Owens, Edwin C, et al. *Vehicle Acceleration and Fuel Consumption When Operated on JP-8 Fuel*. Southwest Research Institute (SwRI). 1989.

58. Lacey, Paul I, and Sidney J Lestz. *Failure Analysis of Fuel Injection Pumps from Generator Sets Fueled with Jet A-1*. Southwest Research Institute (SwRI). 1991.

59. Lacey, Paul I. *Wear Analysis of Diesel Engine Fuel Injection Pumps from Military Ground Equipment Fueled with Jet A-1*. Southwest Research Institute (SwRI). 1991.

60. Lacey, Paul I, and Sidney J Lestz. *Effect of Low-Lubricity Fuels on Diesel Injection Pumps-Part I: Field Performance*. SAE Technical Paper. 1992.

61. Lacey, Paul I, and Sidney J Lestz. *Effect of Low-Lubricity Fuels on Diesel Injection Pumps-Part II: Laboratory Evaluation*. SAE Technical Paper. 1992.

62. Yost, Douglas M, et al. *US Army investigation of diesel exhaust emissions using JP-8 fuels with varying sulfur content*. SAE Technical Paper. 1996.

63. Kouremenos, DA, et al. *Experimental investigation of the performance and exhaust emissions of a swirl chamber diesel engine using JP-8 aviation fuel*. International journal of energy research, 1997. 21.12: p. 1173-1185.

64. Stoecklein, KE, et al. *Initial Effects of Converting Army Diesel-Powered Ground Vehicles to Operate on JP-8+ 100 Fuel*. U.S. Army TARDEC Fuels and Lubricants Research Facility (SwRI). 2000.

65. Kotsiopoulos, P, et al. 2001. *Diesel and JP-8 fuel performance on a Petter AV1 diesel engine*. 39th Aerospace Sciences Meeting and Exhibit. 2001.

66. Arkoudeas, P, et al. *Study of using JP-8 aviation fuel and biodiesel in CI engines*. Energy Conversion and Management, 2003. 44.7: p. 1013-1025.

67. Rakopoulos, Constantinos D, et al. *Comparative environmental evaluation of JP-8 and diesel fuels burned in direct injection (DI) or indirect injection (IDI) diesel engines and in a laboratory furnace*. Energy & fuels, 2004. 18.5: p. 1302-1308.

68. Korres, Dimitrios M, et al. *Use of JP-8 Aviation Fuel and Biodiesel on a Diesel Engine*. SAE transactions, 2004. p. 2027-2037.

69. Frame, Edwin A, and Matthew G Blanks. *Emissions from a 6.5 L HMMWV engine on low sulfur diesel fuel and JP-8*. Southwest Research Institute (SwRI). 2004.

70. Fernandes, Gerald, et al. *Impact of military JP-8 fuel on heavy-duty diesel engine performance and emissions*. Proceedings of the Institution of Mechanical Engineers, Part D: Journal of Automobile Engineering, 2007. 221.8: p. 957-970.

71. Papagiannakis, RG, et al. *Single fuel research program comparative results of the use of jp-8 aviation fuel versus diesel fuel on a direct injection and indirect injection diesel engine*. SAE Technical Paper. 2006.

72. Schihl, Peter, et al. *Modeling JP-8 fuel effects on diesel combustion systems*. Tank Automotive Research, Development & Engineering Center. 2006.

73. Kalligeros, S, et al. *Exhaust Emissions of a Diesel Engine Using Aviation Fuel Blends with Biodiesel*. Proceedings of the 10th International Conference on Environmental Science and Technology, pp. A.

74. Kotsiopoulos, Petros, et al. *Experimental investigation concerning the effect of the use of Biodiesel and F-34 (JP-8) aviation fuel on performance and emissions of a DI Diesel engine*. SAE Technical Paper. 2007.

75. Mosburger, Michael, et al. *Impact of High Sulfur Military JP-8 Fuel on Heavy Duty Diesel Engine EGR Cooler Condensate*. SAE International.2008.

76. Korres, Dimitris, et al., *Aviation fuel JP-5 and biodiesel on a diesel engine*.2008.

77. Pandey, Anand Kumar, and MR Nandgaonkar. *Performance, emission and pump wear analysis of JP-8 fuel for military use on a 558 kW, CIDI diesel engine*. SAE International Journal of Fuels and Lubricants, 2010. 3.2: p. 238-245.

78. Nargunde, Jagdish, et al. *Comparison between Combustion, Performance and Emission Characteristics of JP-8 and Ultra Low Sulfur Diesel Fuel in a Single Cylinder Diesel Engine*. SAE Technical Paper. 2010.

79. Smith, Michael, et al. 2010. *Effect of High Sulfur Military JP-8 Fuel on Heavy Duty Diesel Engine Emissions and EGR Cooler Condensate*. ASME 2010 Internal Combustion Engine Division Fall Technical Conference. 2010.

80. Wadumesthrige, Kapila, et al. *Performance, Durability, and Stability of a Power Generator Fueled with ULSD, S-8, JP-8, and Biodiesel*. SAE International. 2010.

81. Lee, Jinwoo, and Choongsik Bae. *Application of JP-8 in a heavy duty diesel engine*. Fuel, 2011. 90.5: p. 1762-1770.

82. Brandt, Adam C, and Douglas M Yost. *Evaluation of Military Fuels Using a Ford 6.7 L Powerstroke Diesel Engine*. Southwest Research Institute. 2011.

83. Henein, Naeim, et al. *Autoignition Characteristics of Low Cetane Number JP-8 and Approaches for Improved Operation in Military Diesel Engines*. Army Tank Automotive Research Development And Engineering Center. 2011.

84. Lutz, Tim, and Rajani Modiyani, *Brake Thermal Efficiency Improvements of a Commercially Based Diesel Engine Modified for Operation on JP 8 Fuel*.2011.

85. Murphy, Lucas, and David Rothamer. *Effects of Cetane Number on Jet Fuel Combustion in a Heavy-Duty Compression Ignition Engine at High Load*. 2011.

86. Lee, Jinwoo, et al. *Combustion process of JP-8 and fossil Diesel fuel in a heavy duty diesel engine using two-color thermometry*. Fuel, 2012. 102.p. 264-273.

87. Soloiu, Valentin, et al. *Performance of JP-8 Unified Fuel in a Small Bore Indirect Injection Diesel Engine for APU Applications*. SAE Technical Paper. 2012.

88. Yost, D.M, and A.C Brandt. *Evaluation of JP-8 at high temperature in the Ford 6.7L high pressure common rail diesel engine*. 2012.

89. Yu, Xin, et al. *Comparison of In-Cylinder Soot Evolution in an Optically Accessible Engine Fueled with JP-8 and ULSD*. SAE International Journal of Fuels and Lubricants, 2012. 5.2: p. 875-891.

90. Mangus, Michael, and Christopher Depcik. *Comparison of ULSD, Used Cooking Oil Biodiesel, and JP-8 Performance and Emissions in a Single-Cylinder Compression-Ignition Engine*. SAE Int. J. Fuels Lubr., 2012. 5.3: p. 1382-1394.

91. Jayakumar, Chandrasekharan, et al. *Effect of biodiesel, jet propellant (Jp-8) and ultra low sulfur diesel fuel on auto-ignition, combustion, performance and emissions in a single cylinder diesel engine*. Journal of Engineering for Gas Turbines and Power, 2012. 134.2: p. 022801.

92. Jayakumar, Chandrasekharan, et al. *Effect of swirl and injection pressure on performance and emissions of JP-8 fueled high speed single cylinder diesel engine*. Journal of Engineering for Gas Turbines and Power, 2012. 134.2: p. 022802.

93. Labeckas, Gvidonas, et al. 2013. *Combustion, performance and emission characteristics of diesel engine operating on jet fuel treated with the cetane improver*. Proceedings of 12th International Scientific Conference “Engineering for Rural Development”, Latvia, Jelgava, LUA. 2013.

94. Soloiu, Valentin, et al. *Combustion and Emissions Characteristics of JP-8 Blends and ULSD# 2 with Similar CN in a Direct Injection Naturally Aspirated Compression Engine*. SAE Technical Paper. 2013.

95. Rothamer, David A, and Lucas Murphy. *Systematic study of ignition delay for jet fuels and diesel fuel in a heavy-duty diesel engine*. Proceedings of the combustion institute, 2013. 34.2: p. 3021-3029.

96. Uyumaz, Ahmet, et al. *Experimental examination of the effects of military aviation fuel JP-8 and biodiesel fuel blends on the engine performance, exhaust emissions and combustion in a direct injection engine*. Fuel Processing Technology, 2014. 128.p. 158-165.

97. Labeckas, Gvidonas, et al. *The effect of aviation fuel JP-8 and diesel fuel blends on engine performance and exhaust emissions*. Journal of KONES, 2015. 22.p.

98. Labeckas, Gvidonas, et al. *Dependency of the Autoignition Delay, Combustion and Exhaust Emissions of a Diesel Engine on the Cetane Number of Aviation-Turbine JP-8 Fuel*. Agricultural Engineering, 2014. 46.p. 23-39.

99. Solmaz, Hamit, et al. *Investigation of the effects of civil aviation fuel Jet A1 blends on diesel engine performance and emission characteristics*. 2014. p.

100. Yamik, Hasan, et al. *A comparative study on engine performance and emissions of biodiesel and JP-8 aviation fuel in a direct injection diesel engine*. 2014. p.

101. Lee, Jeongwoo, et al. *Emission reduction potential in a light-duty diesel engine fueled by JP-8*. Energy, 2015. 89.p. 92-99.

102. Chu, Sanghyun, et al. *An Experimental Investigation of Injection and Operating Strategies on Diesel Single Cylinder Engine under JP-8 and Dual-Fuel PCCI Combustion*. SAE Technical Paper. 2015.

103. Labeckas, Gvidonas, and Stasys Slavinskas. *Combustion phenomenon, performance and emissions of a diesel engine with aviation turbine JP-8 fuel and rapeseed biodiesel blends*. Energy Conversion and Management, 2015. 105.p. 216-229.

104. Soloiu, Valentin, et al. *Comparison of Combustion and Emissions Properties of Jet-A vs. ULSD in Both Indirect and Direct Compression Ignition Engines at Same IMEP*. SAE International. 2016.

105. Szedlmayer, Michael T., et al. *Combustion and Performance Sensitivity to Fuel Cetane Number in an Aviation Diesel Engine*.

106. Solmaz, Hamit, et al. *An experimental study on the effects of diesel and jet-A1 fuel blends on combustion, engine performance and exhaust emissions in a direct injection diesel engine*. J. of Therrmal Science and Technollogy, 2016. 36.2: p. 51-60.

107. Szedlmayer, Michael, and Chol-Bum M Kweon. *Effect of Altitude Conditions on Combustion and Performance of a Multi-Cylinder Turbocharged Direct-Injection Diesel Engine*. SAE Technical Paper. 2016.

108. Sane, Sahil, et al. *Autoignition and Combustion of ULSD and JP8 during Cold Starting of a High Speed Diesel Engine*. SAE Technical Paper. 2017.

109. Szedlmayer, Michael T., et al. *The effect of fuel aromatic content and cetane number on combustion in a UAV diesel engine*.

110. Kim, Kenneth, et al., *The effect of outside air temperature and cetane number on combustion and performance in a UAV diesel engine at various altitude conditions*.2017.

111. Williams, Robert H, and Eric D Larson. *A comparison of direct and indirect liquefaction technologies for making fluid fuels from coal*. Energy for Sustainable Development, 2003. 7.4: p. 103-129.

112. Fischer, Franz, and Hans Tropsch. *The preparation of synthetic oil mixtures (synthol) from carbon monoxide and hydrogen*. Brennstoff-Chem, 1923. 4.p. 276-285.

113. Brathwaite, J, et al. *Maximizing efficiency in the transition to a coal-based economy*. Energy Policy, 2010. 38.10: p. 6084-6091.

114. Lamprecht, Delanie. *Fischer− Tropsch fuel for use by the US military as battlefield-use fuel of the future*. Energy & fuels, 2007. 21.3: p. 1448-1453.

115. de Smit, Emiel, and Bert M. Weckhuysen. *The renaissance of iron-based Fischer–Tropsch synthesis: on the multifaceted catalyst deactivation behaviour*. Chemical Society Reviews, 2008. 37.12: p. 2758-2781.

116. Saib, AM, et al. *Fundamental understanding of deactivation and regeneration of cobalt Fischer–Tropsch synthesis catalysts*. Catalysis Today, 2010. 154.3-4: p. 271-282.

117. Liu, Guangrui, et al. *Technical review on jet fuel production*. Renewable and Sustainable Energy Reviews, 2013. 25.p. 59-70.

118. Abanteriba, Sylvester, et al. *Derived Cetane Number, Distillation and Ignition Delay Properties of Diesel and Jet Fuels Containing Blended Synthetic Paraffinic Mixtures*. SAE International Journal of Fuels and Lubricants, 2016. 9.3: p. 703-711.

119. Striebich, Richard, et al. *Dependence of Fuel Properties During Blending of Iso-Paraffinic Kerosene and Petroleum-Derived Jet Fuel*. University of Dayton. 2008.

120. Moses, C.A., Stavinoha, L.L., Roets, P. *Qualification of Sasol Semi-Synthetic Jet A-1 as Commercial Jet Fuel: 1997*. 1997. p.

121. Smith, Beverly L., and Thomas J. Bruno. *Application of a Composition-Explicit Distillation Curve Metrology to Mixtures of Jet-A and S-8*. Journal of Propulsion and Power, 2008. 24.3: p. 618-623.

122. Zhang, Chi, et al. *Recent development in studies of alternative jet fuel combustion: Progress, challenges, and opportunities*. Renewable and Sustainable Energy Reviews, 2016. 54.p. 120-138.

123. DeWitt, Matthew J, et al. *Effects of aromatic type and concentration in Fischer− Tropsch fuel on emissions production and material compatibility*. Energy & Fuels, 2008. 22.4: p. 2411-2418.

124. Schubert, Paul F., et al. *Expanding Markets for GTL Fuels and Specialty Products*. Elsevier. 2001.

125. Moses, Clifford A. *Comparative evaluation of semi-synthetic jet fuels*. Contract, 2008. 33415.02-D: p. 2299.

126. Frame, Edwin A, and Matthew G Blanks. *Exhaust Emissions from a 6.5 L Diesel Engine Using Synthetic Fuel and Low-Sulfur Diesel Fuel*. Southwest Research Institute (SwRI). 2003.

127. Frame, EA, et al. *Alternative Fuels: Assessment of Fischer-Tropsch Fuel for Military Use in 6.5 L Diesel Engine*. SAE transactions, 2004. p. 1826-1842.

128. Frame, Edwin A, et al. *Evaluation of Synthetic Fuel for Army Ground Applications Tasks II-VI*. Southwest Research Institute (SwRI). 2007.

129. Alvarez, Ruben, and Edwin A Frame. *Evaluation of Synthetic Fuel in Military Tactical Generators*. Southwest Research Institute (SwRI). 2008.

130. Schulman, Matthew E, and Edwin A Frame. *Engine Durability Evaluation Using Synthetic Fuel, Caterpillar C7 Engine*. Southwest Research Institute (SwRI). 2008.

131. Hansen, Gregory, et al. *Fischer-Tropsch Synthetic Fuel Evaluations HMMWV Test Track Evaluation*. Southwest Research Institute (SwRI). 2009.

132. Hoogterp-Decker, Laura, and Peter Schihl. *The use of synthetic JP-8 fuels in military engines*. Army Tank Automotive Research Development and Engineering Center. 2010.

133. Subramanian, Swami Nathan, and Stephen Ciatti. 2011. *Low Cetane Fuels in Compression Ignition Engine to Achieve LTC*. ASME 2011 Internal Combustion Engine Division Fall Technical Conference. 2011.

134. Claus, Michael, et al. *Durability Evaluation of the Effects of Fischer-Tropsch Derived Synthetic Paraffinic Kerosene Blended up to 50% With Petroleum JP-8 on a Detroit Diesel/MTU 8V92TA Engine*. US Army Tank Automotive Research Development and Engineering Center (TARDEC). 2011.

135. Jayakumar, Chandrasekharan, et al. *Effect of Intake Pressure and Temperature on the Auto-ignition of Fuels with different Cetane Number and Volatility*. SAE Technical Paper. 2012.

136. Schihl, Peter, et al. *The Ignition Behavior of a Coal to Liquid Fischer-Tropsch Jet Fuel in a Military Relevant Single Cylinder Diesel Engine*. SAE International Journal of Fuels and Lubricants, 2012. 5.2: p. 785-802.

137. Muzzell, Pasty A, et al. *US Army Qualification of Alternative Fuels Specified in MIL-DTL-83133H for Ground Systems Use*. US Army Tank Automotive Research Development and Engineering Center (TARDEC). 2013.

138. Gowdagiri, Sandeep, et al. *A diesel engine study of conventional and alternative diesel and jet fuels: Ignition and emissions characteristics*. Fuel, 2014. 136.Supplement C: p. 253-260.

139. Zheng, Ziliang, et al. *Effect of Cetane Improver on Combustion and Emission Characteristics of Coal-Derived Sasol IPK in a Single Cylinder Diesel Engine*. 2014. 46162: p. V001T02A009.

140. Schihl, Peter, et al. *The Combustion and Ignition Characteristics of Varying Blend Ratios of JP-8 and a Coal to Liquid Fischer-Tropsch Jet Fuel in a Military Relevant Single Cylinder Diesel Engine*. SAE International Journal of Fuels and Lubricants, 2015. 8.2: p. 501-514.

141. Soloiu, Valentin, et al. *RCCI of Synthetic Kerosene With PFI of N-Butanol-Combustion and Emissions Characteristics*. 2015. 57274: p. V001T02A016.

142. Soloiu, Valentin, et al., *Combustion and Emissions Characteristics of Dual Fuel Premixed Charge Compression Ignition with Direct Injection of Synthetic FT Kerosene Produced from Natural Gas and Port Fuel Injection of n-Butanol*.2016.

143. Soloiu, Valentin, et al. *Performance of an Indirect Injected Engine Operated with ULSD#2 Blended with Fischer-Tropsch Synthetic Kerosene*. 2017.

144. Muinos, Martin, et al. *Experimental Investigation on the Combustion and Emissions Characteristics of n-Butanol/GTL and n-Butanol/Diesel Blends in a Single-Cylinder MD-CI Engine*. SAE Technical Paper. 2017.

145. Soloiu, Valentin, et al. *Performance of a Supercharged Engine Fueled With a CTL Binary Mixture at Different Injection Pressures*. 2017. 57601: p. V001T04A045.

146. Cao, Yan, et al. *Synthesis Gas Production with an Adjustable H2/CO Ratio through the Coal Gasification Process: Effects of Coal Ranks And Methane Addition*. Energy & Fuels, 2008. 22.3: p. 1720-1730.

147. Heywood, John B., *Internal combustion engine fundamentals*. New York : McGraw-Hill.1988.

148. Tao, Ling, et al. *Techno-economic and resource analysis of hydroprocessed renewable jet fuel*. Biotechnology for biofuels, 2017. 10.1: p. 261.

149. Hughes, JP. *Hydrogenation of fatty oils*. Journal of the American Oil Chemists Society, 1953. 30.11: p. 506-515.

150. Edwards, James T, et al. *US Air Force hydroprocessed renewable jet (HRJ) fuel research*. Air Force Research Lab, Wright-Patterson AFB. 2012.

151. Vasquez, Maria Cecilia, et al. *Hydrotreatment of vegetable oils: A review of the technologies and its developments for jet biofuel production*. Biomass and bioenergy, 2017. 105.p. 197-206.

152. Shaw, Robert W. *Supercritical water a medium for chemistry*. Chemical Engineering News, 1991. 69.p. 26-39.

153. *"Drop-in" Jet and Diesel Fuels from Renewable Oils*. https://apps.dtic.mil/dtic/tr/fulltext/u2/a566458.pdf.

154. Wang, Wei-Cheng, et al. *Review of biojet fuel conversion technologies*. National Renewable Energy Lab (NREL). 2016.

155. Li, Lixiong, et al. *Catalytic hydrothermal conversion of triglycerides to non-ester biofuels*. Energy & Fuels, 2010. 24.2: p. 1305-1315.

156. Pearlson, Matthew, et al. *A techno-economic review of hydroprocessed renewable esters and fatty acids for jet fuel production*. Biofuels, Bioproducts and Biorefining, 2013. 7.1: p. 89-96.

157. Greenbaum, William, and Flying Away From Oil. *Alternative Jet Fuels*. Retrieved July, 2012. 15.p. 2017.

158. de Jong, SA, et al., *Renewable Jet Fuel in the European Union: Scenarios and Preconditions for Renewable Jet Fuel Deployment towards 2030*. Copernicus Institute, Department IMEW, Energy & Resources.2017.

159. Eller, Zoltán, et al. *Advanced production process of jet fuel components from technical grade coconut oil with special hydrocracking*. Fuel, 2016. 182.p. 713-720.

160. Hamilton, Leonard J, et al. 2011. *Renewable fuel performance in a legacy military diesel engine*. ASME 2011 5th International Conference on Energy Sustainability. 2011.

161. Cowart, Jim S, et al. 2012. *Hydrotreated Renewable Jet Fuel Ignition Delay Performance in a Military Diesel Engine: An Experimental and Modeling Study*. ASME 2012 Internal Combustion Engine Division Fall Technical Conference. 2012.

162. Hansen, Gregory A, et al. *Generator Set Durability Testing*. Southwest Research Institute/TARDEC Fuels and Lubricants Research Facility. 2012.

163. Jackman, Andrew, et al. *Durability Evaluation of the Effects of Hydro-processed Renewable Jet (HRJ) Blended at 50% with Petroleum JP-8 on a Navistar Maxxforce D10 9.3 L Engine*. US Army Tank Automotive Research Development and Engineering Center. 2012.

164. Cowart, Jim, et al. *Alternative Diesel Fuel Combustion Acceptance Criteria for New Fuels in Legacy Diesel Engines*. SAE Technical Paper. 2013.

165. Rothamer, David, and Nicholas Neal. *Fundamental Investigation of Jet Fuel Spray and Ignition Process in an Optically Accessible Piston Engine*. U.S. Army Research Office. 2015.

166. McDaniel, Andrew, et al. *A Technical Evaluation of New Renewable Jet and Diesel Fuels Operated in Neat Form in Multiple Diesel Engines*. 2016.

167. EIA, US. *US fuel ethanol plant production capacity*.2018.

168. Brooks, K. P., et al. *Chapter 6 - Low-Carbon Aviation Fuel Through the Alcohol to Jet Pathway*. Academic Press. 2016.

169. Liew, FungMin, et al. *Gas Fermentation—A Flexible Platform for Commercial Scale Production of Low-Carbon-Fuels and Chemicals from Waste and Renewable Feedstocks*. Frontiers in Microbiology, 2016. 7.694: p.

170. Geleynse, Scott, et al. *The Alcohol-to-Jet Conversion Pathway for Drop-In Biofuels: Techno-Economic Evaluation*. ChemSusChem, 2018. 11.21: p. 3728-3741.

171. Lapuerta, Magín, et al. *Strategies to introduce n-butanol in gasoline blends*. Sustainability, 2017. 9.4: p. 589.

172. Won, Sang Hee, et al. *Predicting the global combustion behaviors of petroleum-derived and alternative jet fuels by simple fuel property measurements*. Fuel, 2016. 168.p. 34-46.

173. Mawhood, Rebecca, et al. *Production pathways for renewable jet fuel: a review of commercialization status and future prospects*. Biofuels, Bioproducts and Biorefining, 2016. 10.4: p. 462-484.

174. Brandt, Adam C, and Edwin A Frame. *Evaluation of 25-Percent ATJ Fuel Blends in the John Deere 4045HF 280 Engine*. US Army TARDEC Fuels and Lubricants Research Facility (SWRI). 2014.

175. Dickerson, Terrence, et al. *Start-up and steady-state performance of a new renewable alcohol-to-jet (ATJ) fuel in multiple diesel engines*. SAE Technical Paper. 2015.

176. Yost, Douglas M, Frame, Edwin A. *GEP 6.5 LT Engine Cetane Window Evaluation for ATJ/JP-8 Fuel Blends*. US Army TARDEC Fuels and Lubricants Research Facility Southwest Research (SWRI). 2015.

177. Brandt, Adam C, et al. *Caterpillar C7 and GEP 6.5 L (T) Fuel System Durability Using 25% ATJ Fuel Blend*. US Army TARDEC Fuels and Lubricants Research Facility (SWRI). 2015.

178. Hansen, Gregory A, and Edwin A Frame. *Generator Set Durability Testing Using 25% ATJ Fuel Blend*. US Army TARDEC Fuels and Lubricants Research Facility (SwRI). 2016.

179. Vozka, Petr, et al. *Jet fuel density via GC × GC-FID*. Fuel, 2019. 235.p. 1052-1060.

180. International, ASTM. *ASTM D7566-18a, standard specification for aviation turbine fuel containing synthesized hydrocarbons*. ASTM 2017 Annual Book of Standards, 2017. p.

181. Millo, Federico, et al. *Influence on the performance and emissions of an automotive Euro 5 diesel engine fueled with F30 from Farnesane*. Fuel, 2014. 138.p. 134-142.

182. Groendyk, Michael A, and David Rothamer. *Effects of fuel physical properties on auto-ignition characteristics in a heavy duty compression ignition engine*. SAE International Journal of Fuels and Lubricants, 2015. 8.1: p. 200-213.

183. Soriano, José Antonio, et al. *Influence on performance and emissions of an automotive diesel engine fueled with biodiesel and paraffinic fuels: GTL and biojet fuel farnesane*. Energy & fuels, 2018. 32.4: p. 5125-5133.

184. Martel, Charles R. *Properties of JP-8 Jet Fuel*. AIR FORCE WRIGHT AERONAUTICAL LABS WRIGHT-PATTERSON AFB OH. 1988.

185. F. Montemayor, Alan, et al., *Potential Benefits from the Use of JP-8 Fuel in Military Ground Equipment*.1989.

186. Lacey, Paul I., and Sidney J. Lestz. *Effect of Low-Lubricity Fuels on Diesel Injection Pumps - Part I: Field Performance*. 1992.

187. Blakeley, Katherine. 2012. *DOD alternative fuels: policy, initiatives and legislative activity*. 2012.

188. Anderson, Robert Bernard, et al., *The fischer-tropsch synthesis*. Academic Press New York.1984.

189. Bartis, James T, et al., *Producing liquid fuels from coal: prospects and policy issues*. Rand Corporation.2008.

190. Ansolabehere, Stephen. *The future of coal*. 2006. p.

191. Stratton, Russell W, et al. *Life cycle greenhouse gas emissions from alternative jet fuels*. Partner Project, 2010. 28.p. 133.

192. Mattis, Jim. *Summary of the 2018 national defense strategy of the United States of America*. Department of Defense Washington United States. 2018.

193. Lewis, Kristin C, et al. *US alternative jet fuel deployment scenario analyses identifying key drivers and geospatial patterns for the first billion gallons*. Biofuels, Bioproducts and Biorefining, 2018. p.

194. Telsnig, Thomas, et al. *Assessment of selected CCS technologies in electricity and synthetic fuel production for CO2 mitigation in South Africa*. Energy Policy, 2013. 63.p. 168-180.

195. Elia, Josephine A., et al. *Nationwide energy supply chain analysis for hybrid feedstock processes with significant CO2 emissions reduction*. AIChE Journal, 2012. 58.7: p. 2142-2154.

196. Williams, Robert H, et al. *Fischer–Tropsch fuels from coal and biomass: Strategic advantages of once-through ("polygeneration") configurations*. Energy Procedia, 2009. 1.1: p. 4379-4386.

197. van der Westhuizen, Rina, et al. *Comprehensive two-dimensional gas chromatography for the analysis of synthetic and crude-derived jet fuels*. Journal of Chromatography A, 2011. 1218.28: p. 4478-4486.

198. Klerk, Arno de. *Fischer–Tropsch fuels refinery design*. Energy & Environmental Science, 2011. 4.4: p. 1177-1205.

199. Moses, Clifford A., and Petrus N. Roets. *Properties, Characteristics, and Combustion Performance of Sasol Fully Synthetic Jet Fuel*. Journal of Engineering for Gas Turbines and Power, 2009. 131.4: p. 041502-041502-17.

200. Lovestead, Tara M., et al. *Comprehensive Assessment of Composition and Thermochemical Variability by High Resolution GC/QToF-MS and the Advanced Distillation-Curve Method as a Basis of Comparison for Reference Fuel Development*. Energy & Fuels, 2016. 30.12: p. 10029-10044.

201. Graham, John L., et al. *Swelling of Nitrile Rubber by Selected Aromatics Blended in a Synthetic Jet Fuel*. Energy & Fuels, 2006. 20.2: p. 759-765.

202. Lacey, Paul I, and Sidney J Lestz. *Fuel lubricity requirements for diesel injection systems*. Southwest Research Institute (SWRI). 1991.

203. Ladommatos, Nicos, and John Goacher. *Equations for predicting the cetane number of diesel fuels from their physical properties*. Fuel, 1995. 74.7: p. 1083-1093.

204. Lobo, Prem, et al. *Comparison of PM emissions from a commercial jet engine burning conventional, biomass, and Fischer–Tropsch fuels*. Environmental science & technology, 2011. 45.24: p. 10744-10749.

205. Bhagwan, Robbin, et al. *An experimental comparison of the emissions characteristics of standard jet A-1 and synthetic fuels*. Flow, Turbulence and Combustion, 2014. 92.4: p. 865-884.

206. Huang, Chung-Hsuan, and Randy L Vander Wal. *Effect of soot structure evolution from commercial jet engine burning petroleum based JP-8 and synthetic HRJ and FT fuels*. Energy & Fuels, 2013. 27.8: p. 4946-4958.

207. Lombaert, K, et al. *Analysis of diesel particulate: influence of air-fuel ratio and fuel composition on polycyclic aromatic hydrocarbon content*. International Journal of Engine Research, 2002. 3.2: p. 103-114.

208. Murphy, Lucas, and David Rothamer. *Effects of Cetane Number on Jet Fuel Combustion in a Heavy-Duty Compression Ignition Engine at High Load*. SAE Technical Paper. 2011.

209. Langness, Chenaniah, et al. *Construction, instrumentation, and implementation of a low cost, single-cylinder compression ignition engine test cell*. SAE Technical Paper. 2014.

210. Yanowitz, Janet, et al. *Compendium of experimental cetane numbers*. National Renewable Energy Lab.(NREL), Golden, CO (United States). 2017.

211. Kang, Dongil, et al. *Experimental characterization of jet fuels under engine relevant conditions – Part 1: Effect of chemical composition on autoignition of conventional and alternative jet fuels*. Fuel, 2019. 239.p. 1388-1404.

212. Srivatsa, Charu, et al., *Performance and Emissions Analysis of Partially Pre-Mixed Charge Compression Ignition Combustion*.2018.

213. Ragozin, NA. *Jet Fuels*. AIR FORCE SYSTEMS COMMAND WRIGHT-PATTERSON AFB OH FOREIGN TECHNOLOGY DIVISION. 1966.

214. *ASTM D975-19a, Standard Specification for Diesel Fuel Oils*.2019.

215. *ASTM D7566-19, Standard Specification for Aviation Turbine Fuel Containing Synthesized Hydrocarbons*.2019.

216. Mattson, Jonathan, and Christopher Depcik. 2019. *Availability Analysis of Alternative Fuels for Compression Ignition Engine Combustion*. Proceedings of the 4th International Congress of Automotive and Transport Engineering (AMMA 2018). 2019.

217. Tiron, Roxana. *$400 per gallon gas to drive debate over cost of war in Afghanistan*. Capitol Hill Publishing Corps. 2009.

218. Shen, Mengqin, et al. *Effects of EGR and Intake Pressure on PPC of Conventional Diesel, Gasoline and Ethanol in a Heavy Duty Diesel Engine*. 2013.

219. Bester, Nigel, and Andy Yates, *Assessment of the Operational Performance of Fischer-Tropsch Synthetic-Paraffinic Kerosene in a T63 Gas Turbine Compared to Conventional Jet A-1 Fuel*.2009.

220. Weese, Coleen B, and Joseph H Abraham. *Potential health implications associated with particulate matter exposure in deployed settings in southwest Asia*. Inhalation toxicology, 2009. 21.4: p. 291-296.

221. Bittner, James D, and Jack B Howard. *Role of aromatics in soot formation*. Alternative Hydrocarbon Fuels: Combustion and Chemical Kinetics, 1978. 62.p. 335-358.

222. Ted Biddle, Peter Brook, Chris Bunker, Tim Edwards, Greg Hemighaus. *Handbook of Aviation Fuel Properties* Coordinating Research Council, Inc. .2004.

Appendices

Appendix A: Fuel Specifications

Table 11: U.S. Military Specifications for Turbine Fuels – JP-4, JP-5, JP-8 [222]

Property		*JP-4*	*JP-5*	*JP-8*	*Test Method*
COMPOSITION					
Acidity, Total (mg KOH/g)	Max	0.015	0.015	0.015	D 3242
Aromatics (% by Volume)	Max	25.0	25.0	25.0	D 1319
Sulfur, Mercaptan (% by Mass) *or*	Max	0.002	0.002	0.002	D 3227
Doctor Test		Negative	Negative	Negative	D 4952
Sulfur, Total (% by Mass)	Max	0.40	0.40	0.30	D 129 , D 1266, D 2887, D 2622, D 3120, D 4294 or D 5453
Color, Saybolt		Report	Report	Report	D 156 or D 6045
VOLATILITY					
Distillation					D 86 3, 4 or D 2887
(D 2887 Limits in parentheses)					
Distillation Temperature, (°C)					
Initial Boiling Point	Max	Report	Report	Report	
10% Recovered	Max	Report	206 (185)	205 (186)	
20% Recovered	Min	100	Report	Report	
50% Recovered	Min	125	Report	Report	
90% Recovered		Report	Report	Report	
End Point Temperature	Max	270	300 (330)	300 (330)	
Residue (% by Volume) (for D 86)	Max	1.5	1.5	1.5	
Loss (% by Volume) (for D 86)	Max	1.5	1.5	1.5	
Flash Point (°C)	Min		60	38	D 56, D 93 or D 3828
Density, 15°C (kg/m)		751-802	788-845	775-840	D 1298 or D 4052
°API Gravity, (60°F)		45-57	36-48	37-51	D 1298
Vapor Pressure (37.8°C) kPa		14-21	–	–	D 323, D 4953, D 5190, D 5191
FLUIDITY					
Freezing Point, °C	Max	-58	-46	-47	D 2386,3 D 5901, D 5972
Viscosity at -20°C (cSt)	Max	–	8.5	8.0	D 445
COMBUSTION					
Net Heat of Combustion, MJ/kg	Min	42.8	42.6	42.8	D 3338, D 4809, or
					D 4529 (JP-4 and JP-5)
Calculated Cetane Index			Report	Report	D 9769
Hydrogen Content (% by Mass)	Min	13.5	13.4	13.4	D 3701, D 3343
Smoke Point (mm) ***or***	Min	20.0	19.0	25.0	D 1322
Smoke Point (mm) ***and***	Min	--	--	19.0	D 1322
Naphthalenes, vol %	Max			3.0	D 1840

Table 12: U.S. Military Specifications for Turbine Fuels – JP-4, JP-5, JP-8 (Continued)

Property		***JP-4***	***JP-5***	***JP-8***	***Test Method***
CORROSION					
Copper Strip (2 hr at 100°C)	Max	1	1	1	D 130
THERMAL STABILITY JFTOT					D 3241
Pressure Drop (mm Hg)	Max	25	25	25	
Tube Color Code	Max	< 3, No *peacock* or *abnormal* color. Such deposits result in failure			
CONTAMINANTS					
Existent Gum (mg/100 mL)	Max	7.0	7.0	7.0	D 381
Particulates (mg/liter)	Max	1.0	1.0	1.0	D 2276 or D 5452
Water Reaction Interface	Max	1b	1b	1b	D 1094
Water Separation Index	Min	70	85	70	D 3948
Filtration Time (minutes)	Max	10	15	15	
ADDITIVES					
Anti-Icing (% by Volume)		0.10 to 0.15	0.15 to 0.20	0.10 to 0.15	D 5006 (DiEGME)
Antioxidant		Required	Required	Required	
Conductivity (pS/m)		150 to 600		150 to 450	D 2624

Table 13: U.S. Commercial Turbine Fuel Specifications – Jet A, Jet A-1, Jet B [222]

Property		***Jet A***	***Jet A-1***	***Jet B***	***ASTM Test Method***
COMPOSITION					
Acidity Total (mg KOH/g)	Max	0.10	0.10	--	D 3242
Aromatics (% by Volume)	Max	25	25	25	D 1319
Sulfur Mercaptan (% by Weight)	Max	0.0030	0.0030	0.0030	D 3227
Sulfur Total (% by Weight)	Max	0.30	0.30	0.3	D 1266, D 1552, D 2622
VOLATILITY					
Distillation Temperature (°C)					D 86
10% Recovered	Max	205	205	--	
20% Recovered	Max			145	
50% Recovered	Max	Report	Report	190	
90% Recovered	Max	Report	Report	245	
Final Boiling Point	Max	300	300	--	
Residue (% by Volume)	Max	1.5	1.5	1.5	
Loss (% by Volume)	Max	1.5	1.5	1.5	
Flash Point (°C)	Min	38	38		D 56 or D 3828
Density at 15°C (kg/m3)		775 to 840	775 to 840	751 to 802	D 1298 or D 4052
Vapor Pressure, 38°C (kPa)	Max			14 to 21	D 323 or D 5191
FLUIDITY					
Freezing Point (°C)5	Max	-40	-47	-50	D 2386 or D 5972
Viscosity at -20°C (cSt)	Max	8.0	8.0	--	D 445
COMBUSTION					

Net Heat of Combustion	Min	42.8	42.8	42.8	D 4529, D3338, D 4809
One of the following requirements shall be met					
Smoke Point, mm	Min	25	25	25	D 1322
Smoke Point, mm and	Min	18	18	18	D 1322
Naphthalenes (% by Volume)	Max	3.0	3.0	3.0	D 1840
CORROSION					
Copper Strip (2 hrs at 100°C)	Max	No. 1	No. 1	No. 1	D 130
STABILITY					
Jet Fuel Thermal Oxidative Tester 2.5 hr					D 3241
at Control Temperature of 260ºC					
Filter Pressure Drop (mm Hg)	Max	25	25	25	
Tube Deposit10 Rating	Max	< 3, No peacock or abnormal color deposits			
CONTAMINANTS					
Existent Gum (mg/100 mL)	Max	7	7	7	D 381
Water Reaction Interface	Max	lb	lb	lb	D 1094
ADDITIVES					
Electrical Conductivity (pS/m)	If electrical conductivity additive is used, the conductivity shall not exceed 450 pS/m				

Table 14: ASTM Properties of Fischer Tropsch Synthetic Paraffinic Kerosene (FT-SPK)

Property		***FT-SPK***	***Test Method***
COMPOSITION			
Acidity, total mg KOH/g	Max	0.015	D3242/IP 354
VOLATILITY			
Distillation—both of the following requirements shall be met:			
1. Physical Distillation			D86*C* or IP 123 or D7345
Distillation temperature, °C:			
10 % recovered, temperature (T10)	Max	205	
50 % recovered, temperature (T50)		report	
90 % recovered, temperature (T90)		report	
Final boiling point, temperature	Max	300	
T90-T10, °C	Min	22	
Distillation residue, %	Max	1.5	
Distillation loss, %	Max	1.5	
2. Simulated Distillation			D2887/IP 406
Distillation temperature, °C:			
10 % recovered, temperature (T10)		report	
50 % recovered, temperature (T50)		report	
90 % recovered, temperature (T90)		report	

Final boiling point, temperature		report	
Flash point, °C	Min	38	D56, D3828 , IP 170 or IP 523
Density at 15 °C, kg/m3		730 to 770	D1298/IP 160, D4052, IP 365
Freezing point, °C	Max	–40	D5972 / IP 435, D7153/IP 529, D7154/IP528/D2386
Thermal Stability (2.5 hr at control temperature)			
Temperature, °C	Min	325	D3241 /IP 323*G*
Filter pressure drop, mm Hg	Max	25	
Tube rating: One of the following requirements shall be met:			
(1) Annex A1 VTR, VTR Color Code		< 3	
		No peacock or abnormal color deposits	
(2) Annex A2 ITR or Annex A3 ETR, nm avg over area of 2.5 mm2	Max	85	
ADDITIVES			
Antioxidants, mg/L	Min	17	
	Max	24	

Table 15: Additional ASTM properties of FT-SPK

Property		***FT-SPK***	***Test Method***
HYDROCARBON COMPOSITION			
Cycloparaffins, mass %		15C	D2425
Aromatics, mass %		0.5	D2425
Paraffins, mass %		report	D2425
Carbon and hydrogen, , mass %			%
NON-HYDROCARBON COMPOSITION			
Nitrogen, mg/kg	Max	2	D4629/IP 379
Water, mg/kg	Max	75	D6304/IP 438
Sulfur, mg/kg	Max	15	D5453
Metals, mg/kg			
(Al, Ca, Co, Cr, Cu, Fe, K, Li, Mg, Mn, Mo,	Max	0.1 per metal	D7111
Na, Ni, P, Pb, Pd, Pt, Sn, Sr, Ti, V, Zn), mg/kg			
Halogens, mg/kg	Max	1	D7359

Table 16: ASTM Properties of alcohol to jet (ATJ) fuel

Property		***SPK/A***	***Test Method***
COMPOSITION			
Acidity, total mg KOH/g	Max	0.015	D3242/IP 354
1. Aromatics, vol %	Max	20	D1319/IP 156
2. Aromatics, vol %	Max	21.2	D6379/IP 436
VOLATILITY			
Distillation—both of the following requirements shall be met:			
1. Physical Distillation			D86*C* or IP 123*C*
Distillation temperature, °C:			
10 % recovered, temperature (T10)	Max	205	
50 % recovered, temperature (T50)		report	
90 % recovered, temperature (T90)		report	
Final boiling point, temperature	Max	300	
T90-T10, °C	Min	22	
Distillation residue, %	Max	1.5	
Distillation loss, %	Max	1.5	
2. Simulated Distillation			D2887
Distillation temperature, °C:			
10 % recovered, temperature (T10)		report	
50 % recovered, temperature (T50)		report	
90 % recovered, temperature (T90)		report	
Final boiling point, temperature		report	
Flash point, °C Density at 15 °C, kg/m3	Min	38 755 to 800	D56, D3828*E* , IP 170*E* or IP 523 D1298/IP 160, D4052 or IP 365
Freezing point, °C	Max	–40	D5972/IP 435, D7153/IP 529, D7154/IP 528, or D2386/IP 16
THERMAL STABILITY			
(2.5 h at control temperature)			
Temperature, °C	Min	325	D3241 /IP 323
Filter pressure drop, mm Hg	Mix	25	
Tube rating: One of the following			
requirements shall be met:G			
(1) Annex A1 VTR, VTR Color Code			
(2) Annex A2 ITR or Annex A3 ETR			
nm avg over area of 2.5 mm2			
CONTAMINANTS			
Existent gum, mg/100 mL	Max	4	D381/IP 540
MSEP	Min	90	D3948
ADDITIVES			
Antioxidants, mg/L	Min	17	
	Max	24	

Table 17: Additional ASTM properties of ATJ fuel

Property		***SPK/A***	***Test Method***
HYDROCARBON COMPOSITION			
Cycloparaffins, mass %	Max	15	D2425
Aromatics, mass %	Max	0.5	D2425
Paraffins, mass %		report	D2425
Carbon and hydrogen, , mass %	Min	99.5	
NON-HYDROCARBON COMPOSITION			
Nitrogen, mg/kg	Max	2	D4629/IP 379
Water, mg/kg	Max	75	D6304/IP 438
Sulfur, mg/kg	Max	15	D5453
Metals, mg/kg			
(Al, Ca, Co, Cr, Cu, Fe, K, Li, Mg, Mn, Mo,	Max	0.1 per metal	D7111/UOP389
Na, Ni, P, Pb, Pd, Pt, Sn, Sr, Ti, V, Zn), mg/kg			
Halogens, mg/kg	Max	1	D7359

Table 18: Modified Yanmar L100V Engine Specifications

Parameter	
Engine Type	Vertical Direct Injection CI Engine
Engine Intake	Naturally Aspirated
Cooling	Air Cooled
Cycle	4 Stroke
Displacement	435 cc
Number of Cylinders	1
Number of Valves	1 Intake, 1 Exhaust
Bore	86 mm
Stroke	75 mm
Connecting Rod Length	118 mm
Crank Radius	38 mm
Clearance Volume	2.1611×10^{-5} m^3
Piston Area	0.0058088 m^2
Compression Ratio	21.2
Injection Timing	0 To 100 degrees BTDC
Intake Valve Close	122^{o} BTDC
Exhaust Valve Open	144^{o} ATDC
Continuous Rated Output	8.3 hp SAE, 6.2 kW
Rated Speed	3600 rpm
Injector Pressure	40 MPa To 180 MPa
Engine Oil	Shell 15w-40

Appendix B: Composition of Sasol CTL Fuel from the Agilent Mass Spectrometry Machine

Sr	*Area %*	*Library/ID*	*CAS #*	*Quality*
1	2.5073	Naphthalene, decahydro-, trans-	000493-02-7	97
2	2.2886	trans-Decalin, 2-methyl-	1000152-47-3	97
3	1.9694	1,1'-Bicyclohexyl	000092-51-3	91
4	1.8409	Tetradecane, 2,2-dimethyl-	059222-86-5	35
5	1.7491	Tetratriacontyl heptafluorobutyrate	1000351-84-1	80
6	1.6618	2-Butanone, 4-cyclohexyl-	002316-85-0	35
7	1.6216	Naphthalene, 1,2,3,4-tetrahydro-	000119-64-2	96
8	1.4914	Cyclohexane, propyl-	001678-92-8	50
9	1.4754	Octane, 6-ethyl-2-methyl-	062016-19-7	64
10	1.4031	Undecane, 4-methyl-	002980-69-0	43
11	1.3942	trans-anti-trans-Tetra-decahydroanthracene	028071-99-0	99
12	1.3289	1-Methyldecahydronaphthalene	002958-75-0	95
13	1.2722	Naphthalene, 1,2,3,4-tetrahydro-6-methyl-	001680-51-9	98
14	1.2661	Undecane, 3,6-dimethyl-	017301-28-9	59
15	1.2058	Heptane, 2,3,6-trimethyl-	004032-93-3	83
16	1.2036	Octane, 2,2,6-trimethyl-	062016-28-8	59
17	1.203	Naphthalene, decahydro-, cis-	000493-01-6	96
18	1.1012	1,1'-Bicyclohexyl, 2-methyl-, cis-	050991-08-7	50
19	1.0991	Undecane, 3,6-dimethyl-	017301-28-9	59
20	1.0886	cis-Decalin, 2-syn-methyl-	1000155-85-6	97
21	1.0815	Naphthalene, 1,2,3,4-tetrahydro-2,6-dimethyl-	007524-63-2	91
22	0.9882	Tetradecane	000629-59-4	98
23	0.9484	trans-Decalin, 2-methyl-	1000152-47-3	93
24	0.9297	Dodecane	000112-40-3	96
25	0.9156	Spiro(5,6)dodecane	000181-15-7	42
26	0.9067	Naphthalene, 2-ethyldecahydro-	001618-23-1	90
27	0.9055	Undecane, 3,6-dimethyl-	017301-28-9	59
28	0.888	Anthracene, tetradecahydro-	006596-35-6	98
29	0.8853	Cyclohexane, (1-methylpropyl)-	007058-01-7	41
30	0.8632	1H-Fluorene, dodecahydro-	005744-03-6	92
31	0.8552	Decane, 2,5,6-trimethyl-	062108-23-0	78
32	0.8497	Tridecane	000629-50-5	53
33	0.8482	Pentadecane	000629-62-9	98
34	0.825	2-methyloctacosane	1000376-72-8	59
35	0.8208	Naphthalene, 1,2,3,4-tetrahydro-6-methyl-	001680-51-9	96
36	0.8178	Heptane, 3,3,5-trimethyl-	007154-80-5	72

37	0.8053	Cyclohexane, 1-(cyclohexylmethyl)-4-methyl-, cis-	054823-97-1	70
38	0.7691	Tetracontane, 3,5,24-trimethyl-	055162-61-3	43
39	0.766	Oxirane, decyl-	002855-19-8	45
40	0.7551	Decane, 3,7-dimethyl-	017312-54-8	83
41	0.7511	Naphthalene, decahydro-2,6-dimethyl-	001618-22-0	55
42	0.7479	Pentane, 2,2,3,4-tetramethyl-	001186-53-4	53
43	0.7376	1H-Fluorene, dodecahydro-	005744-03-6	94
44	0.7375	Ether, hexyl pentyl	032357-83-8	64
45	0.7368	Naphthalene, decahydro-2-methyl-	002958-76-1	93
46	0.7076	Hexane, 2,3,3-trimethyl-	016747-28-7	64
47	0.6887	Tridecane	000629-50-5	96
48	0.6844	Octane, 2,4,6-trimethyl-	062016-37-9	52
49	0.6814	Decane, 2-methyl-	006975-98-0	64
50	0.6728	Decane, 2,5,6-trimethyl-	062108-23-0	78
51	0.6633	Naphthalene, 6-ethyl-1,2,3,4-tetrahydro-	022531-20-0	58
52	0.6632	1,13-Tetradecadiene	021964-49-8	46
53	0.6604	Naphthalene, decahydro-2,6-dimethyl-	001618-22-0	64
54	0.6597	Naphthalene, decahydro-2,6-dimethyl-	001618-22-0	86
55	0.6558	Benzene, 1-cyclohexyl-3-methyl-	004575-46-6	96
56	0.646	Undecane, 2,9-dimethyl-	017301-26-7	64
57	0.6392	Heptylcyclohexane	005617-41-4	90
58	0.6325	1,1'-Bicyclohexyl, 2-methyl-, cis-	050991-08-7	72
59	0.6278	Naphthalene, 2-butyldecahydro-	006305-52-8	93
60	0.6233	Isobutyl nonyl carbonate	959311-27-4	64
61	0.6161	Cyclohexane, 1,1'-methylenebis-	003178-23-2	70
62	0.6128	Oxalic acid, isobutyl nonyl ester	1000309-37-4	59
63	0.5641	Undecane, 5,6-dimethyl-	017615-91-7	72
64	0.5591	Octane, 3,6-dimethyl-	015869-94-0	64
65	0.5514	Cyclohexane, (1-methylbutyl)-	061208-94-4	64
66	0.5476	Heptane, 2,4-dimethyl-	002213-23-2	43
67	0.5383	Naphthalene, decahydro-2,6-dimethyl-	001618-22-0	94
68	0.528	Octane, 3-ethyl-	005881-17-4	68
69	0.5268	trans, cis-3-Ethylbicyclo(4.4.0)decane	066660-43-3	86
70	0.524	Nonane, 4,5-dimethyl-	017302-23-7	91
71	0.5216	Naphthalene, decahydro-2,3-dimethyl-	001008-80-6	83
72	0.5183	Decalin, syn-1-methyl-, cis-	1000158-89-1	91
73	0.518	Perhydroanthracene,(4a.alpha, 8a.beta, 9a.alpha, 10a.beta.)	029863-91-0	51
74	0.5098	Hexane, 2,4-dimethyl-	000589-43-5	64
75	0.508	Bicyclo(4.2.0)octa-1,3,5-triene, 7-isopropyl-	027087-54-3	42
76	0.5045	Undecane, 3,5-dimethyl-	017312-81-1	72

77	0.4877	Naphthalene, 1,2,3,4-tetrahydro-2-methyl-	003877-19-8	96
78	0.4785	1H-Indene, 2,3-dihydro-4,7-dimethyl-	006682-71-9	55
79	0.4783	Naphthalene, decahydro-2-methyl-	002958-76-1	55
80	0.4676	Octane, 2,6-dimethyl-	002051-30-1	59
81	0.4525	1H-Fluorene, dodecahydro-	005744-03-6	90
82	0.4513	4a(2H)-Naphthalenemethanol, octahydro-	099992-19-5	70
83	0.4495	1H-Inden-1-one, 2,4,5,6,7,7a-hexahydro-4,4,7a-trimethyl-	060713-96-4	60
84	0.4295	Cyclohexane, 1-ethyl-4-methyl-, cis-	004926-78-7	94
85	0.4229	Undecane, 3-methyl-	001002-43-3	59
86	0.4208	Perhydroanthracene, (4a.alpha,8a.alpha, 9a.alpha, 10a.beta.)	002109-05-9	98
87	0.4193	Tetrapentacontane, 1,54-dibromo-	1000156-09-4	49
88	0.4187	Octane, 2,6-dimethyl-	002051-30-1	87
89	0.4122	(2Z,4E)-3,7-Dimethyl-2,4-octadiene	1000374-08-4	70
90	0.4102	Decane, 2,3,5-trimethyl-	062238-11-3	50
91	0.4098	Octadecane, 1-chloro-	003386-33-2	38
92	0.4078	1-Ethyl-4-methylcyclohexane	003728-56-1	90
93	0.4045	Tetratriacontyl heptafluorobutyrate	1000351-84-1	52
94	0.4023	Undecane, 2,6-dimethyl-	017301-23-4	78
95	0.4006	1H-Indene, 2,3-dihydro-4,7-dimethyl-	006682-71-9	92
96	0.3957	Decane, 2,5-dimethyl-	017312-50-4	78
97	0.3902	Naphthalene, 1,2,3,4-tetrahydro-6,7-dimethyl-	001076-61-5	96
98	0.3897	2,2,7,7-Tetramethyloctane	001071-31-4	64
99	0.3858	Perhydrophenanthrene (4a,4b.alpha,8a.alpha, 10a.beta.)-	027425-35-0	99
100	0.381	Naphthalene, 1,2,3,4-tetrahydro-1,4-dimethyl-	004175-54-6	86
101	0.3749	Octane, 2,6-dimethyl-	002051-30-1	64
102	0.3716	Dodecane, 2,6,11-trimethyl-	031295-56-4	35
103	0.3708	Pentane, 2,3,4-trimethyl-	000565-75-3	47
104	0.3665	Undecane	001120-21-4	60
105	0.3534	Sulfurous acid, butyl decyl ester	1000309-17-7	43
106	0.3493	Octadecane, 1-chloro-	003386-33-2	30
107	0.3441	Heptylcyclohexane	005617-41-4	64
108	0.34	Sulfurous acid, nonyl 2-pentyl ester	1000309-15-8	86
109	0.335	2-Butyl-3,4,5,6-tetrahydropyridine	001462-94-8	38
110	0.3324	Decane, 2,2,8-trimethyl-	062238-01-1	78
111	0.3253	cis-anti-cis-Tricyclo(7.3.0.0(2,6))dodecane	030159-15-0	89
112	0.3166	Tetracontane, 3,5,24-trimethyl-	055162-61-3	43
113	0.315	Cyclohexane, 1,1-dimethyl-	000590-66-9	38
114	0.3109	Naphthalene, decahydro-2,3-dimethyl-	001008-80-6	95
115	0.3014	1H-Pyrrole, 2,3-dihydro-1-methyl-	033838-11-8	58
116	0.2955	Octane, 3,5-dimethyl-	015869-93-9	53

117	0.2952	Hexacosane	000630-01-3	59
118	0.2866	7-Hexadecyne	074685-28-2	46
119	0.2744	Cyclohexane, 1,1'-ethylidenebis-	002319-61-1	53
120	0.2618	Octane, 4-methyl-	002216-34-4	72
121	0.2612	Tetratetracontane	007098-22-8	50
122	0.2574	9-Tetradecenal, (Z)-	053939-27-8	35
123	0.2568	Naphthalene, 1,2,3,4-tetrahydro-1,4-dimethyl-	004175-54-6	93
124	0.2562	1,7,7-Trimethylbicyclo(2.2.1)heptan-2-ol	010385-78-1	38
125	0.2531	Octane, 3,3-dimethyl-	004110-44-5	86
126	0.2492	Hexadecane, 2,6,11,15-tetramethyl-	000504-44-9	46
127	0.2466	Tetracontane, 3,5,24-trimethyl-	055162-61-3	72
128	0.2453	Sulfurous acid, 2-propyl undecyl ester	1000309-12-2	46
129	0.2452	Cyclohexane, 1-(cyclohexylmethyl)-4-ethyl-, cis-	054934-95-1	25
130	0.2328	Sulfurous acid, butyl heptadecyl ester	1000309-18-4	38
131	0.2317	1,2,5-Oxadiborolane, 2,3,3,4,5-pentaethyl-	139688-18-9	30
132	0.2302	Naphthalene, 1,2,3,4-tetrahydro-2,5,8-trimethyl-	030316-17-7	93
133	0.2298	1H-Indene, octahydro-, trans-	003296-50-2	91
134	0.2281	2-methyltetracosane	1000376-72-6	52
135	0.2274	2-Propylcyclohexanol	090676-25-8	38
136	0.2267	Perhydrophenanthrene,(4a, 4b.alpha., 8a.alpha., 10a.beta.)-	027425-35-0	98
137	0.2247	Cyclohexane, ethyl-	001678-91-7	95
138	0.2239	Cyclododecene, 1-methyl-	023070-53-3	64
139	0.2222	Tridecane, 4-methyl-	026730-12-1	64
140	0.2215	Oxalic acid, bis(6-ethyloct-3-yl) ester	1000309-34-6	72
141	0.2211	Dispiro(4.2.4.2)tetradecane	079273-13-5	53
142	0.2199	Cyclohexene, 1-octyl-	015232-87-8	50
143	0.2195	Heptane, 2,2,4-trimethyl-	014720-74-2	72
144	0.2176	Undecane, 5,7-dimethyl-	017312-83-3	64
145	0.2118	m-Menthane, (1S,3R)-	013837-66-6	70
146	0.2053	Cyclohexane, 1-(cyclohexylmethyl)-3-methyl-, trans-	054823-95-9	68
147	0.1975	Decane, 2,5,6-trimethyl-	062108-23-0	64
148	0.1948	1,4-Dimethyl-2-cyclohexylbenzene	004501-52-4	50
149	0.1892	Cyclohexane, 1-methyl-2-pentyl-	054411-01-7	38
150	0.186	2,2,6,6-Tetramethylheptane	040117-45-1	59
151	0.1853	cis,cis-2,9-Dimethylspiro(5.5)undecane	095472-51-8	49
152	0.1847	Hexane, 2,3,4-trimethyl-	000921-47-1	43
153	0.1833	Heptane, 2,3,4-trimethyl-	052896-95-4	78
154	0.1816	Octadecane, 1-bromo-	000112-89-0	49
155	0.1807	Decane, 1,1'-oxybis-	002456-28-2	49
156	0.178	Naphthalene, 1,2,3,4-tetrahydro-2,5,8-trimethyl-	030316-17-7	92

157	0.1769	Naphthalene, 6-butyl-1,2,3,4-tetrahydro-	030654-45-6	95
158	0.1752	1,4-Dimethyl-2-cyclohexylbenzene	004501-52-4	83
159	0.1741	Pentane, 2,2,3,4-tetramethyl-	001186-53-4	43
160	0.1704	Heptane, 3-ethyl-2-methyl-	014676-29-0	59
161	0.1698	Cyclohexane, 1-ethyl-4-methyl-, trans-	006236-88-0	94
162	0.1684	Cyclohexene, 1,2-dimethyl-	001674-10-8	35
163	0.1659	Octatriacontyl pentafluoropropionate	1000351-89-1	38
164	0.1633	Cyclohexanecarboxaldehyde, 4-(hydroxymethyl)-	092385-32-5	38
165	0.1567	Tetradecane, 3-methyl-	018435-22-8	56
166	0.1472	Dispiro(4.2.4.2)tetradecane	079273-13-5	89
167	0.1451	Heptane, 3,4-dimethyl-	000922-28-1	97
168	0.144	1-Cyclohexyl-2-cyclohexylidenethane	059986-23-1	53
169	0.1439	cis-3-Methyl-endo-tricyclo(5.2.1.0(2.6))decane	1000215-29-0	47
170	0.1371	7-Octadecyne, 2-methyl-	035354-38-2	62
171	0.1369	Tetradecahydro-1-methylphenanthrene	1000080-19-6	50
172	0.1317	N-Methoxy-2-carbomethoxy-2-carbethoxyaziridine	063859-01-8	70
173	0.1312	Benzene, 1,2,3-trimethyl-	000526-73-8	78
174	0.1261	1H-Indene, 2,3-dihydro-1,1,3-trimethyl-	002613-76-5	56
175	0.1221	Benzene, 1-heptenyl-	000829-99-2	50
176	0.1193	Thioctic acid	001077-28-7	38
177	0.1026	Perhydrophenanthrene,(4a.,4b.alpha., 8a.alpha., 10a.beta.)	027425-35-0	80
178	0.1007	1-(4-Tolyl)-1-cyclohexene	001821-23-4	43
179	0.1004	Naphthalene, 1,2,3,4-tetrahydro-2,5,8-trimethyl-	030316-17-7	94
180	0.0971	1H-Indene, 3-butyl-1-methyl-	111400-84-1	86
181	0.0967	Hexane, 2,4-dimethyl-	000589-43-5	49
182	0.094	Cyclohexanecarboxaldehyde, 4-(hydroxymethyl)-	092385-32-5	38
183	0.0907	Cyclohexane, 1-ethyl-2-methyl-	003728-54-9	62
184	0.0899	1,2-Propanediol, 3-benzyloxy-1,2-diacetyl-	013754-10-4	43
185	0.0875	Perhydrophenanthrene,(4a.alpha,4b.beta,8a.alpha,10a.alpha)	027389-73-7	84
186	0.0874	2-Ethylbutyric acid, 4-octyl ester	1000369-51-1	53
187	0.0869	Heptane, 2,3-dimethyl-	003074-71-3	91
188	0.085	5-Dodecyne	019780-12-2	50
189	0.084	Heptane, 2,5-dimethyl-	002216-30-0	87
190	0.0829	o-Xylene	000095-47-6	90
191	0.0789	1H-1,2,4-Triazole-5(4H)-thione, 4-phenyl-3-(3-pyridyl)-	057600-03-0	32
192	0.075	1H-Indene, 3-butyl-1-methyl-	111400-84-1	30
193	0.0739	p-Xylene	000106-42-3	95
194	0.0723	Hexadecane	000544-76-3	97
195	0.0713	Cyclohexene, 1,6-dimethyl-	001759-64-4	64
196	0.0641	Benzene, propyl-	000103-65-1	55

197	0.0633	Hexane, 2,3,4-trimethyl-	000921-47-1	81
198	0.0628	p-Menth-8(10)-en-9-ol, cis-	015714-13-3	45
199	0.0565	Hexanedioic acid, bis(2-ethylhexyl) ester	000103-23-1	95
200	0.0558	Perhydrophenanthrene,(4a.alpha,4b.beta,8a.alpha,10a.beta)-	002108-89-6	84
201	0.0479	Hexane, 3-ethyl-	000619-99-8	86
202	0.0424	3,4-Dimethyl-1-(phenylthio)-2-pentene	1000197-07-1	38
203	0.0412	Hexane, 2,3,5-trimethyl-	001069-53-0	87
204	0.038	p-Menth-8(10)-en-9-ol, cis-	015714-13-3	38
205	0.034	Cyclohexane, 1,2,4-trimethyl-, (1.alpha.,2.beta.,4.beta.)-	007667-60-9	90
206	0.0287	Heptane, 4-ethyl-	002216-32-2	60
207	0.028	Cyclohexane, 1,2-dimethyl-, cis-	002207-01-4	95
208	0.0269	Cyclohexane, 1,2,3-trimethyl-, (1.alpha.,2.beta.,3.alpha.)-	001678-81-5	96
209	0.0254	Cyclohexane, 1,4-dimethyl-, trans-	002207-04-7	96
210	0.025	2-methyltetracosane	1000376-72-6	60
211	0.025	Benzimidazol-5-amine, 1-(4-ethoxyphenyl)-	007104-62-3	43
212	0.025	Silane, diethylpentadecyloxy(2-phenylethoxy)-	1000363-17-0	22
213	0.0249	Octane, 2-methyl-	003221-61-2	83
214	0.0216	Pentadecane, 8-hexyl-	013475-75-7	58
215	0.0167	Heptane, 2,4-dimethyl-	002213-23-2	81
216	0.0163	9-Octadecenoic acid, methyl ester, (E)-	001937-62-8	99
217	0.0146	Cyclohexane, 1,3,5-trimethyl-	001839-63-0	93
218	0.0134	Cyclohexane, 1,2-dimethyl-, trans-	006876-23-9	95
219	0.0126	Cyclohexane, 1,3-dimethyl-, cis-	000638-04-0	91
220	0.0126	Pentadecane	000629-62-9	35
221	0.0107	6,6-Diethylhoctadecane	1000360-41-8	62
222	0.0073	Benzamide, 2-methoxy-N-allyl-	1000339-10-5	38
223	0.0069	Adamantane-1-carboxamide, N-(2-benzoyl-4-nitrophenyl)-	1000286-06-7	43
224	0.0061	2,2,7,7-Tetramethyloctane	001071-31-4	53
225	0.005	Hexane, 2,2,4-trimethyl-	016747-26-5	72
226	0.0048	1,3-Benzodioxin-4-one, 2-(1,1-dimethylethyl)-5-ethenyl-perhydro	1000197-46-5	38